Quantification of macromolecular interactions in *GAL* network

Inauguraldissertation
zur
Erlangung der Würde eines Doktors der Philosophie
vorgelegt der
Philosophisch-Naturwissenschaftlichen Fakultät
der Universität Basel

von

Mümün Gençoğlu

Von Bulgaria/Turkey

Basel, 2015

Genehmigt von der Philosophisch-Naturwissenschaftlichen Fakultät

auf Antrag von

Prof. Dr. Attila Becskei and Prof. Dr. Dirk Bumann

Basel, 10.11.2015
(Date of approval by the Faculty)

Prof. Dr. J. Schibler
The Dean of Faculty

Acknowledgements

I would like to express my gratitude to my supervisor, Prof. Dr. Attila Becskei, whose expertise added considerably to my graduate experience.

I would like to thank our dear lab members who have created an extremely collegial atmosphere and especially my lovely Amir and Farzan for their unconditional support that made me feel at home at all times.

I would also like to thank my family for the support they provided me through my entire life and in particular, I must acknowledge my girlfriend, Jenny, without whose love, encouragement and editing assistance, I would not have finished this thesis.

Abstract

The functioning of cellular networks is governed by nonlinear system dynamics. The yeast *Saccharomyces cerevisiae* has long been a preferred model organism for studying such cellular regulatory systems. Perhaps, the most extensively studied genetic switch in yeast is the GAL network. Its behaviour arises from the complex interplay of multiple feedback loops the interaction of which is determined by their biochemical parameters. Direct estimation of these parameters is possible only with modeling, which often remains seriously unconstrained. In order to overcome this barrier we opened each feedback loop genetically and titrated the protein concentration of the signal transducers. Using quantitative proteomics, we were able to determine in vivo macromolecular interaction constants by minimizing the interference from other feedback loops. Some of these in vivo parameter values were in good agreement with previously published in vitro measurements. Moreover the resulting open loop relations along with equivalence relations, mapped the parameter space of deterministic bistability for the *GAL* network. Feedback splitting and transition rates successfully predicted bistability region both correlating with the hysteresis behaviour of the system and validating the parameter determination in our models.

List of Figures

List of Tables

Contents

Chapter 1 Introduction

The systems approach to problem solving uses both computational and experimental data and is composed of several steps. These include modelling of the system based on information about the interactions between its components, testing of the model for perturbations in structure and parameters of the system, and validation of the model by experiments. Mathematical models can then be used to identify the recurring dynamic organizational principles. Interactions identified by *in vitro* experiments can lead to the candidate models explaining the *in vivo* mechanism. Although some system-level properties depend on the time independent or steady-state stimulus response curves, others depend on the temporal behaviour of the system.

Cellular regulation is a result of complex interplay among various mechanisms such as DNA–protein and protein–protein binding, autoregulation, compartmentalization, and shuttling of regulatory proteins. The yeast *Saccharomyces cerevisiae* has long been a preferred organism for studying such cellular regulatory systems.[1] The regulatory circuits of a number of yeast genes have been well characterized. One of the most extensively studied genetic switch in yeast is that of the *GAL* (Galactose network) genes. In the absence of glucose in the environment, *S. cerevisiae* can use galactose as the carbon and energy source through Leloir pathway. The regulatory network that controls the Leloir pathway enzymes is called *GAL* system (or *GAL* switch).[2] The molecular interactions inherent in the *GAL* system have been established through experiments in molecular biology. Over the past decade, numerous mathematical models have been proposed to explain the system behaviour of the *GAL* genetic switch.[3]

In our work we aim to further understand the GAL network dynamic behaviour and explain network memory by using a deterministic approach. In order to

model the network behaviour we aim to establish the most important parameters experimentally which are namely binding constants of the interacting regulatory proteins and their decay rates using mass spectrometry.

1.1 Galactose network in *Saccharomyces cerevisiae*

The galactose network (*GAL)* gene family in *S. cerevisiae* consists of three regulatory (*GAL4, GAL80,* and *GAL3*) and five structural genes (*GAL1, GAL2, GAL7, GAL10,* and *MEL1*), which enables it to use galactose as the carbon source.[4] The structural genes *GAL1, GAL7,* and *GAL10* are clustered but separately transcribed from individual promoters. However, structural genes *GAL2* and *MEL1* lie on different chromosomes. The regulatory gene *GAL4* encodes a transcriptional activator Gal4p that binds to the upstream activation sequences (UASG) of *GAL* genes as a homodimer and activates the transcription of the genes.[5 6 7] The *GAL* genes account for the binding of dimer Gal4p to genes with one binding site (*MEL1, GAL3*, and *GAL80*) and genes with multiple binding sites (*GAL1, GAL2, GAL7*, and *GAL10*). Among these, *GAL2* has three, *GAL7* has two binding sites, genes *GAL1* and *GAL10* share four binding sites and are transcribed in opposite directions. The repressor protein, Gal80p, self-associates to form a dimer and subsequently binds to the gene–Gal4p dimer complex and prevents it from recruiting RNA polymerase II mediator complex, thereby preventing the activation of *GAL* genes.[8 9 10 11] Gal3p is a signal transducer that interacts with Gal80p in response to galactose. Galactokinase encoded by *GAL1*, the first enzyme of the galactose catabolic pathway, is bifunctional and also has Gal3p signal transduction activity, albeit with a weak response.[12 13] This is a direct consequence of gene duplication that is known to have occurred in its evolutionary history.[2]

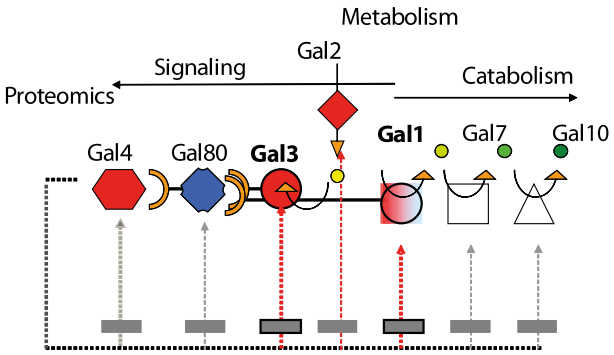

Figure 1.1 Galactose network (Courtesy of Becskei, Attila. 2013). Import of galactose into the cell by Gal2p activates the signaling cascade and the catabolism. Galactose activates Gal3p and Gal1p. They form a complex with Gal80p freeing Gal4p to induce expression of the GAL genes.

1.2 Summary of the *GAL* switch

In the presence of inducer, galactose and adenosine triphosphate (ATP), Gal3p is activated to form a complex with Gal80p in the cytoplasm. This leads to shuttling of Gal80p from the nucleus to the cytoplasm, thereby reducing the availability of Gal80p for binding with Gal4p in the nucleus.[14] Thus, galactose relieves the repression through nucleocytoplasmic shuttling of Gal80p. Once the switch is turned on, the product of the gene *GAL2* (permease Gal2p) mediates transport of galactose into the cells, which further activates Gal3p/Gal1p (*Figure 1.1*). *GAL* system consists of three feedback loops, a positive activation of galactose uptake by Gal2p, an upregulation of the inducer Gal3p/Gal1p to sense intracellular galactose, and a negative feedback caused by upregulation of the repressor Gal80p.

1.2.1 Glucose repression

Glucose is the most abundant and preferred source of carbon and energy. Microorganisms in particular have evolved complex genetic regulatory mechanisms to shut off the expression of proteins required for the metabolic pathways that are unnecessary when glucose is used as the source of carbon and energy. Negative regulation by glucose probably allows microorganisms to sustain with the minimum metabolic machinery required to propagate itself. This phenomenon is referred to as carbon catabolite repression or simply glucose repression.

In yeast, glucose repression is exerted at multiple levels such as transcription, protein and/or mRNA stability, translation post-translational modification, etc. In the presence of glucose (inhibitor media), the synthesis of Gal4p is inhibited through Mig1p-mediated repression of *GAL* genes.[15] Among these, *GAL80, GAL7*, and *GAL2* are indirectly repressed through Mig1p-dependent repression of Gal4p, whereas *GAL1, GAL10, GAL4, GAL3*, and *MEL1* are directly repressed by Mig1p in addition to the indirect repression. In a non-inducing and non-repressing medium (NINR, such as raffinose), Gal80p is bound to the DNA–Gal4p dimer complex in the nucleus and maintains the switch in a repressed state. With respect to *GAL* switch glucose inhibition occurs at three levels. One, at the level of galactose transport by reducing the availability of Gal2p, where both *GAL2* transcription is down regulated and GAL2p decay rate is increased by glucose dependent ubiquitination.[2] Second, by reducing the level of the signal transducer, which is at the level of *GAL3/GAL1* and third by far the most dominant mechanism is repressing the transcription of *GAL4* via Mig1p.

1.3 Hysteresis memory

Although the existence of multiple stable phenotypes of living organisms enables random switching between phenotypes as well as non-random history dependent switching called hysteresis, only random switching has been considered in prior experimental and theoretical models of adaptation to variable environments. Adaptation of organisms to time-varying and often uncertain environments is a classical problem in evolutionary biology. Existence of multiple phenotypes and random switching between them establishes phenotypic diversity within the population and has been suggested as a form of bet-hedging strategy that increases the chances of survival and growth rates of the total population.[16] Phenotypic multi-stability in biological systems is related with persistent memory of history called hysteresis. The term "hysteresis" seems to have been coined by James Alfred Ewing[17] in connection with the ability of some magnetic materials to retain their magnetization state long after the magnetizing magnetic field has been removed. Today it is used much more broadly to

refer to any memory based relationship between an input and state of a system that does not depend on the rate at which the input varies in time.[18] The most basic, yet non-trivial, hysteresis is exemplified by a bi-stable relay in Figure 1.2, where the current state of the relay is determined not only by the external input, but also by the previous relay state. The key characteristic of the bi-stable relay hysteresis is the threshold separation, which is the difference between the values of the external input at which the state switches.

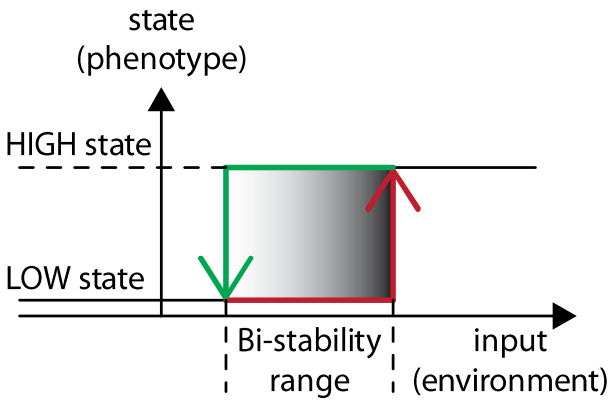

Figure 1.2: When the state is high, the relay switches to low state at the lower input threshold, while starting from low state the relay switches to high state at an upper threshold. Thus, as long as the current input is within the bi-stability range (i.e. between the thresholds), the relay remembers whether the input has entered this range from below or from above.

1.4 Long term adaptation of *GAL* network

One of the examples of a bi-stable relay hysteresis in biological systems is the history dependent behaviour of the *GAL network* studied in *Saccharomyces cerevisiae* yeast. *GAL network* can be viewed as a collection of genes associated with transport and metabolism of galactose. Acar and Becskei[22] along with prior work of others, demonstrated that two phenotypes each associated with "on" and "off" state of the *GAL network* expression can be obtained from the same culture of genetically identical yeast. The fraction of each corresponding sub-population depended on the history of the exposure to the inducer. The GAL network was induced (switched on) when the extracellular inducer concentration (input, galactose) exceeded an upper threshold. The network was switched off when the inducer concentration fell below the lower threshold. Both phenotypes remain

stable through multiple generations of the yeast culture after the extracellular concentration of the inducer is reduced to lower levels, but not removed completely.

Complex networks constituting positive feedbacks can store cellular memory by creating two or more stable states.[19 20] Bistability by simple feedback loops in synthetic circuits is well understood.[21] However, naturally occurring networks that possess multiple feedback loops, are much more complicated when making an analysis of system's dynamics.[22] One of the examples of these naturally occurring networks is the *GAL*, galactose signalling pathway in the yeast *Saccharomyces cerevisiae*.

The *GAL* system has three positive feedback loops mediated by synthesis of Gal1p, Gal3p and Gal2p and a negative feedback effect achieved by synthesis of Gal80p. These feedbacks prevent the reversion of established phenotypes in the presence of fluctuations in the environment. Experiments indicate that the positive feedback effect through Gal3p or Gal1p positive feedback is necessary to reliably store long term memory on previous galactose expressions over hundreds of generations.[22 67] However, the negative feedback effect via Gal80p competes with the positive feedback effect of Gal3p to reduce memory storage.[22] Thus, the *GAL* system presents two stable expression states depending on previous exposure to galactose or raffinose media (*Figure 1.3*).

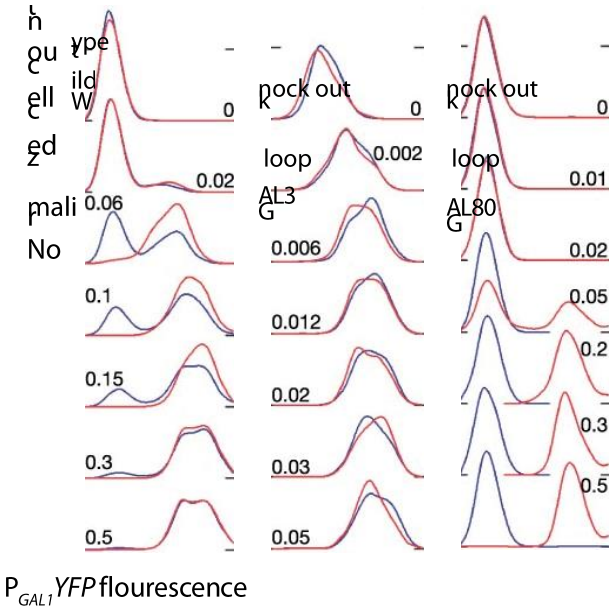

Figure 1.3: Blue distributions represent cells that were initially grown in 2% raffinose and red distributions represent the cells that were initially grown in 2% galactose for 12 hours. After this 12 hours cells were grown for 27 h in a galactose gradient (Figure taken from Acar M, Becskei A, van Oudenaarden A. Nature 2005. [22]).

1.5 *GAL* network signalling layers

The GAL network constitutes a four layer signalling cascade. In the uppermost layer there is Gal2p, which imports extracellular galactose into the cell (purple layer *Figure 1.4*). Subsequently, intracellular galactose binds to Gal3p and Gal1p to activate them. At this stage (third or green layer in *Figure 1.4*) Gal3p and Gal1p sequesters Gal80p from Gal4p. Gal1p and Gal3p binds to Gal80p in the cytoplasm, depleting Gal80p from the nucleus. The transcriptional activator Gal4p (first or orange layer in *Figure 1.4*), which is constitutively bound to promoters of the *GAL* genes, is then released from the inhibitory action of Gal80p (second or blue layer in *Figure 1.4*) and induces the transcription of *GAL* network genes, including *GAL1*, *GAL2*, *GAL3* and *GAL80*. Since Gal1p, Gal2p, and Gal3p induces transcriptional activity in GAL genes they constitute the three positive feedback loops. The opposite effect happens when there is an increase in Gal80p where the GAL gene expression is repressed. Hence, Gal80p creates the negative feedback loop.

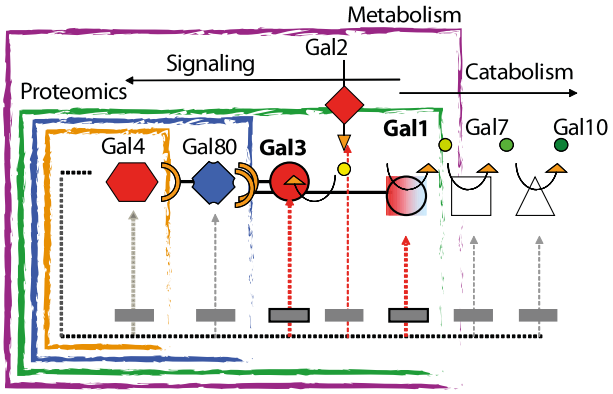

Figure 1.4: GAL network signalling layers. Import of galactose into the cell by Gal2p activates the signalling cascade and the catabolism. Galactose induce the sequestration of Gal80p by forming a complex with Gal80p enabling Gal4p to activate the expression of the GAL genes.

When you have a relatively big network like *GAL*, one needs to establish most of the parameters individually. For this purpose, we isolate different layers of galactose regulatory interactions (*Figure 1.4*) and measure the previously unpublished *in vivo* values. We use mass spectrometry in order to measure the absolute protein concentrations and decay rates. Which then we use to fit the dissociation constants of the regulatory proteins that form the feedback loops using the response of mRNA of the regulated genes to calculate the interactions between regulatory proteins regulate the feedback loops in the galactose network which are governed by four major complexes exist (Gal4p-DNA, Gal4p-Gal80p, Gal1p-Gal80p, and Gal3p-Gal80p).

Evidently, GAL network's actual behaviour arises from the complex interplay of feedback architecture with microscopic biochemical parameters. However, in order to understand this interplay it seems we must first comprehensively characterize a vast number of relevant parameters – species concentrations, reaction rates, binding constants, and so on. This expanse of biochemical detail presents a fundamental barrier to developing a predictive, experimentally falsifiable description of *GAL* network. In order to overcome this barrier we determine the needed details with quantitative proteomics using mass spectrometry selected reaction monitoring.

1.6 Quantitative proteomics

The objective of some proteomics experiments is simply to identify the proteins that are found in a given sample, and this form of analysis is quite descriptive. Once identified, the accurate quantitation of proteins is a vital aspect of proteomics. There are several well-established methods for the quantitation of individual proteins, either in solution or using a solid-phase assay.

The quantity of an individual protein can be detected using Immunoassays in which specific antibodies are used as labelled probes. The western blot or immunoblot is a convenient way to compare the abundances of proteins. In this technique, proteins separated by gel electrophoresis, with different samples represented in different lanes. The antibody may be conjugated on its own radioactive, fluorescent, or enzymatic label which provides a direct detection or a secondary antibody may be used that recognizes the primary antibody and therefore amplifies the signal (indirect detection). This allows very small amounts of protein to be detected. The accurate quantitation of individual proteins in solution can be achieved using a solid-phase immunoassay in which a capture antibody specific for the target protein is immobilized on a polymeric sheet. The adaptation of such assays for proteomic analysis is difficult because even if antibodies could be found to bind to every protein in the proteome, the signal intensity for each antigen-antibody interaction would depend not only on the abundance of the target protein but also on the strength of the antigen–antibody binding.

There are several methods for determining the total concentration of proteins in solution, each of which exploits properties that are general to all proteins. One widely used method is the measurement of UV (ultraviolet) absorbance. This is a non-destructive method, allowing the proteins to be recovered for further analysis. Therefore, it is used not only for quantitation but also to detect protein and peptide fractions eluting from HPLC columns. The UV light is absorbed by aromatic amino acid residues (tyrosine and tryptophan) as well as by peptide bonds. Other protein assay methods are colorimetric or fluorometric and are

based on covalent or noncovalent dye binding or chemical reactions. The Bradford assay measures the degree of binding to Coomassie Brilliant Blue dye. The Lowry assay and the related BCA (bicinchoninic acid) assay are based on the reduction of copper ions in the presence of proteins, resulting in the chelation of a colourless substrate and the production of a coloured complex that can be detected using a spectrophotometer. Most of the methods that we describe are both destructive such as radioactive labelling and immunoassays or are general to all proteins such as absorbance using different assays. However, it is necessary to compare the abundances of thousands of proteins in parallel across multiple samples in typical proteomics experiments. One of the most commonly used and precise ways is based on comparing the abundance of ions across samples by mass spectrometry.

Systems biology require the detection and quantification of large numbers of analytes. Proteomic studies are commonly performed using a shotgun approach, in which the sample proteins are enzymatically degraded to peptides, which are then analysed by mass spectrometry (MS).[23] Selected reaction monitoring (SRM) has improved upon shotgun proteomic approaches. SRM exploits the unique capabilities of triple quadrupole (QQQ) MS for quantitative analysis. In SRM, the first and the third quadrupoles act as filters to specifically select predefined *m/z* values corresponding to the peptide ion and a specific fragment ion of the peptide, whereas the second quadrupole serves as collision cell (Figure 1.5).

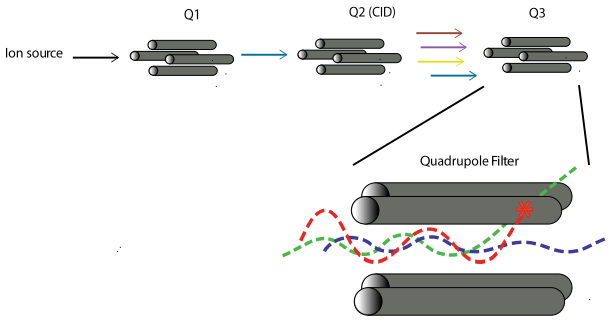

Figure 1.5: Triple quads contain 3 quadrupoles in series that are programed to selectively stabilize your ion of interest. Quadrupoles act as a mass filter. The DC and RF voltages are tuned to stabilize particular m/z ranges.

Several such transitions (precursor/fragment ion pairs) are monitored over time, yielding a set of chromatographic traces with the retention time and signal intensity for a specific transition as coordinates. The two levels of mass selection with narrow mass windows result in a high selectivity, as co-eluting background ions are filtered out very effectively (Figure 1.6).[24]

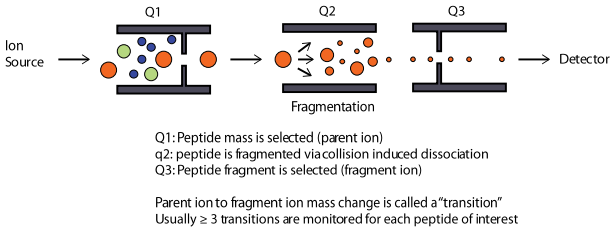

Figure 1.6: Schematic depiction of triple quads contain 3 quadrupoles in series that are programed to selectively stabilize your ion of interest.

Unlike in other MS-based proteomic techniques, full mass spectra are not recorded in QQQ-based SRM. The selective nature of this mode translates into an increased sensitivity three orders of magnitude compared with conventional techniques.[25] In addition, it results in a linear response over a wide dynamic range up to six orders of magnitude. This enables the detection of low-abundance proteins in highly complex mixtures. Absolute quantification using SRM (selected reaction monitoring) is solemnly dependent on the ratio between selected standard heavy peptides and their endogenous counterparts (Figure 1.7).[26]

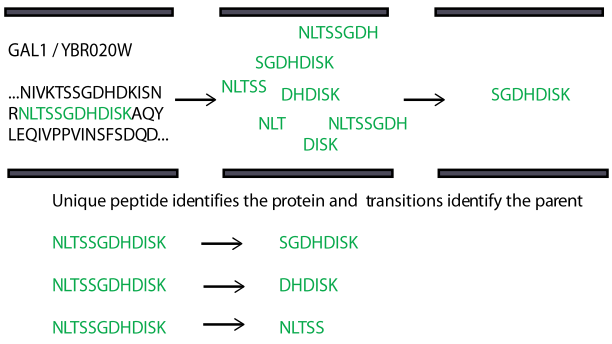

Figure 1.7: Schematic depiction of peptide selection and fragmentation in triple quads system.

1.7 Detection of bistability and hysteresis in *GAL* network using input output method

One appealing class of systems in which to study this phenomenon is that of *monotone systems with inputs and outputs* motivated by applications in molecular biology modelling. Monotone systems with inputs and outputs constitute a natural generalization of classical (no inputs and outputs) monotone dynamical systems, which are those for which flows preserve a suitable partial ordering on states. Our work is grounded upon the rich and elegant theory of monotone dynamical systems,[67] which provides results on generic convergence to equilibria, and, more generally, on the precise determination of the locations and number of steady states.

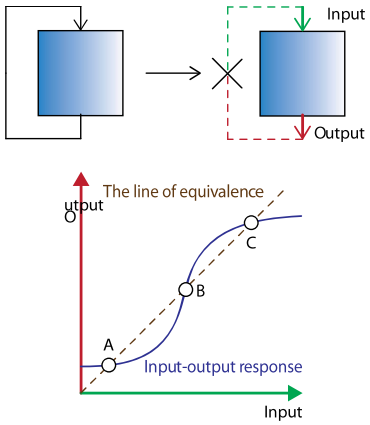

Figure 1.8: Steady-state I/O (input-output) response curve. The blue line represents output as a function of input and the dashed black line represents the line of equivalence. There are three intersection points (A, B, and C), which represent two stable steady states (A and C) and one unstable steady state (B). Figure has been inspired from Angeli, 2003.[67]

The model-independent strategy that is described by Angeli[67] is powerful and broadly applicable: the steady-state response of a feedback system, *if it exists*, will be at one of the self-consistent points where the input-output characteristic intersects the line of equivalence. However the converse is not true: not all these self-consistent intersections represent feedback steady-states. It is theoretically possible to predict stability properties if the system under consideration is monotone, a subtle technical requirement related to the internal structure of the

black box; however, there is no direct method to determine if a given black box is monotone.

Chapter 2 Results

We have determined the in vivo values of decay rate and the binding constants of galactose regulatory proteins layer by layer. When you have a relatively big network like *GAL*, one needs to establish the parameters individually by isolating different parts of the network. Using the feedback splitting, we have determined galactose regulatory interactions and measured the previously unpublished *in vivo* values. We used mass spectrometry in order to measure the absolute protein concentrations and decay rates. Which then we fit the response by measuring the mRNA of the *GAL* genes to calculate the interactions between regulatory proteins that control the *GAL* network. Galactose network feedback loops are governed by four major complexes (Gal4p-DNA, Gal4p-Gal80p, Gal1p-Gal80p, and Gal3p-Gal80p). In order to have a more comprehensive picture of the GAL network dynamic behaviour, we carry our experiments in both galactose and glucose media. Glucose is a key regulators of *GAL* network (see section 1.2.1).

2.1 Measurement of *in Vivo* decay rates of *GAL* regulatory proteins

In this section, we are going to measure the decay rates of GAL regulatory proteins using the total concentrations we measure through targeted mass spectrometry. Efficient regulation of the proteins were achieved through synthetic regulation using a tetOFF system (*Figure 2.8*). Addition of doxycycline stops the expression of the gene whose protein we are interested in (Gal1p, Gal3p, Gal4p, and Gal80p).

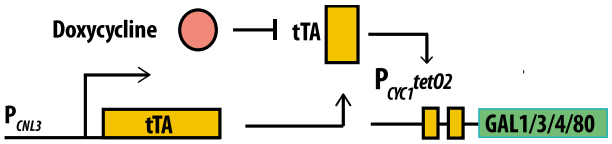

Figure 2.1: Efficient regulation of the proteins were achieved through synthetic regulation using a tetOFF system.

Before measuring the decay rate of GAL regulatory proteins there are two necessary control experiments to be done. First is to measure the sensitivity of the SRM measurements by titrating a fully induced cell with a deletion strain to create a gradient and check the precision during the measurement (Figure 2.2).

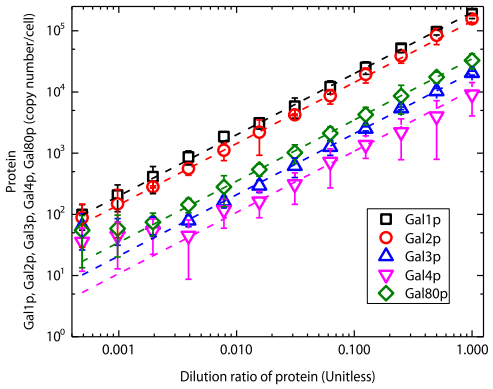

Figure 2.2: Actin normalized dilution series results for Galactose network proteins (protein/cell). Cells have been grown overnight and refreshed in the morning afterwards a dilution series been made with their deletion strains to check the precision of mass spectrometry.

We calculate the protein concentration in the cell pellet by simply measuring the ratio between the peak intensities of our proteins peptide and the labelled heavy peptide. By measuring the number of cells by total weight of the protein we can reach the absolute number of proteins in cell (see section 4.3.1.1-Absolute quantification of protein concentration by targeted LC-MS).

Equation 2.1: $$Protein_{number/cell} = N_{injected\ cell\ number} N_{avogadro} H_{conc} \frac{P_{peak\ area}}{H_{peak\ area}}$$

We can see in the upper figure that the proteomics measurements are reliable until the 150 protein/cell noise level. Secondly, we have considered the fact that translational interference due to a stable remaining mRNA could have an impact on the protein decay rate. We measure the mRNA decay rates of GAL regulatory

genes, where we determined that the decay rate of RNA is quite fast compared to the protein data that we obtained (*Figure 2.3*).

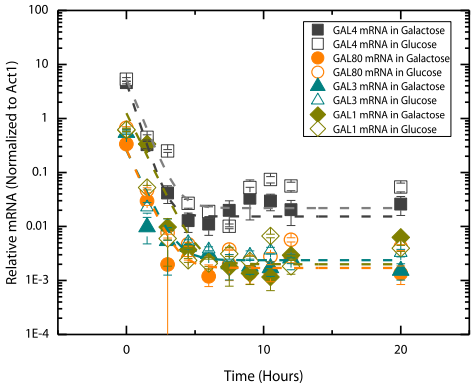

Figure 2.3 GAL mRNA decay over time after addition of 10 µg/µl of doxycycline. Half-life gal4 mRNA: 7.55 min.

After making sure that there is no interference from mRNA and linear range of detection with proteomics is at least 100 fold. We measure the decay rates of GAL regulatory proteins.

We assume that protein is produced at a basal rate of b and is degraded at the rate of ɣ. The production and decay process for the total concentration of protein is simply modelled by the following differential equation,

Equation 2.2: $$\frac{d}{dt}GAL_{PT}(t) = b_{GAL} - \gamma_{GAL}\, GAL_{PT}(t),\ GAL_{PT}(0) = GAL_0.$$

The exact solution of system (*Figure 2.4*) is given by the following function of time,

Equation 2.3: $$GAL_{PT}(t) = Y_0 + A\, e^{R_0 t},$$

Where,

Equation 2.4: $$R_0 = -\gamma_{GAL},\ A = GAL_0 - \frac{b_{GAL}}{\gamma_{GAL}},\ Y_0 = \frac{b_{GAL}}{\gamma_{GAL}}.$$

In what follows, we perform the nonlinear regression using Equation 2.3 and estimate the parameter values given in equation Equation 2.4.

Remark 1: In using the nonlinear regression, we will always use the relative weighting (weighting by $\frac{1}{Y^2}$) in our entire data analysis.

Remark 2: In the decay experiments the initial OD 600 was 0.4. We have diluted the samples every 1.5 hours (during sample taking) keeping the cell concentration lower than OD600=1 over the course of the whole experiment making sure the cells were in exponential growing conditions (see Figure 4.25 in section 4.3.1.2.1-Using GFP fluorescent protein and measuring growth during decay experiments).

2.1.1 Gal4p decay measurement

In this section, we are going to measure the decay rate of the total concentration of Gal4 protein. Efficient regulation of the key transcription factor Gal4p is reached by promoter replacement with tetOFF system. Addition of doxycycline stops the expression of the transcriptional activator (Gal4p).

The concentration of total Gal4p in galactose and glucose media for different times is given in *Table 2.1*.

Table 2.1: The total concentration of Gal4 protein in galactose and glucose media.

Gal4p decay in Galactose			**Gal4p decay in Glucose**		
Time (Hours)	Gal4p (nM)	SD (nM)	Time (Hours)	Gal4p (nM)	SD (nM)
0	42.36	11.81	0	50.25	9.27
1.5	23.04	7.77	1.5	26.06	5.03
3	11.20	5.33	3	12.84	1.44
4.5	6.00	2.69	4.5	6.20	1.72
6	3.75	1.08	6	3.26	1.42
7.5	1.76	0.47	7.5	2.05	0.31
9	1.95	2.49	9	2.12	1.61
10.5	2.17	0.48	10.5	1.97	1.80
12	2.55	1.65	12	2.13	1.32
20	1.81	0.29	24	2.13	1.68

Equation 2.3 is now used to find the estimates for the decay rate of Gal4p (Equation 2.4). Results of nonlinear regression are illustrated in *Figure 2.4*.

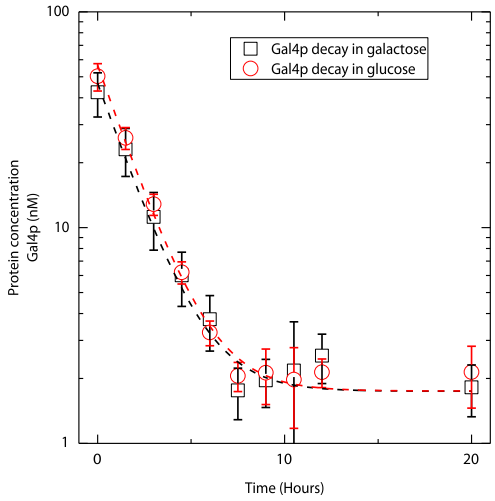

Figure 2.4: Gal4p decay in galactose and glucose media. Expression has been stopped with 10 µg/µl of doxycycline then samples have been taken every 1.5 hours. Decay measurements of the Gal4p (black squares) in 0.5% galactose and in 0.2% glucose (red circles). The expression of GAL4 gene was shut off at t=0 hours.

The parameter estimates with the corresponding standard errors and confidence intervals are given in .

Table 2.2.

Table 2.2 Parameter estimates for Gal4p decay in galactose and glucose media. Expression has been stopped with 10 µg/µl of doxycycline then samples have been taken every 1.5 hours.

Galactose		Glucose	
ϑGal80p	0.501	ϑGal80p	0.460
SE $_{\vartheta Gal80p}$	0.017	SE $_{\vartheta Gal80p}$	0.013

For the lower concentrations of Gal4p in galactose medium, the data points are a bit scattered around the curve. However, the parameter estimates and the corresponding errors suggest that the results of data fitting are good and reliable. For the data values in glucose, at lower concentrations, data points are more deviated from the fit and the errors are higher compared to galactose medium.

This can be explain by the fact that we are getting closer to the detection limits of MS/MS.

2.1.2 Gal80p decay measurement

In this section, we are going to investigate the decay process of the total concentration of Gal80 protein. Like previous section, the efficient regulation of Gal80p is reached by synthetic regulation. Addition of doxycycline stops the expression of the transcriptional repressor (Gal80p) and permits us to determine its decay rate. The concentration of total Gal80p in galactose and glucose media for different times is given in

Table 2.3.

Table 2.3: The total concentration of Gal80 protein in galactose and glucose media.

Gal80p decay in Galactose			Gal80p decay in Glucose		
Time (Hours)	Gal80p (nM)	SD (nM)	Time (Hours)	Gal80p (nM)	SD (nM)
0	1254.47	151.04	0	1378.81	283.84
1.5	739.21	55.96	1.5	676.45	28.99
3	398.84	3.28	3	363.07	16.57
4.5	208.91	45.06	4.5	156.86	27.11
6	149.04	6.19	6	84.04	18.80
7.5	70.45	9.83	7.5	44.20	16.08
9	52.24	10.60	9	32.06	10.41
10.5	58.91	9.64	10.5	53.37	13.46
12	57.35	5.63	12	57.95	16.23

Equation 2.3 is now used to find the estimates for the parameters of system (Equation 2.2). Results of nonlinear regression are illustrated in *Figure 2.5*.

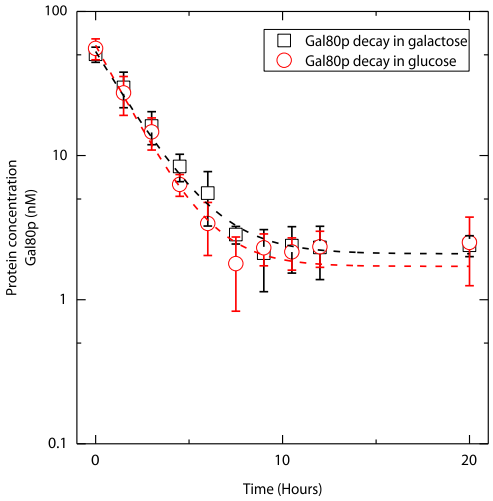

Figure 2.5: Gal80p decay in galactose and glucose media. Expression has been stopped with 10 µg/µl of doxycycline then samples have been taken every 1.5 hours. Decay measurements of the Gal80p (black squares) in 0.5% galactose and in 0.2% glucose (red circles). The expression of GAL4 gene was shut off at t=0 hours.

The parameter estimates with the corresponding standard errors and confidence intervals are given in *Table 2.4*.

Table 2.4 Parameter estimates for Gal80p decay in galactose and glucose media. Expression has been stopped with 10 µg/µl of doxycycline then samples have been taken every 1.5 hours.

Galactose		Glucose	
ϑGal80p	0.461	ϑGal80p	0.503
SE $_{\vartheta Gal80p}$	0.017	SE $_{\vartheta Gal80p}$	0.013

2.1.3 Gal3p decay measurement

In this section, we measure the decay rate of Gal3 protein. Efficient regulation of the key transcription factor Gal3p is reached by synthetic Tet-OFF system (Figure 2.1). Addition of doxycycline stops the expression of the transcriptional repressor (Gal80p) and permits us to determine its decay rate. The concentration of total Gal3p in galactose and glucose media for different times is given in *Table 2.5*.

Table 2.5: The total concentration of Gal3 protein in galactose and glucose media.

Time	Galactose	Glucose
0	524.9	665.7
1.5	358.4	354.5
3	213.7	197.9
4.5	114.1	111.1
6	75.7	79.4
7.5	37.2	39.6
9	22.4	17.1
10.5	11.4	8.1
13	5.3	4.4
20	4.9	3.2

Equation 2.3 is now used to find the estimates for the parameters of system. Results of nonlinear regression are illustrated in *Figure 2.6*.

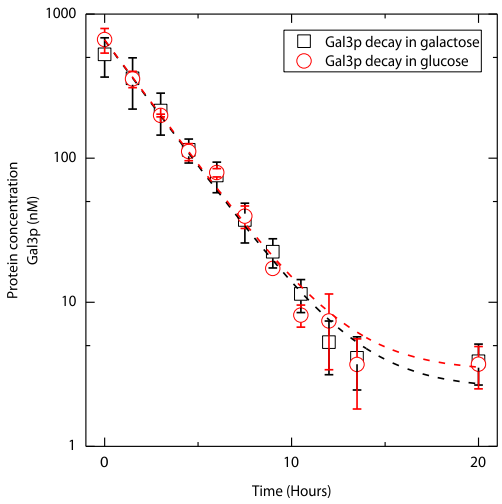

Figure 2.6: Gal3p decay in galactose and glucose media. The expression of GAL3 gene was shut off at t=0 hours. Expression has been stopped with 10 µg/µl of doxycycline. Samples have been taken every 1.5 hours. Decay measurements of the Gal4p (black squares) in 0.5% galactose and in 0.2% glucose (red circles).

The parameter estimates with the corresponding standard errors and confidence intervals are given in *Table 2.6*.

Table 2.6 Parameter estimates for Parameter estimates for Gal4p decay in galactose and glucose media. Expression has been stopped with 10 µg/µl of doxycycline then samples have been taken every 1.5 hours.

Galactose		Glucose	
ϑ_{Gal1p}	0.446	ϑ_{Gal1p}	0.528
SE ϑ_{Gal1p}	0.011	SE ϑ_{Gal1p}	0.014

2.1.4 Gal1p decay measurement

In this section, we measure the decay rate of Gal1 protein. Efficient regulation of the key transcription factor Gal1p is reached by synthetic Tet-OFF system. Addition of doxycycline stops the expression of the signal transductor (Gal1p) and permits us to determine its decay rate.

Table 2.7: The total concentration of Gal1 protein in galactose and glucose media.

Time	Galactose	Glucose
0	3863.0	3641.5
1.5	3127.2	2050.5
3	1655.6	1426.7
4.5	919.8	844.3
6	551.9	584.6
7.5	367.9	357.8
9	184.0	161.1
10.5	90.2	120.2
13	51.7	79.8
20	42.9	32.9

Equation 2.3 is now used to find the estimates for the parameters of system (*Figure 2.7*).

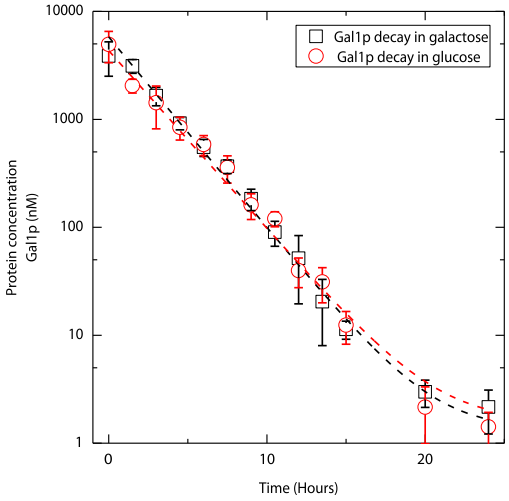

Figure 2.7: Gal1p decay in galactose and glucose media. Expression has been stopped with 10 µg/µl of doxycycline then samples have been taken every 1.5 hours. Decay measurements of the Gal1p (black squares) in 0.5% galactose and in 0.2% glucose (red circles). The expression of GAL1 gene was shut off at t=0 hours.

The parameter estimates with the corresponding standard errors and confidence intervals are given in *Table 2.8*.

Table 2.8 Parameter estimates for Parameter estimates for Gal4p decay in galactose and glucose media. Expression has been stopped with 10 µg/µl of doxycycline then samples have been taken every 1.5 hours.

Galactose		Glucose	
ϑ_{Gal1p}	0.425	ϑ_{Gal1p}	0.515
SE $_{\vartheta Gal1p}$	0.013	SE $_{\vartheta Gal1p}$	0.018

2.1.5 Conclusion

Having established a synthetic control on transcription of *GAL* genes and a method to precisely measure absolute protein concentration, we looked at the effect of media on protein degradation and profiled *in vivo* protein turnover in the presence of the carbon source galactose and glucose. Growth in galactose causes a significant change in the metabolic profile of yeast, resulting in an increase in their doubling time from ~1.5 to 2 hours. [27] However, the overall distribution of half-lives measured in this condition was similar to the turnover profile generated for yeast grown in glucose, with an average half-life of 1.5 to 2 hours.

Thus, glucose dependent ubiquitination of Gal2p is the single example of change in GAL regulatory protein decay rate. RNA decay does not interfere with our measurements since it has a much faster decay rate than proteins.[28]

2.2 Determination of *in vivo* dissociation constants of *GAL* regulatory proteins

GAL network's dynamic behaviour arises from the complex interplay of feedback architecture with microscopic biochemical parameters. However, in order to understand this interplay it seems we must first comprehensively characterize a vast number of relevant parameters – one of the most important being the protein binding constants.

When fitting the binding constants of the regulatory *GAL* proteins we can use the decay data. Samples we obtain from our decay experiments, described in the previous section (2.1-Measurement of *in Vivo* decay rates of *GAL* regulatory proteins), gives a concentration gradient of *GAL* proteins. This enables us to use the same data to fit the binding constants of the regulatory proteins. By this way we hit two birds with one stone.

We determine the binding coefficients by fitting a function where the absolute number of the regulatory proteins control *GAL* gene's transcription levels. In other words, we measure the response of the network by using the transcription levels of GAL genes which is controlled by the gradient of the regulatory protein. We already know that the mRNA decay is much faster than protein which means they reach steady state levels instantly relative to proteins.

We use three genes with different binding sites to measure the response to the regulatory protein concentration change. Using genes with different binding properties enables us to get a better fit and provides a better information about cooperative binding of the proteins. We choose genes that are present consistently in every one of our constructs to protect the symmetry of our work. We use GCY1 which is a GAL4 induced Glycerol dehydrogenase; involved in an alterna-

tive pathway for glycerol catabolism used under micro aerobic. GCY1 is similar to GAL3 is controlled by GAL4 and has a single binding site. Another gene we use is the GAL7, Galactose-1-phosphate uridyl transferase; synthesizes glucose-1-phosphate and UDP-galactose from UDP-D-glucose and alpha-D-galactose-1-phosphate in the second step of galactose catabolism. One of the main reasons we use GAL7 is that it has a good dynamic range and is present in all of our constructs. The third gene we use is the YFP, Yellow fluorescent protein is a genetic mutant of green fluorescent protein originally derived from the jellyfish Aequorea victoria. In all of our strains, YFP is controlled by a GAL1 promoter. It has three binding sites and it's important along with GAL7 to establish our parameters involved in cooperative binding. Using YFP is also important for the fact that we are using GAL1-YFP mRNA input out system to explain the hysteresis memory in GAL network.

To demonstrate how we use the GAL genes to determine the protein interactions, let's assume that fast decaying *GAL* mRNA is at steady state at that particular time point during our decay measurements. We can fit, for instance, Gal4p protein level and *GAL* mRNA level to find the dissociation constant of Gal4p – DNA with the following formula.

$$\frac{dGAL_{mRNA}}{dt} = \text{basal}_{GALmRNA} - V_{max}\frac{Gal4p}{Gal4p + Kd_{Gal4p-DNA}} - \gamma_{GALmRNA\ decay\ rate}\text{GAL}_{\text{mRNA}}$$

Then for any time point during our experiment the GAL mRNA enables us to fit K_D.

$$GAL_{mRNA} = \frac{basal_{GALmRNA} - V_{max}\frac{Gal4p}{Gal4p + Kd_{Gal4p-DNA}}}{\gamma_{GALmRNA\ decay\ rate}}$$

Likewise we applied this approach to the rest of the regulatory proteins (Gal1p, Gal3p, and Gal80p) in order to measure their decay rates and binding constants to their counterparts. Of course with the addition of each layer (Figure 1.4) our functions become more nonlinear and complicated. This is why we use this layered approach to isolate the parameters and fix in the upper layers. Current efforts are aimed at fitting the data (decay; section 2.1, binding constant; this sec-

tion). Next we are aiming at determining the galactose uptake and its metabolism in order to have a complete overview of the system (section 2.3).

2.2.1 Isolation of *GAL4*: The transcriptional activator Gal4p homodimer binding to DNA

The regulatory gene *GAL4* encodes a transcriptional activator Gal4p that binds to the upstream activation sequences (UASG) of *GAL* genes as a homodimer and activates the transcription of the genes. The *GAL* genes account for the binding of dimer Gal4p to genes with one binding site (*GAL3*, and *GAL80*) and genes with multiple binding sites (*GAL1, GAL2, GAL7*, and *GAL10*).

In the first layer of the *GAL* network, the *GAL80* gene is deleted; as a result, Gal4p can activate the expression of other genes without any repression from Gal80p. It is important for our measurements to determine the dynamic behaviour of Gal4p protein since it is the core transcriptional activator for all the GAL genes and will lay down the foundation for our investigation of upper levels (Figure 1.4). We have replaced the Gal4p endogenous promoter with doxycycline repressible system. Transcriptional control of Gal4p protein with doxycycline enables us to precisely create a gradient where we can measure the response of Gal4p controlled genes. We use targeted mass spectrometry to measure the in vivo Gal4p concentration. By using a *GAL80* deletion strain (ΔGAL80), we omit the negative feedback loop that represses *GAL* gene activation. This basically isolates the Gal4p-DNA interaction and enables us to directly calculate the binding constant of GAL4p to DNA by fitting the concentration of Gal4p with the response of the Gal4p target mRNAs (Figure 2.8).

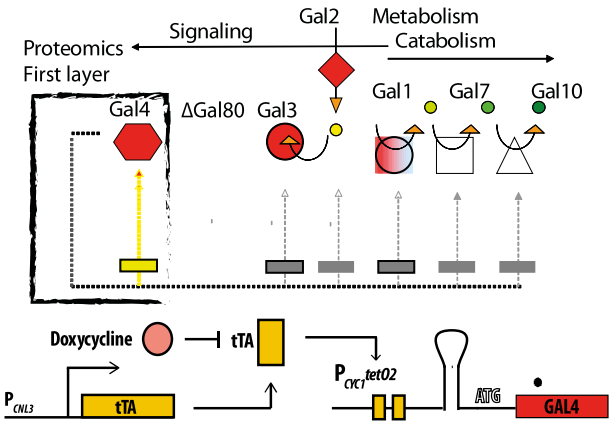

Figure 2.8 GAL network first layer. Control of expression of GAL4 gene. Here we control the Gal4p expression with doxycycline which inhibits the transcription factor, tTA, whose expression is constitutive. Addition of doxycycline stops the expression of the transcriptional activator (Gal4p) and permits us to determine its decay rate. Gal80p feedback loop is deleted to isolate Gal4p and DNA interaction.

Graded expression of Gal4p protein with doxycycline enables us to measure the binding constant of Gal4p to DNA. More specifically we measure the response by using the transcription levels of a target gene which is controlled by given level of Gal4p protein (Figure 2.9).

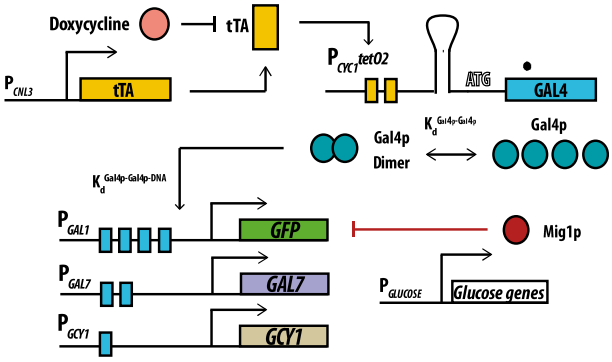

Figure 2.9: Gal network 1st layer protein interaction scheme. Gal4p production is controlled by Tet-OFF synthetic system. Gal4p-Gal4p homodimer binds to GCY1 (galactose inducible glycerol dehydrogenase), GAL7 (Galactose-1-phosphate uridyl transferase), GFP controlled by GAL1 promoter to induce their expression.

We use a set of differential equations for the 1st layer to fit the *GAL7/GCY1/GFP* response (see section 4.4.3). The available biological data expresses the total concentration of proteins; therefore, we need to first express the free protein concentrations with respect to the total concentrations by applying algebraic constrains in our ordinary differential equations. We arrive at the following equations;

$$\frac{dGal4p_{free}}{dt} = \text{basal}_{G4pfree} - 2G4p_{\text{free}}{}^{2} kon_{\text{G4pG4p}} + 2C4p_{complex}\, koff_{\text{G4pG4p}} - {}^{\gamma}{}_{G4pfree}\,\text{G4p}_{\text{free}}$$

$$\frac{dC4p_{complex-homodimer}}{dt} = \text{basal}_{C4pcomplex} - 2C4p_{\text{free}}\, kon_{\text{G4pG4p}} + 2C4p_{complex}\, koff_{\text{G4pG4p}} - {}^{\gamma}{}_{C4pcomplex}\,\text{C4p}_{complex}$$

Where C4 represents [G4:G4] complex. Here, we assume that there is homodimerization. The algebraic constrains are;

$$Gal4p_{total} = Gal4p_{free} + 2\,C4p_{complex-homodimer}$$

We have assumed that Gal4p binds to DNA only as a dimer.[29] It has long been known that Gal4 dimerization is essential for Gal4 function *in vivo* (Keegan et al., 1986). [30] Addition of homodimerization mechanism to the set of equations not only reduces the hill coefficients but also represents a more realistic mechanism for the Gal4p-DNA interaction. (Compare this number with the previous results where there was no homodimerization (section 4.1)). We have switched our equations from hill function to Adair. This not only enabled us to write promoter saturation functions in the 2nd layer where we use incomplete repression but also improved the model according to Akaike's Information Criteria (see section 4.4.3.3.3-Comparing models using Akaike's Information Criterion (AIC)). Following set of ordinary differential equations (ODE) represent the Gal4p homodimerization and GCY1 induction by Gal4p homodimer (for the full set of equations, check section 4.4.3-Gal4p homodimerization and $\text{Gal4p}_{\text{Homodimer}}$-DNA dissociation constant).

$$\frac{d}{dt} G4_{PF}(t) = b_{G4} - 2\, kon_{dim4}\; G4_{PF}(t)^2 + 2\, koff_{dim4}\; C4(t) - \gamma_{G4}\, G4_{PF}(t),$$

$$\frac{d}{dt} C4(t) = \; kon_{dim4}\; G4_{PF}(t)^2 - \; koff_{dim4}\; C4(t) - \gamma_{G4}\, C4(t),$$

$$\frac{dGCY1_{mRNA}}{dt} = \text{basal}_{GCY1mRNA} - V_{max}\,\frac{C4p_{complex}}{C4p_{complex} + Kd_{C4p-DNA}} - {}^{\gamma}{}_{GCY1mRNA}\,\text{GCY1}_{\text{mRNA}}$$

We do a global fit over time where we use the available mRNA data and the total protein concentration data we have from our 1st layer measurements (see section 4.4.3 and *Table 2.1*).

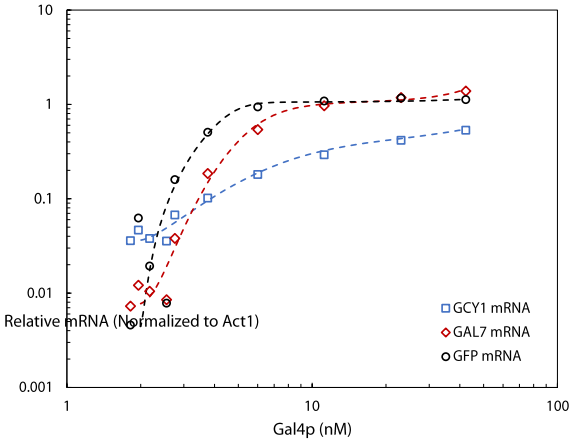

Figure 2.10: Expression levels of the GFP (black circle), GAL7 (red diamonds), GCY1 (blue squares) at different Gal4p concentrations. The measurement was performed in 0.5% galactose. After the differential equation parameter fitting one of the key parameters that we found were: $Kd_{C4\text{-}DNA}$=1.19 nM, $Kd_{Gal4\text{-}Gal4}$=13.90 µM, γ_{Gal4}=0.50 hour^{-1}, Galactose=0.5%. Adair equation has been used for each genes promoter saturation function where enhancement factor for cooperative binding was fit as 35.45.

We have measured the effect of glucose media on Gal4p-DNA binding. Our fitting shows that the effect of glucose is not really visible in 1st layer protein DNA interactions.

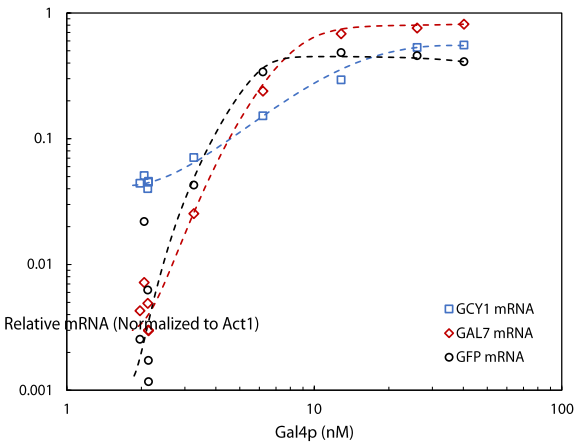

Figure 2.11: Expression levels of the GFP (black circle), GAL7 (red diamonds), GCY1 (blue squares) at different Gal4p concentrations. The measurement was performed in 0.5% galactose+0.2% glucose. After the differential equation parameter fitting one of the key parameters that we found were: $Kd_{C4\text{-}DNA}$=1.33 nM, $Kd_{Gal4\text{-}Gal4}$=16.17 µM, γ_{Gal4}=0.49 hour^{-1}. Adair equation has been used for each genes promoter saturation function where enhancement factor for cooperative binding was fit as 39.45. Another important observation would be the fact that galactose and glucose media does not really affect the Gal4p decay, dimerization and it's binding to DNA.

Table 2.9: Fitted parameters of mRNA response to Gal4p decay in 0.5% Galactose and 0.2% Glucose.

Galactose		Glucose	
$Kd_{GAL4\ homodimerization}$ (μM)	13.90	$Kd_{GAL4\ homodimerization}$ (μM)	16.17
$Kd_{GAL4\text{-}DNA\ binding}$ (nM)	1.19	$Kd_{GAL4\text{-}DNA\ binding}$ (nM)	1.33

We can see in *Table 2.9* that neither the homodimerization not the DNA binding of the Gal4p protein changes due to glucose effect. At this point we can say that the glucose effect is still solemnly on Gal2p.[31]

2.2.2 Isolation of *GAL80*: The repressor Gal80p homodimer forms a tetramer complex with Gal4p homodimer

In the second layer of galactose network we will be focusing on the Gal80p decay and the Gal4p-Gal80p binding (*Figure 2.12*). To determine the affinity of the Gal4p–Gal80p interaction, we engineered a double deletion strain (see section 4.1) where we deleted two signal transductors (Gal1p and Gal3p) that sequesters Gal80p from the nucleus to the cytoplasm. GAL80 is a transcriptional regulator involved in the repression of GAL genes; involved in the repression of GAL genes in the absence of galactose; inhibits transcriptional activation by Gal4p; inhibition relieved by Gal3p or Gal1p binding. Transcriptional control of Gal80p protein was achieved with doxycycline. We use targeted mass spectrometry to measure the in vivo Gal80p concentration. We use a ΔGAL1ΔGAL3 strain where we delete the main two feedback loops upper in the galactose regulatory layer. This basically isolates the Gal4p-Gal80p interaction and enables us to directly calculate the binding constant of GAL80p to Gal4p by fitting the concentrations of Gal80p, Gal4p with the response of the *GAL* network mRNAs.

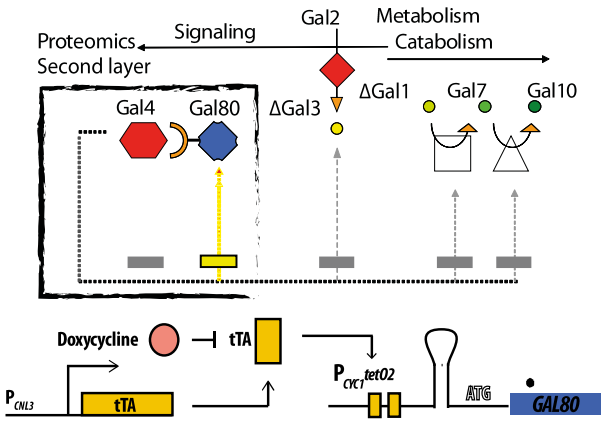

Figure 2.12 Control of expression in target genes. Here we control the Gal80p expression with doxycycline which inhibits the transcription factor, tTA, whose expression is constitutive. Addition of doxycycline stops the expression of the transcriptional repressor (Gal80p) and permits us to determine its decay rate. Gal1p and Gal3p feedback loops are deleted to isolate Gal4p and Gal80 interaction.

In this section we will use the decay data available and the corresponding mRNA values to calculate the Gal4p-Gal80p dissociation constant. Since we isolated the interaction of Gal80p with Gal4 by deleting Gal3p and Gal1p sequestration we can use the graded expression of Gal80p protein with doxycycline to fit the binding constant of Gal80p to Gal4p. More specifically we measure the response by using the transcription levels of a target gene which is controlled by given level of Gal80p protein since Gal4p is constant (*Figure 2.8*). We already know the Gal4p DNA binding we can fit our mRNA response to calculate the Gal4 Gal80p homodimerization.

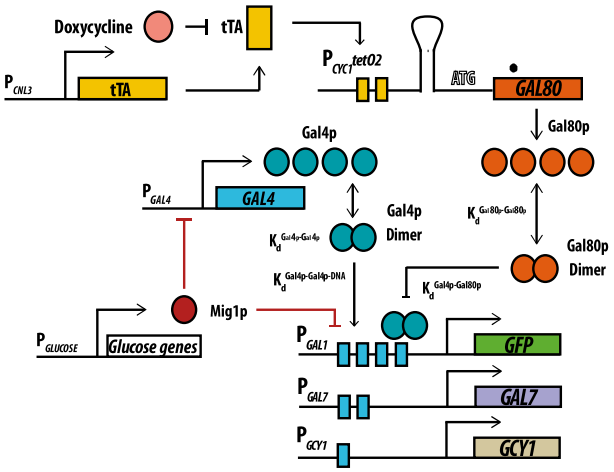

Figure 2.13: Gal network 2nd layer protein interaction scheme. Gal80p production is controlled by Tet-OFF synthetic system. Gal80p homodimer binds to Gal4p homodimer to repress the GCY1 (galactose inducible glycerol dehydrogenase), GAL7 (Galactose-1-phosphate uridyl transferase), GFP controlled by GAL1 promoter expression.

In our model Gal80p-Gal80p homodimer binds to Gal4p-Gal4p homodimer to inhibit transcription. Parameters like Gal4p homodimerization and decay rate from the 1st layer has been fixed. When we are fitting the response of the mRNA we have taken incomplete repression of *GAL7* and GAL1 (Promoters with multiple binding sites) promoters by Gal80p into account.[32] For this, we consider the following promoter configurations.

$$\frac{dGCY1_{mRNA}}{dt} = \text{basal}_{GCY1mRNA} - V_{max}\frac{C4p_{complex}/Kd_{C4p-DNA}}{1 + C4p_{complex}/Kd_{C4p-DNA} + C480p_{complex}/Kd_{C4p-80p-DNA}} - \gamma_{GCY1mRNA}\,\text{GCY1}_{\text{mRNA}}$$

Where C480 represents [G4:G80] complex. Here, we assume that there is homodimerization for both GAL4 and GAL80 and they bind to each other only as dimers forming a quadramer. When we increase the binding sites we need to introduce the incomplete repression by Gal80p which we write it as the factor α as it can be seen in GAL7 promoter function (see also 4.4.4.3.1). For GFP we use a similar approach where we define a different α, and an enhancement factor (see section 4.4.4.3.2).

$$\frac{dGAL7_{mRNA}}{dt} = \text{basal}_{GAL71mRNA} - V_{max}\frac{2b\frac{C4p_{complex}}{Kd_{C4p-DNA}} + c(\frac{C4p_{complex}}{Kd_{C4p-DNA}})^2 + 2\alpha(\frac{C4p_{complex}}{Kd_{C4p-DNA}})^2\frac{C480p_{complex}}{Kd_{C480p-DNA}}}{1 + 2\frac{C4p_{complex}}{Kd_{C4p-DNA}} + c(\frac{C4p_{complex}}{Kd_{C4p-DNA}})^2} - {}^{\gamma}{}_{GAL7mRNA}\,\text{GAL7}_{\text{mRNA}}$$

Where C4 represents [G4:G4] complex, C80 represents [G80:G80] complex and C480 represents [C4:C80] complex. The algebraic constrains are;

$$Gal4p_{total} = Gal4p_{free} + 2\,C4p_{complex-homodimer} + 2\,C480p_{complex-heterodimer}$$

$$Gal80p_{total} = Gal80p_{free} + 2\,C80p_{complex-homodimer} + 2\,C480p_{complex-heterodimer}$$

We write the ODE functions for Gal80p and fit the dissociation constant for Gal4p-Gal80p binding.

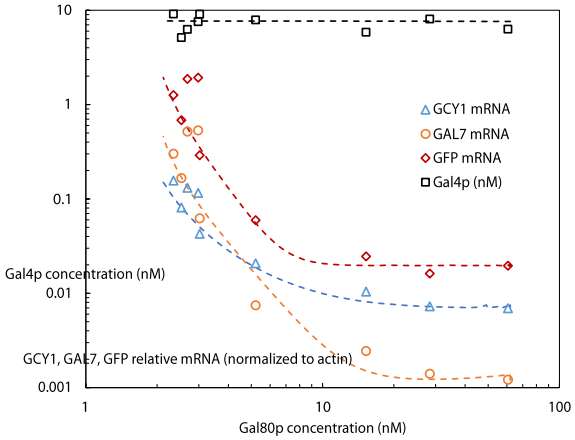

Figure 2.14: Expression levels of the GFP (red diamonds), GAL7 (yellow circles), GCY1 (blue triangles), and Gal4p (black squares) at different Gal80p concentrations. The measurement was performed in 0.5% galactose.

The effects of glucose on galactose network are drastic so we measured if this effect is originated by Gal80p-Gal4p interaction. We have done the same fitting for glucose to see the effect of sugar on the Gal80p-Gal4p dissociation constant. We found that the dissociation constants in both media are quite similar.

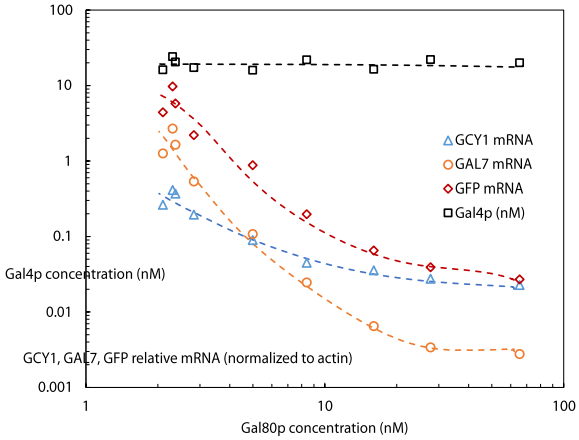

Figure 2.15: Expression levels of the GFP (red diamonds), GAL7 (yellow circles), GCY1 (blue triangles), and Gal4p (black squares) at different Gal80p concentrations. The measurement was performed in 0.5% galactose+0.2% glucose media.

Table 2.10: Fitted parameters of mRNA response to Gal80p decay in 0.5% Galactose and 0.2% Glucose.

Galactose		Glucose	
Kd $_{\text{Gal80p homodimerization}}$ (nM)	39.45	Kd $_{\text{Gal80p homodimerization}}$ (nM)	47.13
Kd $_{\text{Gal80p-Gal4p}}$ (nM)	0.22	Kd $_{\text{Gal80p-Gal4p}}$ (nM)	0.22

We can see in table above that neither the homodimerization nor the Gal4p binding of the Gal80p protein changes due to glucose effect. In our fitting we have also saw that the Gal80p binding to Gal4p is not cooperative (See section 4.4.4.3.3).

2.2.3 Isolation of *GAL3*: The signal transducer Gal3p sequesters Gal80p

Galactose-activated transcription of the *Saccharomyces cerevisiae GAL* genes occurs when Gal3p binds the Gal4p inhibitor, Gal80p. Non-interacting variants of Gal3p or Gal80p render the *GAL* genes non-inducible. GAL80 inhibits the function of GAL4, presumably by direct binding to the GAL4 protein. The presence of galactose triggers the relief of the GAL80 block. The key to this relief is the GAL1 and GAL3 proteins. The long-standing notion has been that a galactose complex formed with GAL1 and GAL3 is the inducer that interacts with GAL80.

In the third layer of our GAL network parameter measurements we determine the Gal3p interaction with Gal80p. GAL3 is a transcriptional regulator; involved in activation of the GAL genes in response to galactose; forms a complex with Gal80p to relieve Gal80p inhibition of Gal4p; binds galactose and ATP but does not have galactokinase activity; like its paralog, GAL1, that arose from the whole genome duplication. As mentioned before (section 2.1) the *GAL* system in *S. cerevisiae* has Gal3p positive feedback loops mediated by Gal3p-Gal80p interaction. Experiments indicate that the positive feedback effect through Gal3p is necessary to reliably store information on previous galactose expressions over hundreds of generations.[3 14]

We use a ΔGAL1ΔGAL2 strain where we delete the main feedback loops by the Gal3p paralog Gal1p and the upper layer Gal2p feedback which we will be dealing with Galactose metabolism and binding section 2.3. By deleting the Gal1p interaction we isolate the Gal3p-Gal80p interaction (Figure 2.16). This enables us to directly calculate the binding constant of GAL3p to Gal80p by fitting the network mRNA response to Gal3p gradient.

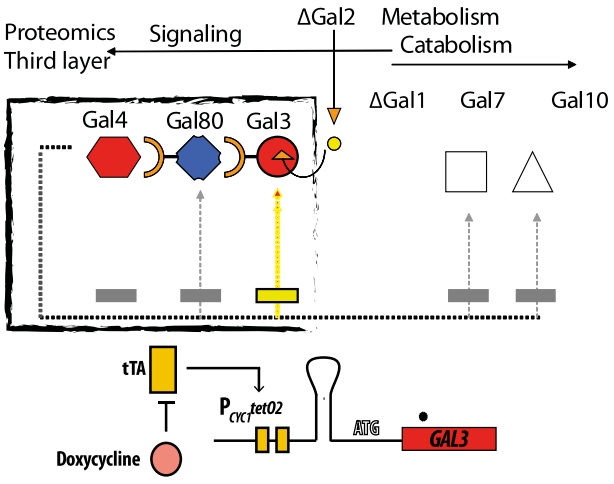

Figure 2.16: Control of expression in target genes. Here we control the Gal3p expression with doxycycline which inhibits the transcription factor, tTA, whose expression is constitutive. Addition of doxycycline stops the expression of the transcriptional activator (Gal3p) and permits us to determine its decay rate. Gal1p and Gal2p feedback loops are deleted to isolate Gal3p and Gal80 interaction.

Galactose-activated transcription of the *Saccharomyces cerevisiae GAL* genes occurs when Gal3 binds the Gal4 inhibitor, Gal80. Non-interacting variants of Gal3 or Gal80 render the *GAL* genes non-inducible. In the absence of galactose

Gal80 binds to Gal4 and prohibits it from activating transcription. In the presence of galactose, Gal3 binds to Gal80 to prohibit its inhibition of Gal4. We measure the strength of Gal3p-Galactose binding by measuring the steady state *GAL* network activation at different galactose concentrations in a Gal3p gradient.

In this section we will use the gradient available for Gal3p concentration and fit the mRNA expression change of the GAL genes to calculate the Gal3p-Gal80p dissociation constant. Since we isolated the interaction of Gal3p with Gal80p by deleting Gal1p which also sequesters Gal80p. More specifically we measure the response by using the transcription levels of GAL genes which is controlled by the interaction of Gal3p, Gal80p, and Gal4p which is constant (*Figure 2.17*). We already calculated the Gal4p-DNA and Gal4p-Gal80p binding from the previous layers. Using the previous layer parameters (see section 2.1, 2.2.1, 2.2.2) we can fit our mRNA response to calculate the Gal3p Gal80p heterodimerization dissociation constant.

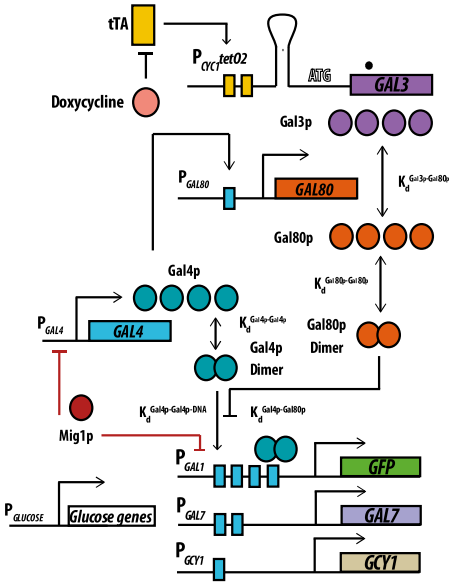

Figure 2.17: GAL network 3rd layer protein interaction scheme. Gal3p production is controlled by Tet-OFF synthetic system. Gal3p sequesters Gal80p to relieve Gal80p homodimer repression on the GCY1 (galactose inducible glycerol dehydrogenase), GAL7 (Galactose-1-phosphate uridyl transferase), GFP controlled by GAL1 promoter transcription.

In our model Gal80p-Gal80p homodimer binds to Gal4p-Gal4p homodimer to inhibit transcription.[1014] Parameters including Gal4p and Gal80 decay rates and

Gal4p-DNA, Gal4p-Gal80 dissociation constants from the 1st layer and 2nd layer have been fixed. We assume that Gal3p monomer binds to Gal80p monomer sequestering the Gal80p homodimer. With increasing Gal3p we reduce the number of Gal80p homodimers. In return this frees the Gal4p homodimers to induce GAL gene expression. Parameters from the first two layers have been fixed so we solemnly fit the Gal3p-Gal80p interaction. When we are fitting the response of the mRNA we have taken incomplete repression of *GAL7* and GAL1 (Promoters with multiple binding sites) promoters by Gal80p into account.[33] We use different levels of Galactose in order to measure the Gal3p-Galactose binding. Our measurements we have confirmed (Figure 2.18) the previous findings by Bhat and Hopper[34] where they have shown that overexpression of Gal3p can activate *GAL* network. We have added the necessary functions to take Gal3p Gal80p galactose independent binding. We use the ODE functions from previous two layers and add the Gal3p components where we consider Gal3p-Galactose binding, Galactose dependent and independent Gal3p-Gal80p binding. For the full set of equations see section (Data fitting, section 4.4.5, page 147).

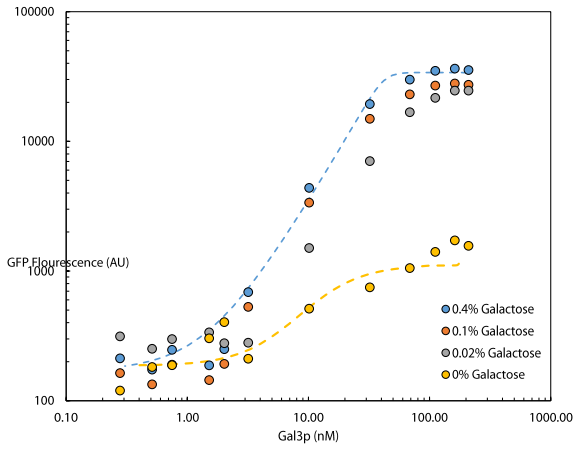

Figure 2.18: Expression levels of the GFP at different Galactose concentration in a Gal1p concentrations. The measurement was performed at steady state after 24 hours of Galactose addition to the media.

Table 2.11: Fitted parameters of mRNA response to Gal3p gradient at different galactose concentrations. The measurement was performed at steady state after 24 hours of Galactose addition to the media.

$Kd_{GAL3\text{-}Galactose\ (Gal3pA)}$ (mM)	15.35
$Kd_{Gal3pA\text{-}Gal80\ with\ galactose}$ (nM)	0.25
$Kd_{Gal3p\text{-}Gal80\ without\ galactose}$ (nM)	12.08

Gal3p binds to Gal80p without galactose with the dissociation constant of 12 nM.

2.2.3.1 Effect of glucose on galactose-dependent interaction of Gal3p and Gal80p

The effects of glucose on galactose network are drastic. We have repeated the previous fitting in glucose media to see the effect of sugar on the Gal80p-Gal3p dissociation constant.

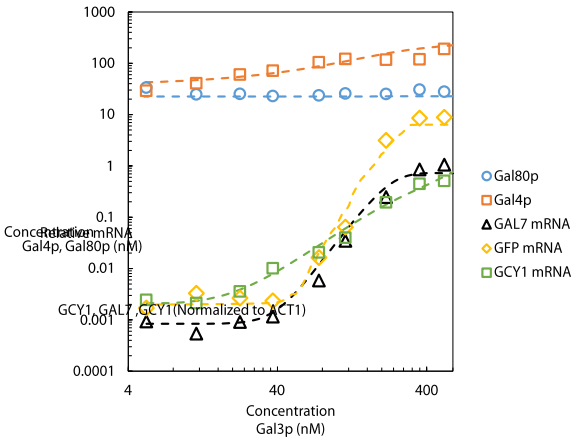

Figure 2.19: Expression levels of the GFP (yellow diamonds), GAL7 (black triangles), GCY1 (green squares), Gal80p (orange squares), and Gal4p (blue circles) at different Gal3p concentrations. The measurement was performed in 0.5% galactose.

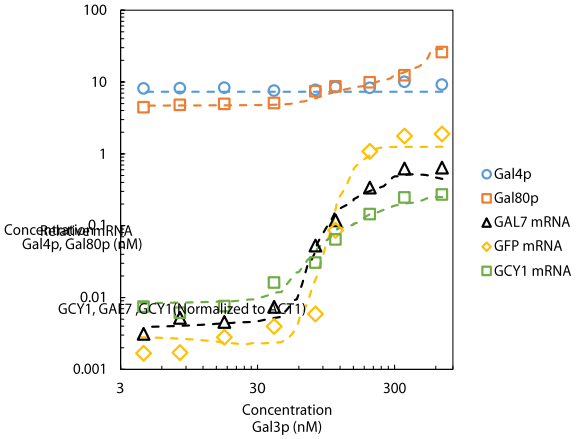

Figure 2.20: Expression levels of the GFP (yellow diamonds), GAL7 (black triangles), GCY1 (green squares), Gal80p (orange squares), and Gal4p (blue circles) at different Gal83p concentrations. The measurement was performed in 0.5% galactose+0.2% glucose.

Table 2.12: Fitted parameters of mRNA response to Gal3p decay in 0.5% Galactose and 0.2% Glucose+0.5%Galactose.

Galactose	Glucose
$Kd_{Gal3a\text{-}Gal80}$=0.26nM	$Kd_{Gal3a\text{-}Gal80}$=0.28nM

We can see in *Table 2.12* that the Gal3p Gal80p interaction is not affected by glucose (see also section 4.4.5). At this point we can say that the glucose effect is still solemnly on Gal2p.[35]

2.2.4 Isolation of *GAL1*: Gal1p is a degenerate signal transducer and sequesters Gal80p

Second part of our 3rd layer parameter measurements we will open the network from GAL1, Galactokinase; which phosphorylates alpha-D-galactose to alpha-D-galactose-1-phosphate in the first step of galactose catabolism; expression regulated by Gal4p; human homolog GALK2 complements yeast null mutant; GAL1 has a paralog, GAL3, that arose from the whole genome duplication. We will be measuring the Gal1p decay and fitting the Gal1p interaction with Gal80p. Galactokinase, *GAL1*, acts as the sole signal transducer in the absence of Gal3p;[36] where Gal4p, the transcriptional activator, is auto regulated;[37] Gal1p is also a nucleocytoplasmic shuttling protein that sequesters Gal80p. Gal80 protein has three binding partners: Gal4p and Gal3p or Gal1p. In the absence of galactose,

Gal80 binds to and inhibits the transcriptional activation domain (AD) of the *GAL* gene activator, Gal4, preventing *GAL* gene expression. Galactose triggers an association between Gal3 and Gal80, relieving Gal80 inhibition of Gal4. We selected for *GAL3* deletion mutants for Gal80p to bind to Gal1p or Gal4p with and without galactose to measure the Gal1p-Galactose dissociation constant.

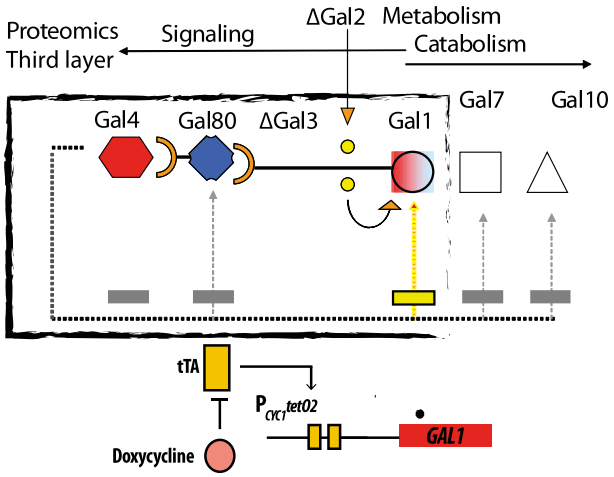

Figure 2.21 Control of expression in target genes. Here we control the Gal4p expression with doxycycline which inhibits the transcription factor, tTA, whose expression is constitutive. Addition of doxycycline stops the expression of the transcriptional activator (Gal4p) and permits us to determine its decay rate.

In this section, the transcriptional control of GAL1 gene with doxycycline enables us to measure the Gal1p decay rate over time. We use targeted mass spectrometry to measure the in vivo Gal1p concentrations over time. We use a ΔGAL2ΔGAL3 strain where we delete the main feedback loop by the Gal1p paralog Gal3p and the upper layer Gal2p feedback which we will be dealing with galactose metabolism and binding 2.3. By deleting the Gal3p positive feedback loop we isolate the Gal1p-Gal80p interaction (*Figure 2.21*). This enables us to directly calculate the binding constant of GAL1p to Gal80p by fitting the network mRNA response to Gal1p gradient.

Overproduction of the GAL1 protein causes constitutive expression of GAL/MEL genes even in the absence of galactose (Figure 2.23). Overproduction of the GAL1 protein (galactokinase) also causes constitutively, consistent with the ob-

servations that GAL1 is strikingly similar in amino acid sequence to GAL3 and has GAL3-like induction activity. A galactose-independent induction by GAL1 is shown in Figure 2.23 where at 0% galactose with over expression we see network activation.

We use the gradient available for Gal1p concentration and fit the mRNA expression change of the GAL genes to calculate the Gal1p-Gal80p dissociation constant. We isolated the interaction of Gal1p with Gal80p by deleting Gal3p which also sequesters Gal80p. More specifically we measure the response by using the transcription levels of GAL genes which is controlled by the interaction of Gal1p, Gal80p, and Gal4p (*Figure 2.17*). We already calculated the Gal4p-DNA and Gal4p-Gal80p binding from the previous layers. Using the previous layer parameters (see section 2.1, 2.2.1, 2.2.2) we can fit our mRNA response to calculate the Gal1p Gal80p heterodimerization dissociation constant.

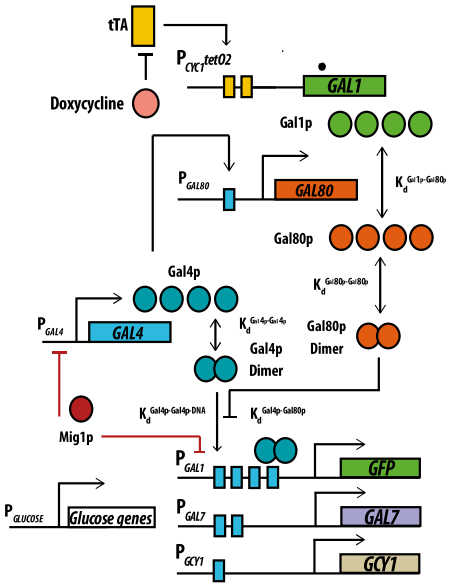

Figure 2.22: GAL network 3nd layer protein interaction scheme. Gal1p production is controlled by Tet-OFF synthetic system. Gal1p sequesters Gal80p to relieve Gal80p homodimer repression on the GCY1 (galactose inducible glycerol dehydrogenase), GAL7 (Galactose-1-phosphate uridyl transferase), GFP controlled by GAL1 promoter transcription.

In our model Gal80p-Gal80p homodimer binds to Gal4p-Gal4p homodimer to inhibit transcription.[1014] Parameters including Gal4p and Gal80 decay rates and Gal4p-DNA, Gal4p-Gal80 dissociation constants from the 1st layer and 2nd layer

have been fixed. In our model Gal1p monomer binds to Gal80p monomer reducing the number of the Gal80p homodimer. With increasing Gal1p we reduce the number of Gal80p homodimers. In return this frees the Gal4p homodimers to induce GAL gene expression. Parameters from the first two layers have been fixed so we solemnly fit the Gal1p-Gal80p interaction. When we are fitting the response of the mRNA we have taken incomplete repression of *GAL7* and GAL1 (Promoters with multiple binding sites) promoters by Gal80p into account.[38] We use high level of Galactose in both media which enables us to assume that the Gal1p molecules are already bound to galactose sugar. The binding of galactose with Gal1p is fitted as well. Our fitting of the data to find the Gal1p Gal80 dissociation constant is quite similar to Gal3p.

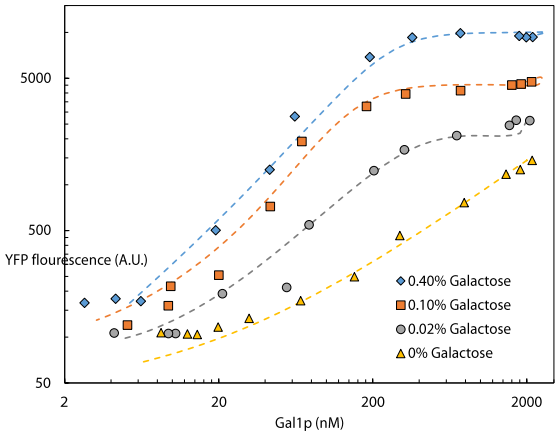

Figure 2.23: Expression levels of the GFP at different Galactose concentration in a Gal1p concentrations. The measurement was performed at steady state after 24 hours of Galactose addition to the media.

Table 2.13: Fitted parameters of mRNA response to Gal1p gradient at different galactose concentrations. The measurement was performed at steady state after 24 hours of Galactose addition to the media.

$Kd_{\text{Gal1p-Galactose (Gal1pA)}}$ (mM)	28.09
$Kd_{\text{Gal1pA-Gal80 with galactose}}$ (nM)	1.52
$Kd_{\text{Gal1p-Gal80 without galactose}}$ (nM)	90.81

Gal1p binds to Gal80p without galactose. This has been previously discussed by Bhat and Hopper.[39] The dissociation constant of galactose independent Gal1p-Gal80p binding is 90.8 nM.

2.2.4.1 Effect of glucose on galactose-dependent interaction of Gal1p and Gal80p

The effects of glucose on galactose network are drastic. We have done previous fitting in glucose media to see the effect of sugar on the Gal80p-Gal3p dissociation constant.

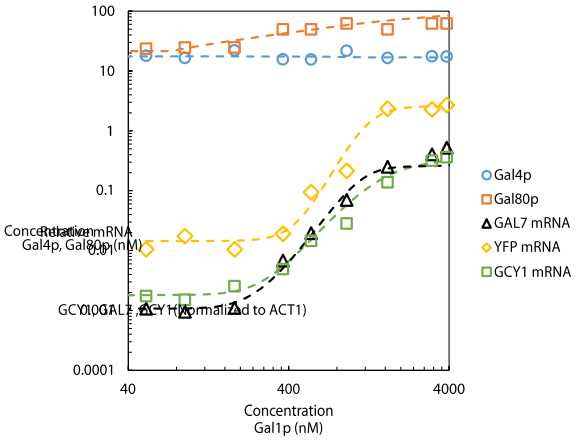

Figure 2.24: Expression levels of the GFP (yellow diamonds), GAL7 (black triangles), GCY1 (green squares), Gal80p (orange squares), and Gal4p (blue circles) at different Gal3p concentrations. The measurement was performed in 0.5% galactose.

Table 2.14: Fitted parameters of mRNA response to Gal1p decay in 0.5% Galactose and 0.2% Glucose+0.5% Galactose.

Galactose	Glucose
$Kd_{Gal1a\text{-}Gal80}$=1.14 nM	$Kd_{Gal1a\text{-}Gal80}$=1.23 nM

We can see in Figure 2.14 that the Gal1p Gal80p interaction is not affected by glucose.

2.2.5 Conclusion

The *GAL* system of *S. cerevisiae* was metabolically engineered by construction of different mutant strains where several layers of *GAL* network were isolated to determine the interaction of regulatory proteins. In the first layer of the GAL network we deleted *GAL80 (ΔGAL80)*. Using a ΔGAL80 strain we have isolated the Gal4p-DNA interaction. We determined the DNA binding activity of Gal4p by

titrating a known amount of protein and fit the dissociation constant (K_D) for both Gal4p homodimerization and Gal4p-DNA binding. With increasing amounts of Gal4p we measured the GAL gene activation. We determined a K_D of 1 nM in good agreement with published results for both the truncated Gal4p DNA binding domain (Vashee et al. 1993) where they found Kd to be 1.3 nM,[40] and for full-length Gal4p (Parthun and Jaehning, 1990) where they claimed the Kd was 6.4 nM.[41] We have found the Gal4p homodimerization to be 13.2 µM which is in agreement with previously published in vitro data (Bhat et al. 1997) for they claimed the a homodimerization in micro molar region.[42] Weak homodimerization of Gal4p plays an important role to reduce the nonlinearity of the response (See section 4.4.3.3.1).

To determine the affinity of the Gal4p–Gal80p interaction, we have engineered a double deletion construct where we removed both Gal3p and Gal1p signal transductors. Using the double deletion strain we have isolated Gal4p-Gal80p binding. Controlling GAL80 transcription with doxycycline we measured the GAL gene response to Gal80p gradient. When Gal80p is at low abundance Gal4p is in a complex with DNA completely. By titrating this complex with increasing amounts of Gal80p, we determined a K_D of 0.22 nM. This value is in agreement with vitro data published by (Melcher et al. 2001) where they claim that Gal4p Gal80p binding is stronger than Gal4p DNA which is lower than 1nM.[8] We assumed a stoichiometric binding, indicating that Gal80 dimer molecules bind one Gal4p dimer complexed with DNA. In our fitting we determined the Gal80p homodimerization to be 39 nM which is again in complete agreement with previous in vitro measurements of Melcher et al. (They claim that Gal80 homodimerization is around 20 nM) Gal80p dimerizes with high affinity, and are significantly stabilized when bound to Gal4p–DNA complexes. In summary, a series of strong protein–protein and protein–DNA interactions appears to stabilize all components of a DNA–$(Gal4p)_2$–$(Gal80p)_2$ complex. It is also important to point out that in our fits we also showed that Gal80p stabilizes the interaction between Gal4p and DNA. Our K_D for the Gal4p–Gal80p interaction is more than one order of magnitude lower than that determined by (Lue et al. 1987)[43] using an electro-

phoretic mobility shift assay which was measured as 6.4 nM, and two orders of magnitude lower than that determined by Wu et al. 1996 (2.4 nM).[11] The difficulty in determining the dissociation constant between Gal4p and Gal80p reflects the complicated linkage between Gal4p and DNA, Gal4p and Gal80p, and Gal80p and Gal80p. All pairwise interactions within the DNA-bound complexes have K_D in the subnanomolar range and are stabilized further by neighbouring interactions. These strong interactions stabilize transient dimer–dimer interactions by positioning dimers in suitable close proximity.

In order to understand the interactions between the regulatory factors, it was important to put them into a quantitative framework. In the first and the second layer of *GAL* network, we have established the model where Gal80p dimerizes in with high affinity and that Gal4p forms a heterotetramer with Gal80p on DNA. Gal80p stabilizes the interaction between Gal4p and DNA. When we moved to the third layer where signal transductors Gal1p, Gal3p comes into play together with galactose sugar itself.

Despite extensive experimental and theoretical analysis of *GAL* network, there are still some questions remain unanswered. For instance, there are certain unresolved issues concerning the molecular mechanisms involved. For example, *in vitro* studies have demonstrated that Gal3p can form a tripartite complex with Gal4p–Gal80p complex. This indicates that Gal3p can potentially translocate to the nucleus and bind to the DNA–Gal4p–Gal80p complex to relieve the repression of Gal80p.[44] This is in contrast to the finding by Peng and Hopper that Gal3p is cytoplasmic protein.[14 45 46] However, recent studies reveal that the inducer, Gal3p, interacts with the repressor protein both in the nucleus and cytoplasm indicating that both Gal3p and Gal80p are nucleocytoplasmic shuttling proteins.[47] This raises further questions regarding the effects of these mechanisms on the working of the switch. In our model we have used the findings of Peng and Hopper to fit our data where binding of Gal3p to the Gal80p monomer competes with Gal80 self-association in cytoplasm, reducing the amount of the Gal80p dimer available for inhibition of Gal4p.

In our fits we found that Gal3p has binds to galactose roughly 2 times stronger to Gal1p, 15mM and 28 mM respectively these values are close to previous work by Platt et al., 2000 where he reported a 21mM for Gal3p and 25 mM for Gal1p. Gal3p-Galactose complex binds to Gal80p almost 10 times stronger than Gal1p-Galactose complex which are close to what Bhat et al 1997[42] suggested as 5nM.

Although Gal3p and Gal80p interact strongly in the presence of galactose, a weaker galactose-independent interaction between Gal3p and Gal80p occurs. Steady-state analysis demonstrates that a 100-fold increase in the Gal3p relative to the basal levels in the wild type switches-on the system in the absence of galactose. The cells achieve roughly 40% of the maximum expression levels. Previously published data argues that a 900-fold excess concentration relative to basal Gal3p expression in galactose is necessary for complete expression. Our measurements we have confirmed (Figure 2.18) the previous findings by Bhat and Hopper[48] where they have shown that overexpression of Gal3p can activate *GAL* network. Our fitted values suggest a dissociation constant of 15nM for Gal3p-Gal80p and 95nM for Gal1p-Gal80p.

2.3 Galactose metabolism

2.3.1 Galactose transport

Gal2p transports galactose from the medium into the cell. Unlike a wild-type strain, a *GAL2* mutant grows on galactose as the sole carbon source, provided its concentration is above 0.02%. In the absence of galactose, its induction is undetectable, but its expression is induced several hundred-fold in response to galactose, which means that *GAL2* is under the positive feedback loop. The biological significance of this loop was evaluated experimentally by expressing *GAL2* independent of the positive feedback loop. Wild-type strains show a switch-like response to varying concentrations while, a *gal2* strain shows a linear response. If Gal2p is expressed constitutively from a promoter independent of the positive feedback loop, the linear response as observed in a *gal2* strain is retained, but

shifts upwards compared to the linear response exhibited by *gal2* strain. This implies that the positive feedback loop of Gal2p expression is an important element of the *GAL* genetic switch that is required for imparting a switch-like response. However, removal of the feedback loops of Gal3p and Gal80p did not result in the loss of the switch-like property.

The inducer galactose enters the cytoplasm of the cell both by Gal2p-independent diffusion mechanism (ex. Hxt transporters[49]) and a galactose permease (Gal2p) –facilitated mechanism.[50 51] The permease, Gal2p, which has both high affinity and low affinity transport mechanism, facilitates the transport of galactose from extracellular medium to the cytoplasm, constituting a positive feedback.[52] The *GAL* switch responses linearly to galactose concentration if Gal2p is expressed independently of the *GAL* regulon. On varying the constitutive levels of Gal2p concentration, the expression of the *GAL* genes can be tuned in a graded manner. In wild type, where Gal2p is regulated, the Gal2p concentration is commensurate with the galactose in the medium yielding a sensitive response. [52] Our aim in this section is to measure the Gal2p facilitated galactose transport. Using a Gal2p gradient we measure the intracellular galactose concentration in Gal2p induced and repressed cells (see section 4.3.3). We fit the transport rate parameters by using the following equation derived from Widda's formula of transport[53] (For the derivation see section Data fitting-Galactose transport-4.4.10):

Equation 2.5: $$J = \frac{D_y E_{HXT}}{L}\left(\frac{Gal_{ext}}{K_{d\,HXT} + Gal_{ext}} - \frac{Gal_{int}}{K_{d\,HXT} + Gal_{int}}\right) + \frac{D_y E_{GAL2}}{L}\left(\frac{Gal_{ext}}{K_{d\,GAL2} + Gal_{ext}} - \frac{Gal_{int}}{K_{d\,GAL2} + Gal_{int}}\right)$$

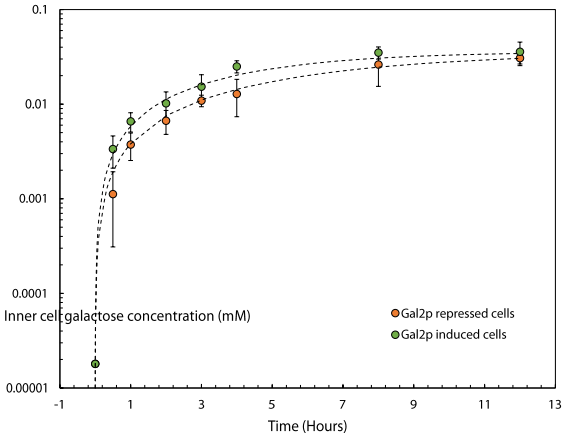

Figure 2.25: Change of intracellular galactose concentration over time. Efficient regulation of the high affinity galactose transporter Gal2p is controlled by synthetic Tet-OFF system. Gal2p repressed cells (orange circles), Gal2p induced cells (green circles).

Transport rates (using Equation 2.5) shows us that Gal2p has a higher affinity to Galactose and increases the galactose transport significantly.

Table 2.15: Fitted parameters of Galactose transport over time with and without Gal2p after addition of 2% Galactose.

	Estimate	Standart error
KdHXT	0.0477393	0.0067476
Kd_{GAL2}	0.0241379	0.0041674
Dy/*L*	1.064351	0.1484977
	from literature	
EHXT (mM)	5.1768152	
	from our measurements	
Induced EGAL2 (mM)	2.3815407	
Repressed EGAL2 (mM)	0.0193621	

Number of HXT molecules has been averaged from previously published data.[54] [55] [56] [57]

2.3.2 Galactose consumption

The final layer of our galactose metabolism chapter is to show the in vivo consumption rate of galactose and try to explain a novel interaction we have discovered on the process.

The galactose metabolic pathway is commonly referred to as the Leloir pathway after Luis Federico Leloir, who discovered that the intracellular galactose is converted to glucose through four distinct enzymatic reactions. Galactokinase catalyses the conversion of intracellular D-galactose to galactose-1-phosphate. Galactose-1-phosphate is converted to glucose-1-phosphate by uridyl transferase. UDP-glucose needed for this reaction is replenished by the conversion of UDP-galactose to UDP glucose by the epimerase. Glucose –1-phosphate is then converted to glucose 6- phosphate by phosphoglucomutase. As phosphoglucomutase is also involved in converting glucose-6-phosphate to glucose-1-phosphate during growth on glucose, it is not generally considered as a member of Leloir pathway.

Metabolic measurements have been done by using galactose kit from megazyme (see section 4.3.3). First we make the cell lysate and measure the concentration of galactose. Experiments have showed us that we do not see any galactose consumption in Gal2 deleted strains. We can see that both in our galactose consumption experiment and growth measurement we did in glycerol. Our initial measurements showed us that there is no galactose consumption in deltaGal1 and deltaGal2 cells. It was expected that galactose would not be consumed in Gal1 deleted cells since Gal1 is the galactokinase which is the first enzyme in galactose consumption pathway Figure 2.26. We measured that a galactose induced wild type cell (Figure 2.26, after t=2 hours) consumes 0.012 mM of galactose per minute (For detailed galactose consumption calculation see section 4.4.9, page 153).

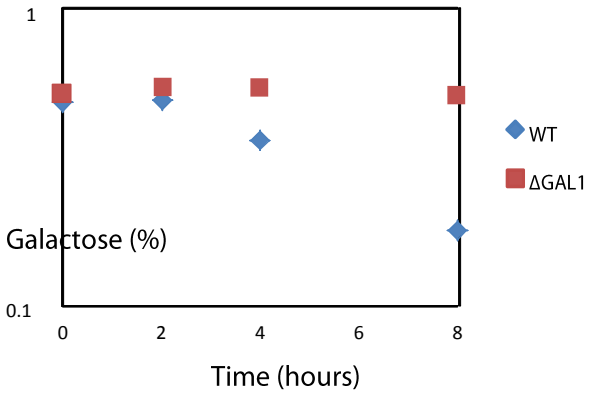

Figure 2.26: Galactose percentage in WT (blue diamonds) and ΔGAL1 (red squares) deletion cultures. Measurement has been done over the course of 8 hours where at t=0 hours 0.5% Galactose was added to each culture.

However the GAL2 deletion strains showed the same behaviour GAL1 deletion strain which was truly unexpected. Since there is no previous publication stating that Gal1p enzymatic activity is directly linked to Gal2p. We see in *Figure 2.27* that Gal2p lacking cells behave as if they are lacking the Gal1p.

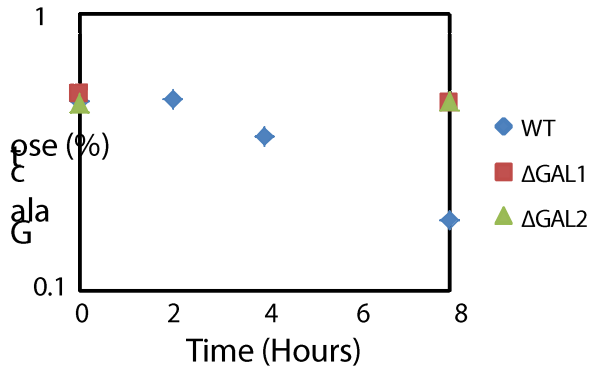

Figure 2.27: Galactose percentage in WT (blue diamonds), ΔGAL1 (red squares), and ΔGAL2 cultures. Measurement has been done over the course of 8 hours where at t=0 hours 0.5% Galactose was added to each culture.

In order to support our findings and exclude the possibility that our intracellular galactose measurements are biased, we grew the cells in glycerol+galactose media. Should the cells were able to consume galactose they would have had a division time of roughly 2 hours which is the case for WT cells. For ΔGAL1 and ΔGAL2 cells we see that the division time is roughly around 6-8 hours which means the deletion strains are not able to metabolize galactose *Figure 2.27*. This also points out that out metabolic measurement are reliable *Figure 2.27*.

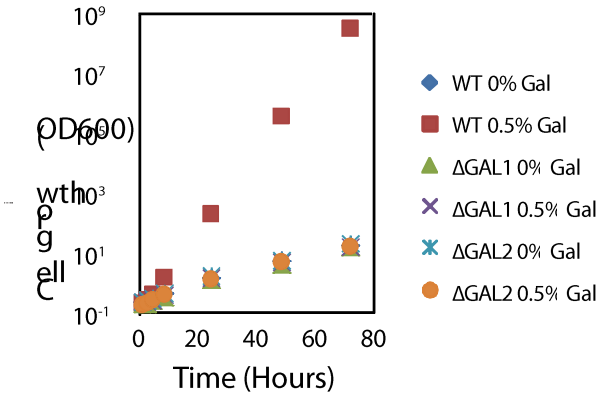

Figure 2.28: Cell growth in 3% glycerol media with and without %0.5 galactose. Initial OD 600 was 0.1 we have diluted the samples every 6 hours and multiplied the OD 600 newer value with the dilution factor to determine cell growth.

Before getting into trying to explain the reasons and mechanism behind the newly found Gal1p-Gal2p interaction. We also checked the whether there was a mutation or a dysfunction in our commercial ΔGAL2 from EUROSCARF© (see section 4.1.1-Deletion strains).

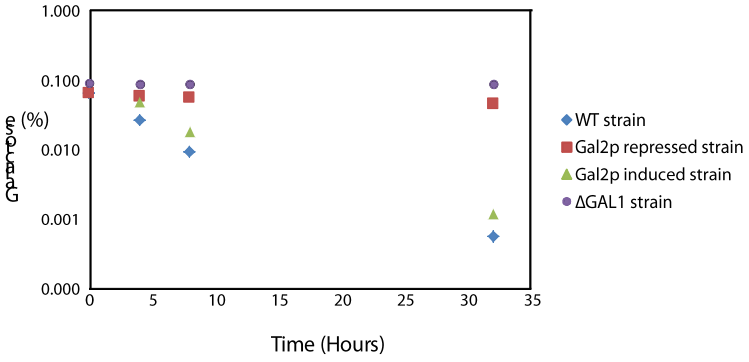

Figure 2.29: Galactose percentage in WT (blue diamonds), ΔGAL1 (purple circle), Gal2 induced cells with tetOFF system (green triangles), and Gal2 repressed cells with tetOFF system (red squares) cultures. Measurement has been done over the course of 32 hours where at t=0 hours 0.1% Galactose was added to each culture.

2.3.2.1 Effect of Gal2p on Galactose metabolism

Our measurements about Gal1p-Gal2p interaction is truly intriguing where there has been no previous publications to state this. One of the main contradictory facts to our finding is the *in vitro* data showing Gal1p activity without Gal2p. From our previous measurements *Figure 2.27*, *Figure 2.28*, and *Figure 2.29*, we trust that there is an interaction between Gal2p and Gal1p. We try to show whether there is a direct or indirect interaction between Gal1p and Gal2p. One

of the clear cut experiments to show whether the Gal1 and Gal2 have a direct interaction was to tag Gal1 with GFP and add a nuclear localization signal. By removing Gal1 from the nucleus we can measure whether this affects galactose consumption or not. GFP has been tagged with YFP and NLS sequences have been added in order to see if there is a direct connection between Gal1p and Gal2p (Figure 2.30).

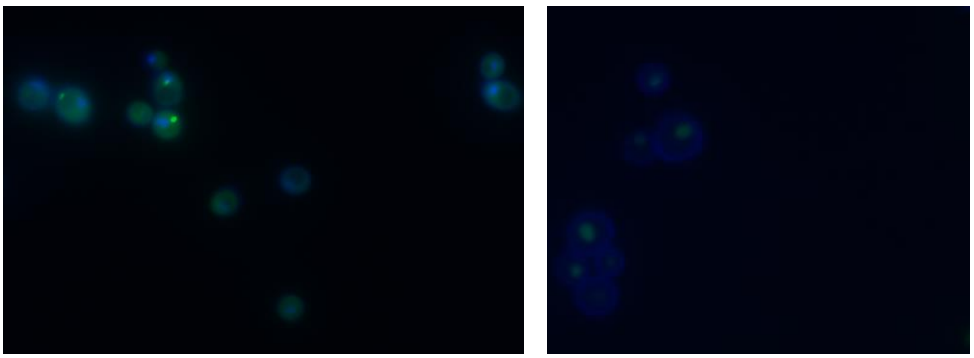

Figure 2.30: NLS cells imaging, Gal1-GFP-NLS construct in BY4742 cells where Gal1 has been tagged with GFP. From the picture we can see that NLS sequence is working well concentrating Gal1 into the nucleus.

After confirming the localization of Gal1 we can measure the galactose consumption by metabolic measurements where we measure the decrease in galactose concentration in media over time (*Figure 2.31*).

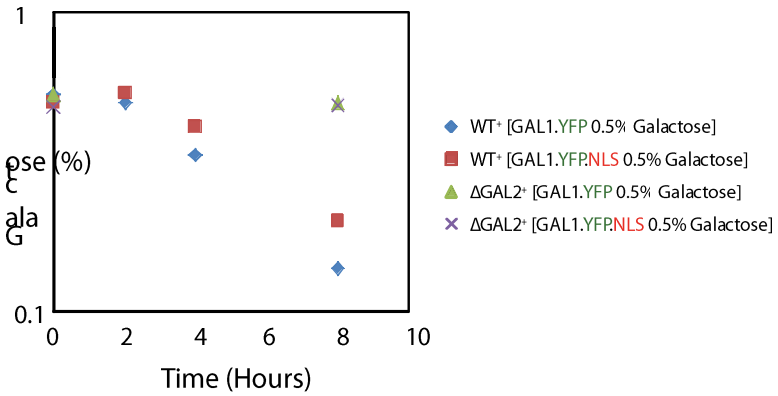

Figure 2.31: Galactose consumption in Gal1 tagged yeast strains.

We can see from the growth measurement that removing galactokinase from cytoplasm doesn't really has an effect on galactose consumption *Figure 2.32*. WT cells with Gal1-YFP and Gal1-NLS-GFP-NLS grow equally good in glycer-

ol+galactose media whereas the growth is slow as expected in only glycerol media.

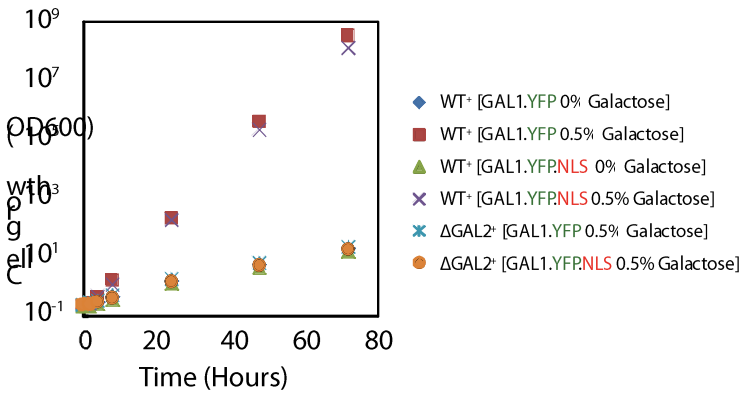

Figure 2.32: Growth of Gal1 tagged cells in 3% glycerol with and without 0.5% galactose media. Initial OD 600 was 0.1 we have diluted the samples every 6 hours and multiplied the OD 600 newer value with the dilution factor to determine cell growth.

Further consumption experiments (*Figure 2.32*) where we integrated the GAL1 tagged plasmids into deletion strains also backs up the previous statement that removing Gal1 from the cytoplasm to nucleus doesn't inhibit the Galactose consumption which means that Gal1-Gal2 interaction is not a direct protein-protein interaction.

Next we have investigated the possibility of an indirect interaction between Gal1p and Gal2p. We have measure galactose consumption in TPK deleted genes. TPK family genes are cAMP-dependent protein kinase catalytic subunits. We have used TPK1, 2, and 3 deletion strains. TPK1, TPK2 and TPK3 encode isoforms of the catalytic subunit of cAMP-dependent protein kinase (PKA), the effector kinase of the Ras-cAMP signalling pathway. [58] [59] Through phosphorylation of various targets, PKA activity regulates processes involved in cell growth and response to nutrients, in our case specifically sugar. We have not seen any effect by TPK genes for galactose consumption (Figure 2.33).

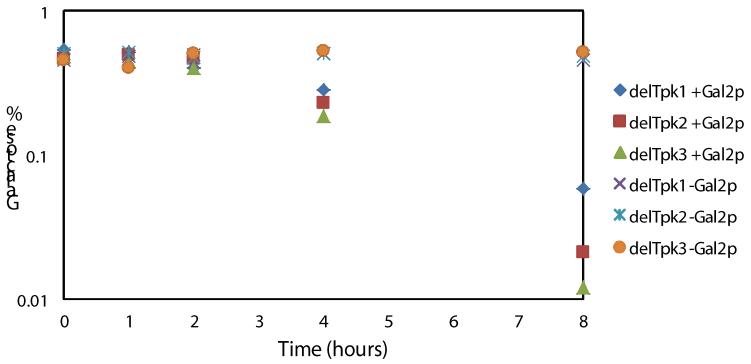

Figure 2.33: Galactose percentage in ΔTPK1 Gal2 induced cells with tetOFF system (blue diamonds), ΔTPK1 Gal2 repressed cells with tetOFF system (purple crosses), ΔTPK2 Gal2 induced cells with tetOFF system (red squares), ΔTPK2 Gal2 induced cells with tetOFF system (purple circle), ΔTPK3 Gal2 repressed cells with tetOFF system (blue diamonds), ΔTPK3 Gal2 repressed cells with tetOFF system (blue crosses), Gal2 induced cells with tetOFF system (orange circles) cultures. Measurement has been done over the course of 8 hours where at t=0 hours 0.5% Galactose was added to each culture.

In addition we have checked the Gal1p for phosphorylation sites using mass spectrometry. We could not detect any candidate site where Gal1p can be phosphorylated.

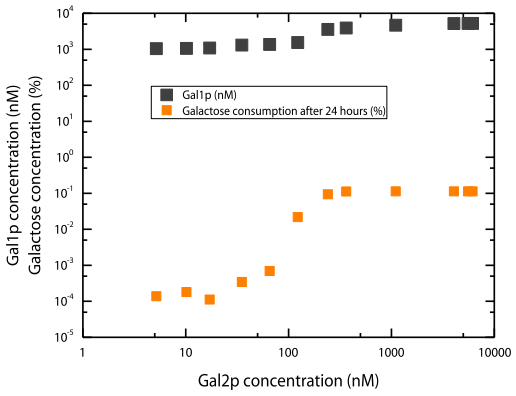

Figure 2.34: Galactose consumption in Gal2p gradient (orange squares) controlled with tetOFF system culture. Gal1p concentration varying in Gal2p gradient (black squares). Measurement has been done over the course of 24 hours where at t=0 hours 0.5% Galactose was added to each culture.

However galactose consumption is somewhat correlated to Gal2p amount in cell. If we write that Gal1p activity directly depends on Gal2p concentration we get a reasonable prediction about galactose consumption in the cell. Although we do have a qualitative picture about galactose consumption depending on

Gal2p concentration it is still not well defined to enable us to work with WT cells (For consumption calculations see section Data fitting-Galactose consumption-4.4.9).

Equation 2.6: $$Gal1p *= Gal1p\left(\frac{\left(\frac{Gal2p(t)}{Gal2pmax}\right)n}{kn+\left(\frac{Gal2p(t)}{Gal2pmax}\right)n}\right)$$

Using the phenomenological *Figure 2.23* we can fit the data where the Gal1p enzymatic reaction depends on the Gal2p concentration (*Figure 2.35*).

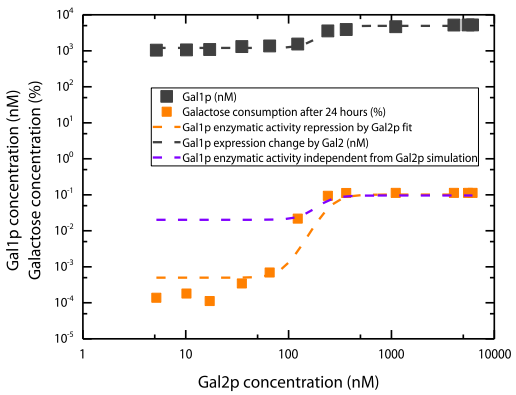

Figure 2.35: Galactose concentration in Gal2p gradient (orange squares) after 24 hours. Controlled with tetOFF system culture. Gal1p concentration varying in Gal2p gradient (black squares). Galactose consumption simulation without Gal1p-Gal2p interaction (purple dash line) Galactose consumption simulation with Gal1p-Gal2p interaction using active Gal1p (orange dash line). Measurement has been done over the course of 24 hours where at t=0 hours 0.5% Galactose was added to each culture.

We see that the Gal1p loses its enzymatic activity when Gal2p is less than 100 nM.

2.3.3 Conclusion

The inducer galactose enters the cytoplasm of the cell both by Gal2p-independent diffusion mechanism (ex. Hxt transporters[60]) and a galactose permease (Gal2p) –facilitated mechanism.[61 62] The permease, Gal2p, which has both high affinity and low affinity transport mechanism, facilitates the transport of

galactose from extracellular medium to the cytoplasm, constituting a positive feedback.[63] We have determined the dissociation rate of Gal2p-Galactose as 0.02 mM and the dissociation rate of HXT transporters were found to be 0.05 mM. Although the difference may not be as big as initially one may think. We have to take into account the fact the measurements have been done in saturating galactose concentrations with little traces of glucose. Meier et al. 2002[60], improving upon prior work, pointed out that HXT transporters have a higher affinity to glucose (as Gal2p having a higher affinity for galactose). Moreover, he has shown that the HXT transporter's glucose preference is regulated by glucose fraction in a competitive media where both glucose and galactose are present. HXTs carry galactose and glucose almost in equal rates until the glucose level reaches one tenth of the galactose concentration. This 10 fold fraction represents the point of switching for HXT transporters where from that point on they mostly transport glucose. This is also true for Gal2p. It has been previously shown by Maier et al. 2002 and Reifenberger et al. 1997 that in the absence of galactose Gal2p transports glucose with almost equal affinity as HXT transporters (HXT with dissociation constant ranging from 0.1mM to 10mM and on average $K_{d\text{-}HXT}$=0.023 mM and Gal2p with $K_{d\text{-}Gal2p}$=0.024). Considering their similar affinities to glucose it is certainly not off the beaten path to assume that their galactose dissociation rates would be in similar range in saturating galactose conditions.

We have calculated that a galactose induced wild type cell should consume roughly 1mM of galactose per hour (For detailed galactose consumption calculation see section 4.4.9, page 153). This finding is in parallel with Sellick et al. 2009 where they showed Gal1p K_m=0.25mM, K_{cat}=20s^{-1}. When these in vitro values are used to calculate the galactose consumption we do get a similar consumption rate. A new interaction between Gal1p and Gal2p has been discovered where we show that without Gal2p, Gal1p does not show any enzymatic activity although its transducing activity is intact. This finding is very interesting since there has been no previous publication to state this. One of the main contradictory facts to our finding is the *in vitro* data showing Gal1p activity without Gal2p. Gal1p phosphorylates galactose which contradicts with our findings.[64] Although

this does not exclude the possibility of an indirect effect by Gal2p on Gal1p, it is certainly discouraging. We went on to trying to explain the basis of this mechanism using different approaches. One of the clear cut experiments to show whether the Gal1 and Gal2 have a direct interaction was to tag *GAL1* with GFP and add a nuclear localization signal. By removing Gal1p from the nucleus we can measure whether this affects galactose consumption or not. We have measured that galactose was consumed with a similar rate in cells where Gal1p accumulated to the nucleus (Figure 2.30 and Figure 2.31). We have also investigated some of the possible mechanisms for indirect interaction between Gal1p and Gal2p. First we have carried a MS/MS shotgun proteomics measurement where we checked for possible phosphorylation and post translational modification sites on Gal1p but our measurements did not yield a viable candidate. Through phosphorylation of various targets, PKA activity regulates processes involved in cell growth and response to nutrients, in our case specifically sugar. We have not seen any effect by TPK genes (PKA proteins) for galactose consumption (Figure 2.33). There is prior work that may explain a decrease in Gal1p activity. Some of the publications include de Jongh et al. reporting that overexpression of GAL1 decreased growth rate by about 30% due to toxicity by Gal-1P accumulation.[65] Moreover, it has been shown that lack of glucose reduces the ATP level in cell effecting the Gal1p activity.[66] Although, there are numerous works published examining the galactokinase activity of Gal1p there is no evidence showing a clear cut repression by Gal2p.

2.4 GAL network analysis by using input/output matching

The analysis and design of nonlinear feedback systems has recently undergone some big changes due to the discovery of certain basic conceptual notions, and the identification of classes of systems for which systematic decomposition approaches can result in effective and easily computable control laws.

Every system consists of nonlinearities due to varying factors and they play an important role on creating multistable systems. Especially in positive feedback loops nonlinearities are accentuated resulting system to diverge into two stable steady states. Bistability is one of the most important phenomena in cellular systems since it holds the key to cellular differentiation and memory.

The model-independent strategy that is described by Angeli et al[67] (discussed in section 1.7) where the steady-state response of a feedback system being at one of the self-consistent points where the input-output characteristic intersects the line of equivalence is used in this section to map the bistability regions in both reduced (Δ*GAL2*Δ*GAL3* strain) and WT *Saccharomyces cerevisiae*. We use this elegant method not only to examine the network behaviour but also to show the validity of our parameter determination from previous layers (parameters fitted in sections 2.1 and 2.2).

2.4.1 Network opening from *GAL1* using a reduced *GAL* network (Δ*GAL2*Δ*GAL3* strain)

In order to better understand the dynamics of the galactose network we decided to use the input/output method (Angeli et al, 2004) by opening the galactose network from GAL1. We are using GAL1 so that we open the network by cutting a positive feedback. One of the main reasons to use this reduced GAL network is to be able to reach steady state intracellular galactose concentration. We have shown in section 2.3.2 that Gal1p does not show any enzymatic activity without Gal2p present. The mathematical work by Angeli et al. suggests that opening of a positive feedback loop enables us to measure steady state values of the system by matching the input/output data. When the input and the output data are equal this gives the steady state values of the system.

2.4.1.1 Hysteretic memory of Δ*GAL2*Δ*GAL3*

It has previously been showed that Gal1p and Gal3p positive feedback loops are the key for the GAL memory and bistability.[22 67] Hysteretic memory (discussed in

section 1.3-Hysteresis memory) in the reduced GAL network reaches almost 5 days. It takes cells to activate from OFF history to on history a long time due to the fact that Gal1p is a weaker signal transductor than Gal3p.

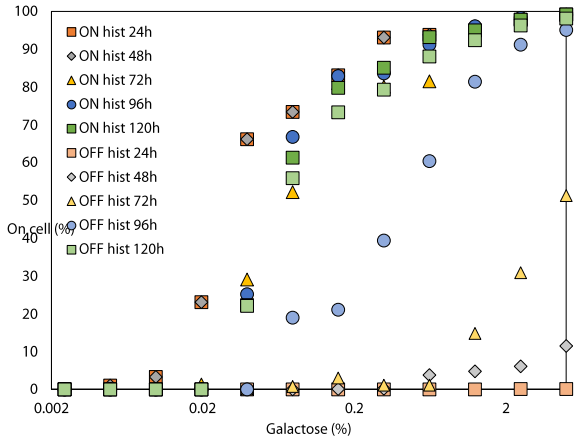

Figure 2.36: Hysteresis experiments with ΔGAL2ΔGAL3 strain. On cell % of the cells with low (darker colours) or high (lighter colours) initial condition were grown at the indicated galactose concentration for 24, 48, 72, 96, and 120 hours.

Gal1p feedback shows a persistent memory. Although with Gal80p feedback reduces the memory storage[21] the slow activation by Gal1p makes the OFF history activation a 5 days process.

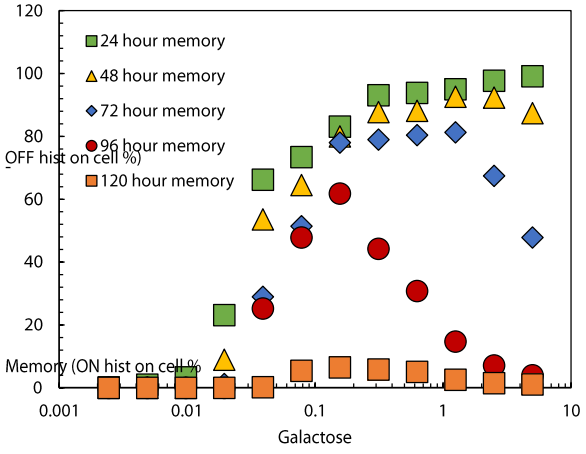

Figure 2.37: Hysteresis memory with ΔGAL2ΔGAL3 strain. Difference between the on cell percentage of the cells with high initial condition and on cell percentage of the cells with low initial condition. Cells were grown at the indicated galactose concentrations for 24, 48, 72, 96, and 120 hours after.

We see that the memory is persistent in Gal1p feedback loop and is enhanced in the bistability region that is mapped by input output matching (*Figure 2.40*). In

our reduced network we use Gal1p feedback splitting to map the bistability regions.

2.4.1.2 Input output matching to map steady states

In order to do our measurements faster we have designed a double colour fluorescent system where we can easily measure the amount of input and the corresponding output. This made our experiments much faster.

We have used blue fluorescent and yellow fluorescent protein in our constructs. One being the input output construct and the other the identity construct which allows us a good graphical representation of where input and the output is equal. In other words identity strain provides us an easy read for the bistability region (see detailed plasmid construct in sections 4.1.2.1.1.1 and 4.1.2.1.2.1).

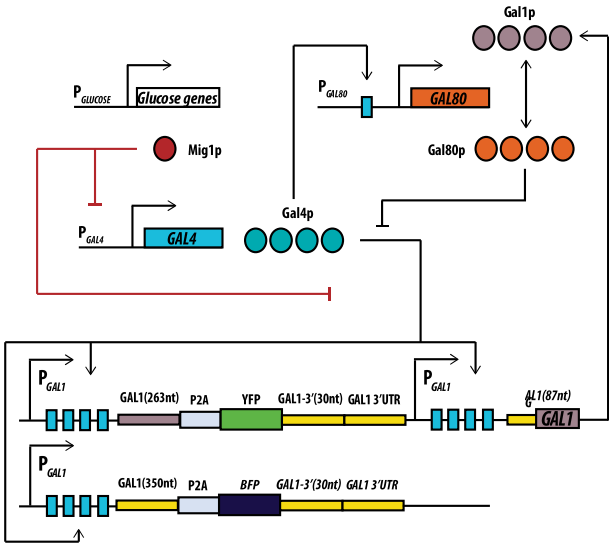

Figure 2.38: Identity construct for the GAL1 opening. GAL1, YFP and BFP transcription is controlled by an endogenous GAL1 promoter.

We have replaced the GAL4 binding sites in the GAL1 promoter with tet operators and used an endogenous GAL1 promoter to measure the YFP output. We have also inserted a second synthetic GAL1 with tet operator promoter to express BFP which then we use to check the input value.

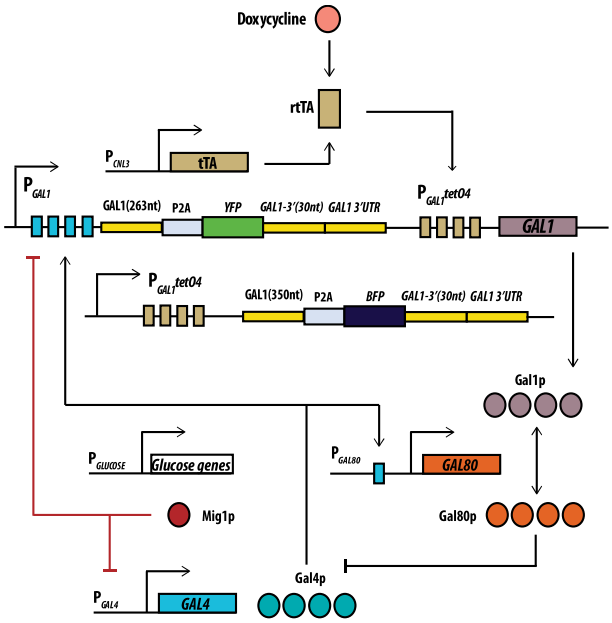

Figure 2.39: Input output construct for the GAL1 opening. We control the GAL1 and BFP transcription with doxycycline and measure the output with YFP expression which is controlled by the endogenous GAL1 promoter.

Assuming the BFP fluorescent corresponds to GAL1 mRNA and YFP fluorescent corresponds YFP mRNA we can reconstruct the input output response as follows (See full set of equations in section 4.4.7):

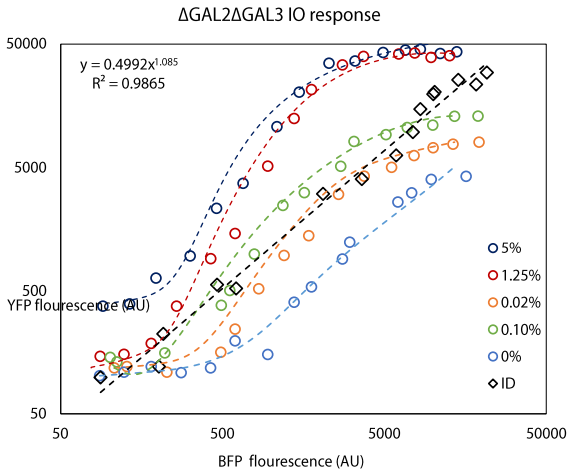

Figure 2.40: Mapping of ΔGAL2ΔGAL3 strain steady states using Gal1p feedback opening. Cells grown for 24 hours at different Galactose concentrations and in a GAL1 mRNA gradient.

Once we mapped the bistability region for the double deletion strain we saw that the memory is enhanced where system shows multistability.[21]

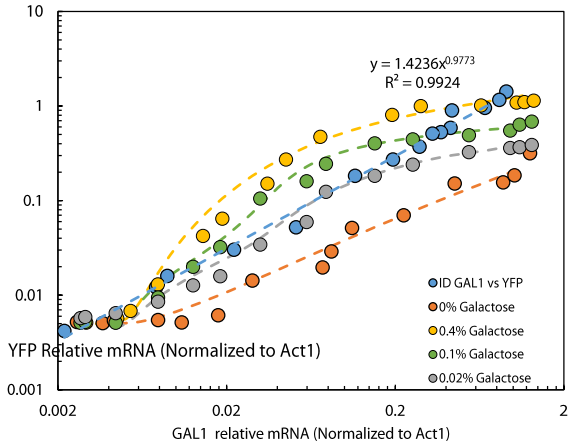

Figure 2.41: Reconstruction of input output response in ΔGAL2ΔGAL3 strain steady states using Gal1p feedback opening. Cells grown for 24 hours at different Galactose concentrations and in a GAL1 mRNA gradient.

Our input output model is quite similar to 3rd layer fitting model (sections 2.2.3 and 2.2.4). However in input output (I/O) we control GAL1 mRNA as input and measure the response as YFP mRNA where the response is regulated by protein concentrations. That's why we needed to integrate the translation rates for proteins in our model (see full set of equations in section 4.4.7-Fitting of the GAL1 input output data). We have measured the translation rates of our regulatory proteins using SRM.

Table 2.16: Parameter estimation of input output response in ΔGAL2ΔGAL3 strain steady states using Gal1p feedback opening.

$Kd_{\text{Gal1p-Galactose (Gal1pA)}}$ (mM)	38.94
$Kd_{\text{Gal1pA-Gal80 with galactose}}$ (nM)	1.529
$Kd_{\text{Gal1p-Gal80 without galactose}}$ (nM)	73.14

We found that translation rates between Gal4p and Gal80p are quite similar but Gal1p translation rate is 4 times higher than Gal4p and Gal80p (Table 2.17). There are examples showing transcriptional factor having a lower translation rate than rest of the genes.

Table 2.17: Translational rates of GAL network regulatory proteins.

Steady state (tranlation rate/decay rate)	
Gal1p	4085.61
Gal4p	1101.69
Gal80p	1070.96

We can see that our input output matches both double fluorescent and mRNA measurements (Figure 2.40 and Figure 2.41 respectively). It has been shown in submitted work by Becskei group that an elegant way to control the validity of the input output matching is to fit the transition rates of the closed loop system and to determine the region where transitions are suppressed. This indicates the region where bistability occurs. We have checked the transition rates from low to high state and high to low state in our closed loop system.

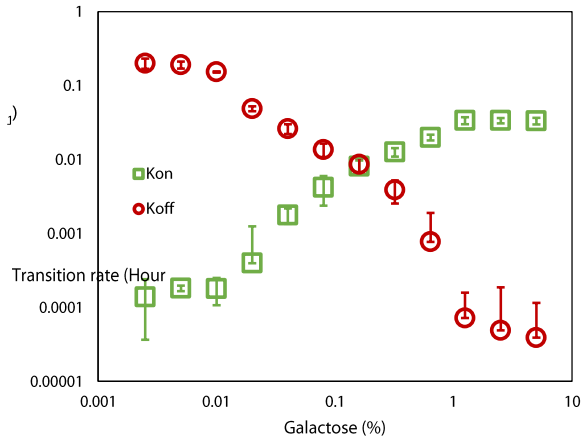

Figure 2.42: Transition rates of ΔGAL2ΔGAL3 cells. In bistable region, the transition rates become slower. Cells grown for 5 days at different Galactose concentrations both with a low and high initial galactose condition.

Transition rates provide an easy way to confirm the prediction of the bistability region from input output measurements. We can see in Figure 2.42 that the transition rates from high to low and low to high in the closed loop system coincides with the bistability region in our input output measurements (*Figure 2.41*).

2.4.2 *GAL* network opening from GAL2

In the second section of IO opening we want to tackle the WT behaviour. Inhibition of the cells in glucose for has a dramatic effect on galactose network memory (Figure 2.43).

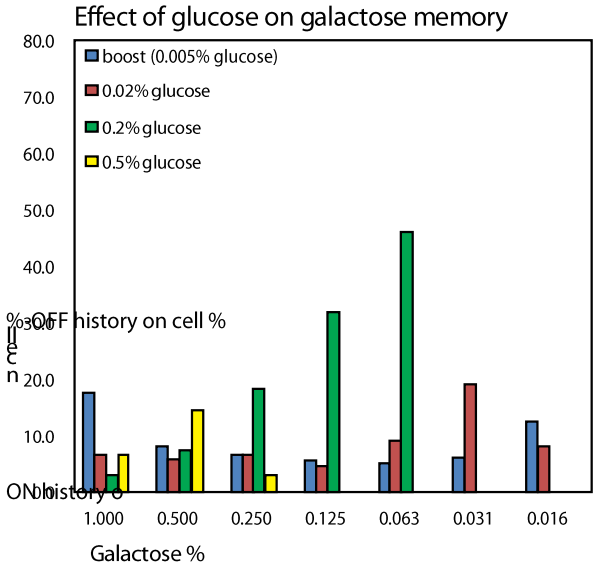

Figure 2.43: Hysteresis memory in GAL network at different glucose concentrations. Cells have been incubated at different glucose concentrations both at high and low galactose initial condition. Then hysteretic memory has been measured after 24 hours.

We want to explain the reasons and reconstruct this dynamic behaviour GAL network. However as described in our previous sections (2.3.2.1-Effect of Gal2p on Galactose metabolism), the unknown mechanism between Gal1p and Gal2p hinders us making a solid conclusion in this section since we could not model the network.

2.4.2.1 Input output matching to map WT steady states

In order to do our measurements faster we have designed a double colour fluorescent system very much similar to GAL1 opening in previous section. We have used blue fluorescent and yellow fluorescent protein in our constructs. One being the input output construct and the other the identity construct which allows

us a good graphical representation of where input and the output is equal. In other words identity strain provides us an easy read for the bistability region (see detailed plasmid construct in sections 4.1.2.1.1.2 and 4.1.2.1.2.2).

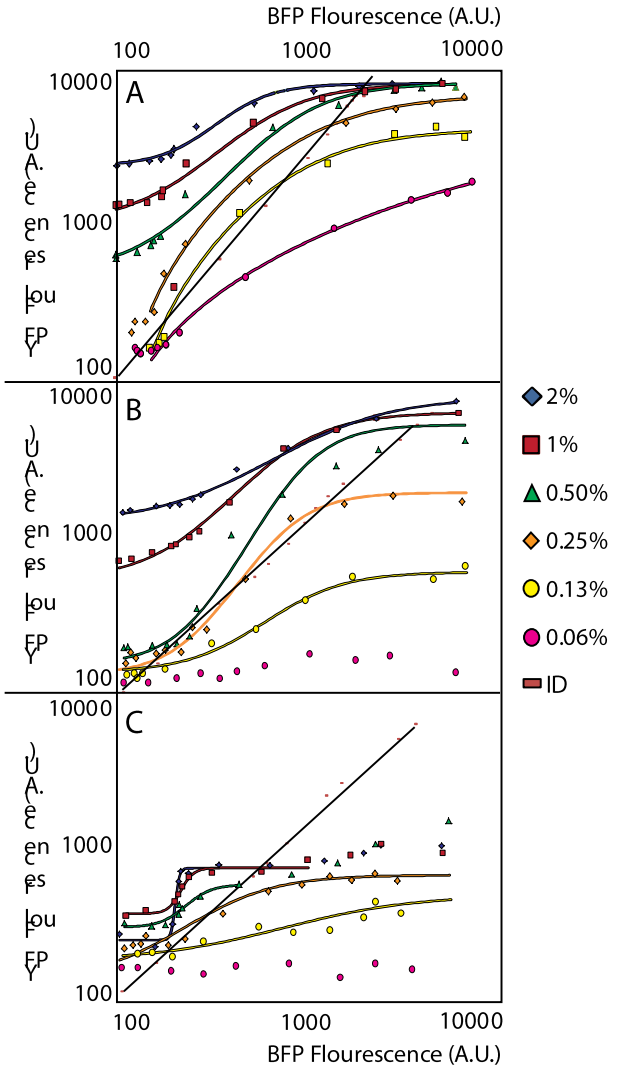

Figure 2.44: Mapping of WT strain steady states using Gal2p feedback opening. Cells grown for 24 hours at different galactose and glucose concentrations and in a GAL2 mRNA gradient (x-axis).

Although we were not able to reconstruct the IO response, we can see that the bistability region in 0.2% glucose is enhanced compared to 0% and 0.5%. This may be one of the first clues suggesting the higher memory in mid-range glucose.

2.4.3 Conclusion

It is clear that bistability is an important recurring theme in cell signalling. Bistability may be of particular relevance to biological systems that switch between discrete states or "remember" previous stimuli. Because the GAL regulatory network contains three positive feedback loops, this network exhibits bistability. A core positive feedback loop through *GAL1* is necessary for this cellular memory, whereas a negative feedback loop through *GAL80* competes with the positive *GAL1* loop and reduces memory. Using feedback splitting we show the bistablity regions in ΔGAL2ΔGAL3 strain in yeast. Matching the input output response we show that the memory stored in Gal1p feedback loop especially enhanced between 0.02% to 1.25% galactose. In this region the system is bistable and the hysteresis memory is still visible after 5 days. The slow activation of the network is due to the weaker sequestration of Gal80p by Gal1p instead of Gal3p. Gal1p feedback deletion strain shows a long memory. Although with Gal80p feedback reduces the memory storage[21] the slow activation by Gal1p makes the OFF history activation a 5 days process. Transition rates provide an easy way to confirm the prediction of the bistability region from input output measurements. It has been previously shown by the submitted work from Becskei group [68] that the transition rates become slower in bistability region. It has been also shown by Scott et. al. the range of bistability is considerably widened as transitions from the low to the high state are suppressed confirming the relation between the transition rates and bistability in our closed loop system (*Saccharomyces cerevisiae* Δ*GAL2*Δ*GAL3* strain). We can see in Figure 2.42 that the transition rates from high to low and low to high in the closed loop system coincides with the bistability region in our input output measurements (*Figure 2.41*). For the WT behaviour of the GAL network we were not able to reconstruct the IO response. One of the main reasons for this of course was the peculiar interaction between Gal1p and Gal2p, nevertheless; qualitatively we did map the bistability region. Our findings were in parallel with the hysteretic memory we have measured where in 0.2% glucose it was enhanced compared to 0% and 0.5%.

2.5 Other projects

2.5.1 Introduction

In mapping of deterministic and stochastic network activity by feedback splitting project in our lab, I performed the proteomics measurements for absolute quantification of rtTA protein concentration by targeted LC-MS (SRM). In their work Becskei group showed that protein homodimerization can generate sufficient nonlinearity to create cellular memory. They compared the strength of this nonlinearity with cooperativity using feedback splitting. With the resulting open loop relations that has captured the nonlinearities and together with equivalence relations, they mapped the bistability region for the positive feedback circuits with different cooperativity and homodimeration. Feedback circuits were created by placing the gene of the TF, rtTA under the control of its own promoter. The inducer doxycycline increases the affinity of the TF to the DNA. I have contributed by determining the decay rate of rtTA protein.

2.5.2 Results

For absolute quantification of rtTA, heavy reference peptides were selected matching the sequence of the endogenous peptide with the highest precursor ion MS-intensity determined in the label-free quantification experiment. Peptides containing missed cleavages or a glutamine at the N-terminus were excluded. The following endogenous peptides were detected after scan run for the full spectrum shotgun proteomics:

Table 2.18: Endogenous rtTA peptides that were detected using shotgun proteomics.

Identified rtTA peptides
ALLDALPIEMLDR
ETPTTDSMPPLLR
FEGDTLVNR
FSVSGEGEGDATYGK
LGVEQPTLYWHVK
LSFLPAGHTR
VHLGTRPTEK
VINSALELLNGVGIEGLTTR
CALLSHR
QAIELFDR

To synthesize heavy peptides, five peptide sequences were selected (Table 2.18 bold blue marked peptides) that had the highest peaks.

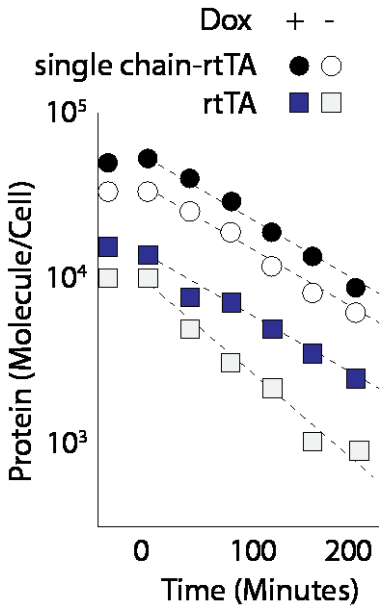

Figure 2.45: Decay of rtTA protein. Decay rate for single chain rtTA is 0.0126 min^{-1} with 20 µM doxycycline, 0.0088 min^{-1} without doxycycline. For rtTA the decay rate is 0.0084 min^{-1} both with and without doxycycline.

Chapter 3 Conclusion

3.1 Achieved results

Having established a synthetic control on transcription of *GAL* genes and a method to precisely measure absolute protein concentration, we looked at the effect of media on protein degradation and profiled *in vivo* protein turnover in the presence of the carbon source galactose and glucose. The overall distribution of half-lives measured in this condition was similar to the turnover profile generated for yeast grown in glucose, with an average half-life of 1.5 to 2 hours. Thus, glucose dependent ubiquitination of Gal2p is the single example of change in GAL regulatory protein decay rate.

The *GAL* system of *S. cerevisiae* was metabolically engineered by construction of different mutant strains where several layers of *GAL* network were isolated to determine the interaction of regulatory proteins. In the first layer of the GAL network we deleted *GAL80 (ΔGAL80)*. Using a ΔGAL80 strain we have isolated the Gal4p-DNA interaction. We determined the DNA binding activity of Gal4p by titrating a known amount of protein and fit the dissociation constant (K_D) for both Gal4p homodimerization and Gal4p-DNA binding We determined a K_D of 1 nM in good agreement with published results for both the truncated Gal4p DNA binding domain (Vashee et al. 1993) where they found Kd to be 1.3 nM.[69] We have found the Gal4p homodimerization to be 13.2 μM which is in agreement with previously published in vitro data (Bhat et al. 1997) for they claimed the a homodimerization in micro molar region.[70] To determine the affinity of the Gal4p–Gal80p interaction, we have engineered a double deletion construct where we removed both Gal3p and Gal1p signal transductors. Using the double deletion strain we have isolated Gal4p-Gal80p binding. By titrating Gal80p, we

determined a K_D of 0.22 nM. This value is in agreement with vitro data published by (Melcher et al. 2001) where they claim that Gal4p Gal80p binding is stronger than Gal4p DNA which is lower than 1nM.[8] In our fitting we determined the Gal80p homodimerization to be 39 nM which is again in complete agreement with previous in vitro measurements of Melcher et al. (They claim that Gal80 homodimerization is around 20 nM) Gal80p dimerizes with high affinity, and are significantly stabilized when bound to Gal4p–DNA complexes. In summary, a series of strong protein–protein and protein–DNA interactions appears to stabilize all components of a DNA–$(Gal4p)_2$–$(Gal80p)_2$ complex. It is also important to point out that in our fits we also showed that Gal80p stabilizes the interaction between Gal4p and DNA. The difficulty in determining the dissociation constant between Gal4p and Gal80p reflects the complicated linkage between Gal4p and DNA, Gal4p and Gal80p, and Gal80p and Gal80p. All pairwise interactions within the DNA-bound complexes have K_D in the subnanomolar range and are stabilized further by neighbouring interactions. In order to understand the interactions between the regulatory factors, it was important to put them into a quantitative framework. In the first and the second layer of *GAL* network, we have established the model where Gal80p dimerizes in with high affinity and that Gal4p forms a heterotetramer with Gal80p on DNA. Gal80p stabilizes the interaction between Gal4p and DNA. When we moved to the third layer where signal transductors Gal1p, Gal3p comes into play together with galactose sugar itself. In our fits we found that Gal3p has binds to galactose roughly 2 times stronger to Gal1p, 15mM and 28 mM respectively these values are close to previous work by Platt et al., 2000 where he reported a 21mM for Gal3p and 25 mM for Gal1p. Gal3p-Galactose complex binds to Gal80p almost 10 times stronger than Gal1p-Galactose complex which are close to what Bhat et al 1997[42] suggested as 5nM. Although Gal3p and Gal80p interact strongly in the presence of galactose, a weaker galactose-independent interaction between Gal3p and Gal80p occurs. Steady-state analysis demonstrates that a 100-fold increase in the Gal3p relative to the basal levels in the wild type switches-on the system in the absence of galactose. Our measurements we have confirmed (Figure 2.18) the previous

findings by Bhat and Hopper[71] where they have shown that overexpression of Gal3p can activate *GAL* network. Our fitted values suggest a dissociation constant of 15nM for Gal3p-Gal80p and 95nM for Gal1p-Gal80p.

The permease, Gal2p, which has both high affinity and low affinity transport mechanism, facilitates the transport of galactose from extracellular medium to the cytoplasm, constituting a positive feedback.[72] We have determined the dissociation rate of Gal2p-Galactose as 0.02 mM and the dissociation rate of HXT transporters were found to be 0.05 mM. Although the difference may not be as big as initially one may think. We have to take into account the fact the measurements have been done in saturating galactose concentrations with little traces of glucose. Meier et al. 2002[60] suggested that HXTs carry galactose and glucose almost in equal rates until the glucose level reaches one tenth of the galactose concentration. This 10 fold fraction represents the point of switching for HXT transporters where from that point on they mostly transport glucose. This is also true for Gal2p. It has been previously shown by Maier et al. 2002 and Reifenberger et al. 1997 that in the absence of galactose Gal2p transports glucose with almost equal affinity as HXT transporters.

We have calculated that a galactose induced wild type cell should consume roughly 1mM of galactose per hour with Gal1p enzymatic activity. This finding is in parallel with Sellick et al. 2009 where they showed Gal1p K_m 0.25mM, K_{cat} 20s^{-1}. During the process of determining galactose consumption and transport in *GAL* network we have stumbled upon a new interaction between Gal1p and Gal2p. WE have shown that without Gal2p, Gal1p does not show any enzymatic activity although its transducing activity is intact. We have further confirmed these findings with several control experiments in contrast to prior *in vitro* data showing Gal1p activity without Gal2p. We went on to trying to explain the basis of this mechanism using different approaches. To show whether the Gal1 and Gal2

have a direct interaction was to tag *GAL1* with GFP and add a nuclear localization signal. We have shown that galactose was consumed with a similar rate in cells where Gal1p accumulated to the nucleus (Figure 2.30 and Figure 2.31). We have also investigated some of the possible mechanisms for indirect interaction between Gal1p and Gal2p such as a MS/MS shotgun proteomics measurement where we checked for possible phosphorylation and post translational modification sites on Gal1p but our measurements did not yield a viable candidate. Although, there are numerous works published examining the galactokinase activity of Gal1p there is no evidence showing a clear cut repression by Gal2p.

After establishing the layer by layer the important parameters that govern the GAL network dynamics. We went on to map the bistability region ΔGAL2ΔGAL3 strain in yeast both to explain its hysteresis behaviour and validate our established parameters from previous layers. It is clear that bistability is an important recurring theme in cell signalling. Bistability may be of particular relevance to biological systems that switch between discrete states or "remember" previous stimuli. Because the GAL regulatory network contains three positive feedback loops, this network exhibits bistability. Using feedback splitting we have shown the bistablity regions in ΔGAL2ΔGAL3 strain in yeast. Matching the input output response we show that the memory stored in Gal1p feedback loop especially enhanced between 0.02% to 1.25% galactose. In this region the system is bistable and the hysteresis memory is still visible after 5 days. The slow activation of the network may be due to the weaker sequestration of Gal80p by Gal1p instead of Gal3p.[22] We have fitted transition rates as an easy way to confirm the prediction of the bistability region from input output measurements. It has been previously shown by the submitted work from Becskei group [73] that the transition rates become slower in bistability region. It has been also shown by Scott et. al. the range of bistability is considerably widened as transitions from the low to the high state are suppressed confirming the relation between the transition rates and bistability in our closed loop system (*Saccharomyces cerevisiae* Δ*GAL2*Δ*GAL3* strain). We have shown the galactose range, where the transition rates from high to low and low to high in the closed loop system are suppressed,

coincides with the bistability region in our input output measurements (*Figure 2.41*). For the WT behaviour of the GAL network we were not able to reconstruct the IO response. One of the main reasons for this was the interaction between Gal1p and Gal2p that we could not explain. Nevertheless, we did map the bistability region. Our findings were in parallel with the hysteretic memory we have measured where in 0.2% glucose it was enhanced compared to 0% and 0.5%.

3.2 Future development

Systems biology attempts to discern the inherent design principles prevailing in the biological network connecting genotype to phenotype. *GAL* genetic network of *S. cerevisiae* offers an opportunity for such a study, as its molecular connectivity at the genetic, signalling, and metabolic levels are well characterized. The system-level studies have demonstrated that the mechanisms prevailing in the *GAL* system offers properties such as ultra-sensitivity, noise reduction, memory, and speedy response for an optimal operation of the switch. However, more studies are essential to incorporate recent findings such as the effect of Gal2p on Gal1p enzymatic activity and the possibility of translocation of Gal3p into the nucleus. Opportunities exist to integrate such data with system-level studies to obtain better insights on system-level properties such as ultra-sensitivity, bistability, autoregulation, and memory among other. One of them being the bistability mapping of WT cells and explaining the effect of glucose on galactose memory.

Chapter 4 Materials and methods

4.1 Design and construction of synthetic circuits and yeast strains

4.1.1 Deletion strains

We have created double deletion strains by mating two single deletion commercially available yeast strains and put them under random sporulation. In response to nitrogen starvation in the presence of a poor carbon source, diploid cells of the yeast *Saccharomyces cerevisiae* undergo meiosis and package the haploid nuclei produced in meiosis into spores. The formation of spores requires an unusual cell division event in which daughter cells are formed within the cytoplasm of the mother cell.[74]

4.1.2 Construct plasmids

The first step was to transform the Y0000 ßY4741 MATa strain with pRS305::pCLN3::tTA plasmid. We used pRS303::Fig1::Tgal7::Pgal1::YFP plasmid as backbone together with tTA to generate the strains in which we measured the protein decay. We transformed this strain with various tetOFF system containing GAL regulatory genes. Strain with the backbone that contained the pCYC1 with two bind sites of tetO2 leads the transcription of the inserted gene; an Amp cassette as bacterial marker and; an URA3 gene as yeast marker.

At the same time of design the model plasmid, some constraints were considered. To avoid losing the effect of the TATA box for a large distance between the TATA box and ORF, we decided shorten the distance between the TATA box and

5'UTR and keep it at 12 bp. The truncated fragment was around 100 bp to provide a large homologous sequence. GAL regulatory protein decay constructs; to efficiently control the interested GAL gene we have used tet-OFF, tetracycline controlled gene expression system [75]

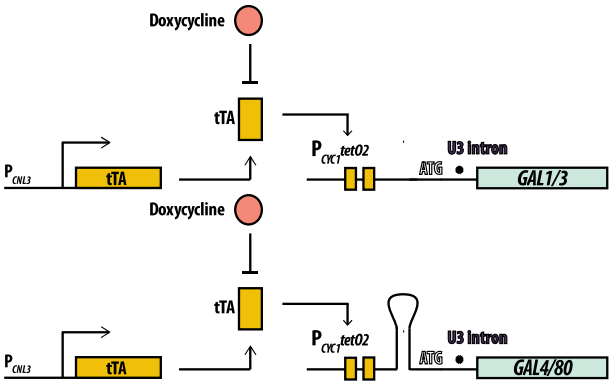

Figure 4.1: Efficient regulation of the proteins were achieved through synthetic regulation using a Tet OFF system.

Strain were optimized to find the best dynamic range with and without step loops. As an option translational initiation was blocked in *cis* by insertion of a strong stem-loop structure into the 5'-UTR. Stem loop hinders the ribosomal binding; therefore, reduces the translational efficiency. The reason we tried constructs with stem loops was because of the discrepancy in the fitting that was caused by the fact that Gal4 expression pattern does not follow the target gene. All constructs were then optimized by a synthetic intron insertion (Figure 4.3).

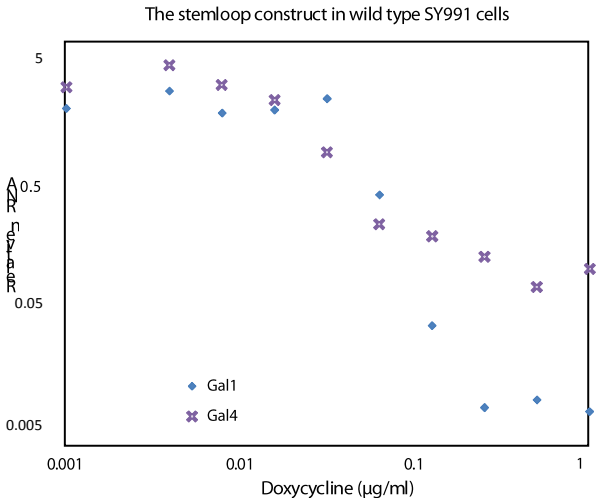

Figure 4.2: real time PCR relative mRNA values GAL4 and GAL1. GAL1 mRNA expression is controlled by GAL4 concentration using a Tet OFF system.

A set of primers have been designed to screen mature mRNA, one of them binds at the 5'UTR, the other lies at the both sides of the splicing sites and binds only if the mRNA is spliced.

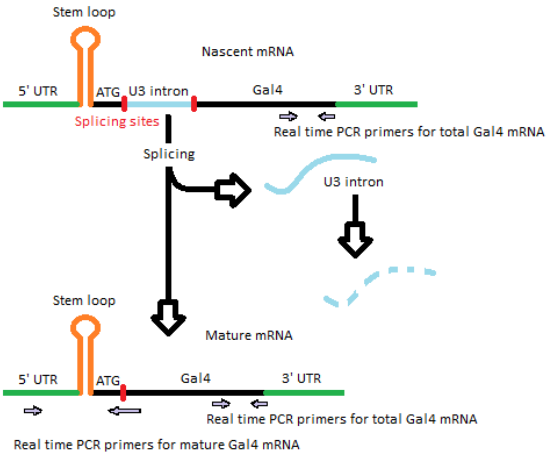

Figure 4.3: Scheme representing GAL4 mRNA maturation and Oligo regions to measure GAL4 mRNA and GAL4 mature mRNA using real time PCR. GAL4 mRNA expression is controlled by a Tet OFF system.

Mature and total mRNA are very similar in the stem loop construct without the intron. In the construct which includes the intron mature mRNA follows the target gene expression closely. Construct has been improved (Figure 4.4).

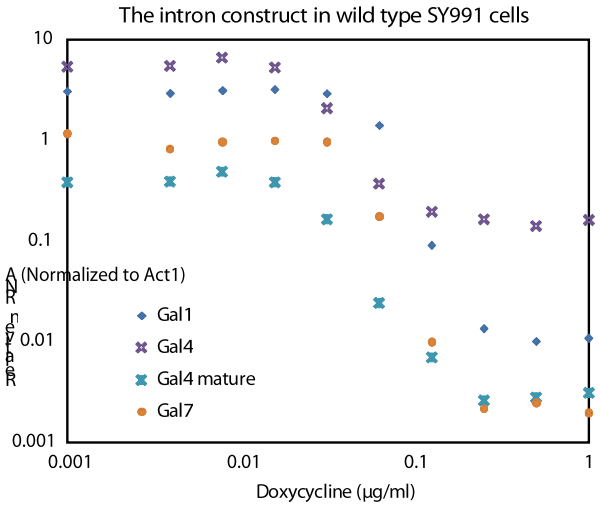

Figure 4.4: real time PCR relative mRNA values GAL4 (nascent, mature and total) and GAL1 (total). GAL1 mRNA expression is controlled by GAL4 concentration (doxycycline gradient) using a Tet OFF system.

Gal1, 3, 80 have been improved in similar way. Dynamic range has been increased with and without stem loops then then the best strain has been used to measure our parameters. For Gal1p and Gal3p decay strains the full data set was reached with two plasmids, where we cover the whole dynamic range.

4.1.2.1 Feedback splitting constructs

4.1.2.1.1 Input/output constructs

4.1.2.1.1.1 Gal1p feedback loop opening

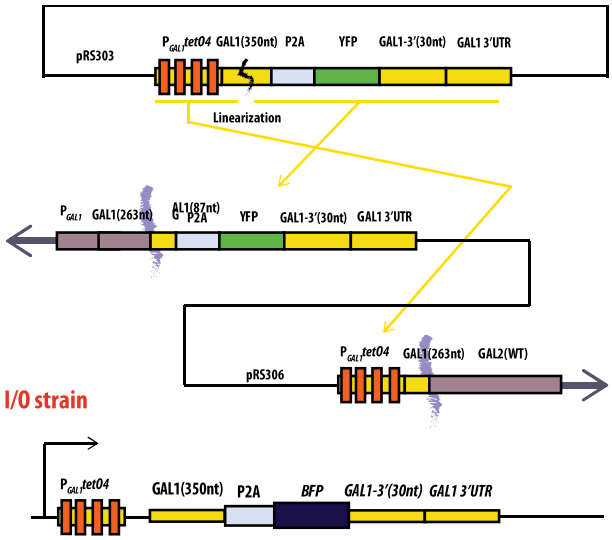

Figure 4.5: Scheme representing GAL1 feedback opening input output plasmids and their integration sites.

4.1.2.1.1.2 *Gal2p feedback loop opening*

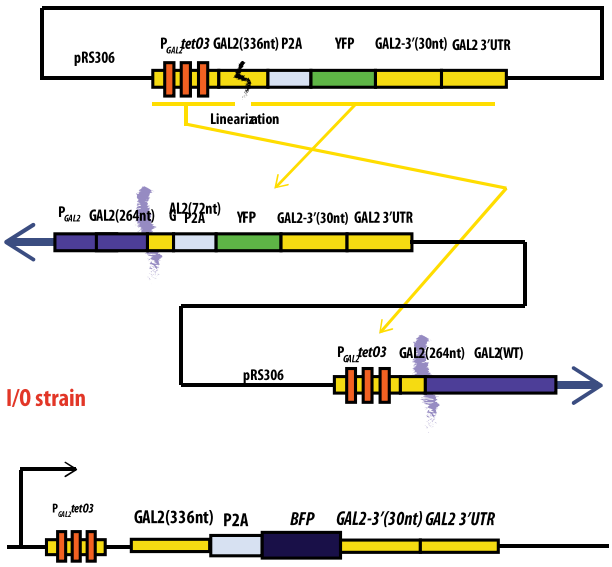

Figure 4.6: Scheme representing GAL2 feedback opening input output plasmids and their integration sites.

4.1.2.1.2 Identity matching constructs

4.1.2.1.2.1 *Gal1p feedback loop opening*

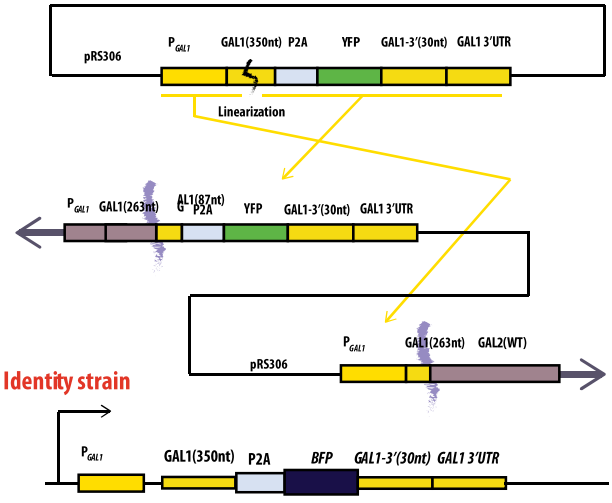

Figure 4.7: Scheme representing GAL1 feedback opening identity plasmids (line of equivalence) and their integration sites.

4.1.2.1.2.2 *Gal2p feedback loop opening*

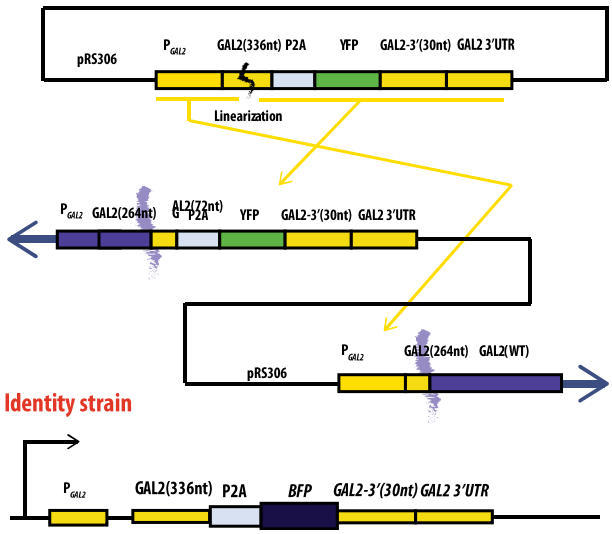

Figure 4.8: Scheme representing GAL2 feedback opening identity plasmids (line of equivalence) and their integration sites.

4.1.3 DNA amplification (PCR)

PCR is a simple and elegant technique to amplify a specific DNA fragment from a DNA template. The amplified fragment is delimited by two oligo with homologous sequences that hybridize with the DNA and exert primers for the DNA polymerase [46],[47]. We performed the PCRs in Eppendorf strips in which we added the reagents. For a single reaction we used 14.75 µl H_2O, 5 µl HF buffer, 2.5 µl primer mix (10 mM each), 2 µl dNTPs (2.5 mM each), 0.5 µl template and 0.25 µl Phusion DNA Polymerase.

Table 4.1: PCR program. Tm (melting temperature) of the primers is given by Genius, the software used to create the oligo.

Step	Temperature (°C)	Time	No. of cycle
Initial Denature	96	4 min	1
Denature	94	40 sec	
Annealing	Primer Tm – 4	45 sec	5
Extension	72	1 min per 1Kb	
Denature	94	40 sec	
Annealing	Primer Tm – 2	45 sec	30
Extension	72	1 min per 1Kb	
Final Extension	72	7 min	1

4.1.4 DH5α competent cells

To perform the cloning of our plasmid, we used the strain DH5α of E.coli. This strain is the most frequently strain used for cloning thus its high efficiency transformations. In addition, it is easy the isolation of the desired plasmid. We inoculated 5 colonies from a freshly LB grown plate in a 200 ml SOC medium. We let them grow overnight at RT with vigorous shaking. The following day, we transferred the cells into sterile Falcon tubes and placed them on ice for 10 min when the OD_{600} was as close to 0.45 as was possible. We span down for 15 min at 3500 rpm and carefully discarded the supernatant. We resuspended the cells in 64 ml of cold HTB and kept on ice for 10 min. We span down again for 15 min at 3500 rpm, carefully discarded the supernatant and resuspended in 16 ml of cold HTB. Following, we slowly added 1.2 ml of filter sterilized DMSO while gently swirled the cells suspension. We aliquoted immediately into Eppendorf tubes (e.g. 210 μl portions) and froze by throwing the tubes into liquid nitrogen. We stored the tubes at -80°C.

4.1.5 Bacterial Transformation of DH5α

The transformation is a basic technique of molecular biology, resulting the incorporation of foreign DNA to the bacteria through its membrane to generate a large amount of the desired DNA. The cells required for the transformation were

melted on ice during 30 min approximately. Afterwards, the cells were mixed gently with the fingers and were aliquoted 50µl into 1.5ml tubes. It was added 5µl of desired ligation into each tube carrying out a gently mix with the fingers. It was let incubate the tubes on ice for 10 min. The next step was the heat shock at 42°C for exactly 1 min and the placement of the tubes on ice again for 2 min. It was 1ml of pre-warmed (37°C) LB without antibiotics and was let the tubes at 37°C for 1 h. After this time, it was performed a spin down of the tubes during 4 min at 14.000rpm, it was added 300µl LB in each tube and was spread this amount onto ampicillin LB plates. The plates were cultivated inverted at 37°C overnight or at RT at the weekend.

4.1.6 Yeast transformation protocol

The day before the transformation, we made a 5 ml overnight culture of strain to transform in YPD. Next morning, we refreshed the cells in fresh YPD at OD_{600} ~ 0.2, and we let them grow for 5 h at 30ºC in the shaking incubator. Usually, we used 50 ml of YPD for 8 transformations. When it was missing 1.5 h to start the transformation, it needed to linearize the DNA for transformation. The linearization was performed like a single plasmid digestion. After the 5 h, we harvested the cells by centrifugation at 3300 rpm for 5 min at room temperature RT. Following, we discarded the supernatant and washed the cells in 50 ml of sterile ddH_2O and span again. In the next step, after discard the supernatant, we resuspend the cells in 25 ml of sterile LiT buffer and let them incubate at RT for 40 min with gentle shaking. During that time, we prepared the PEG solution, 30-60 min to dissolve with gentle shaking; and the carrier DNA, heating it to 95ºC for 10 min (to ensure sterility). For each transformation, we mixed 50 µL LiT, 5 µL carrier DNA in the Eppendorf tube where we had made the plasmid digestion; always, we included a control without transforming DNA. After ended the cell incubation, we span down the cells (3300 rpm, 5 min) and resuspened in 750 µL LiT. We added 100 µL of the cells into the Eppendorf tube and let them incubate at RT for 10 min. In the next step we added 300 µL of PEG solution to each tube and incubate them at RT for 10 min; and at 42ºC for 15 min to do the heat shock.

Following the incubations, we centrifuged the cells for 1 min at V_{max}, discarded the supernatant and, added 1 ml of fresh YPD in each tube and let them at 30ºC for 1 h. Before plate the cells on plates with appropriate selection media, we span down for 1 min at V_{max}, discarded the supernatant and we resuspended in 100 μL of 10mM Tris-Cl pH 7.5. The incubation of the plates was for 2-3 days at 30°C.

4.1.7 Yeast Colony PCR

We tested whether the transformation took place into right position and a single time for several clones of the same strain. Using a pipetman tip, we transferred yeast cells to 30 μl of 0.2% SDS. We mixed very well in a vortex for ~ 20 seconds. To break down the cell membranes, we heated the tubes for four min at 90°C. Then we span down for 1 min at 1000 rpm and transferred the supernatant to a new tube. After, we performed a PCR as it has already described previously (5.2. DNA amplification. PCR) with a PCR program shown below. We tested if the plasmid was integrated into the correct allele to disrupt it. The oligo used to this PCR bound before the 5'UTR chosen by us in the gDNA and, after the truncated fragment in the plasmid. A single integration is necessary to avoid disturbing the measurements. To test the single integration, the oligo bound in the plasmid on the TATA box region and after the truncated fragment. In this case, shouldn't have amplification.

Table 4.2: Program of yeast colony PCR. Tm (melting temperature) of the primers is given by Genius, the software used to create the oligo.

Step	**Temperature (°C)**	**Time**	**No. of cycle**
Initial Denature	96	4 min	1
Denature	94	40 sec	
Annealing	Primer Tm – 2	45 sec	35
Extension	72	1 min per 1Kb	
Final Extension	72	7 min	1

4.1.8 Genomic DNA isolation

We started with the preparation of 2 ml overnight YPD culture of clones we wanted to test. Next morning, we collected them by centrifugation (3500 rpm for 5 min), and resuspended the cells with 1 ml ddH_2O and we transferred them to a 2 ml Eppendorf tube to centrifuge at V_{max} for 1 min to pellet the cells. In a new 2 ml Eppendorf tube, we made a mix of 20 µl Zymolyase (80 U/ml), 2 µl RNase (20 µg/ µl) and 1 µl 2-mercaptoethanol and, we added the suspension of the cells in 150 µl 1.2 M SCE. We let incubate the mixture at 30°C with shaking for 1 h. Following the incubation, we added 500 µl lysis buffer and incubated at RT for 5 min; next, we added 360 µl 7 M NH_4OAc into the tube and we put them at 65°C for 5 min and then put them in ice for another 5 min. The addition of 650 µl chloroform is a critical step to separate the DNA of the proteins and other cell components; we mixed the mixture in a vortex and span down it at V_{max} for 2 min. We transferred the supernatant to a new 2 ml tube containing 1 ml 2-propanol; we mixed and incubated at RT for 5 min. That mixture was centrifuged at V_{max} for 5 min. Afterwards, we washed the pellet with 70% ethanol; span down V_{max} for 1 min and we let air dry the pellet. We dissolved the pellet with100 µl 10 mM Tris-Cl, pH 7.5 at 30°C for 20-60 min. Once the DNA was dissolved, we measured the concentration with the Nanodrop.

4.1.9 Copy number checking using qPCR with gDNA template

We prepared two different concentrations of gDNA: 5 and 50 ng. We used the gDNA of W303 yeast strain at 50 ng as reference. We measured the levels of two genes: URA3 present in the plasmid and ACT1 as reference gene, already present in the yeast genome We used the 384 Well Plate Two Notch Type and we filled each well with 5 µl CyberGreen, 2 µl gDNA, 2 µl diluted primers (1.5 mM) and 1 µl H_2O.

Table 4.3: qPCR Program.

	Preparation		Amplification		Melting Curve		
	Without repeat		40 cycles		Increase 0.3 °C per scan		
Temp	50 °C	95 °C	95 °C	60 °C	95 °C	60 °C	95 °C
Time	2:00	3:00	0:03	0:45	0:15	0:15	0:15

4.2 Yeast culture preparation

4.2.1 Preparing and selecting cell cultures

We prepared two 5 ml overnight cultures of SD CSM 2% raffinose (0.005% glucose) medium at 30°, with and without DOX. We refreshed next morning at OD_{600}~0.1 in 10 ml of the same raffinose medium at the presence or absence of DOX, and we let the cells grow 5h at 30°. We harvested the cells at 3500 rpm during 10 min and froze them in liquid nitrogen. Afterwards, we performed RNA isolation, reverse transcription and qPCR analysis to choose the strains we require for our experiments.

4.2.2 RNA isolation

RNA was isolated from each time point using RNeasy ® Mini-kit of QIAGEN ® with DNase I treatment (Qiagen). We included an optional DNase digestion step because the qPCR is a sensitive application and we wanted to avoid any genomic DNA.

4.2.3 Reverse transcription

The reverse transcription is a technique to synthetize cDNA using RNA as template. In the market there are several kits to performer the cDNA synthesis. We tested three of them to see which one gave us better results. We tested the QuantiTect Reverse Transcription Kit and SuperScript® Reverse Transcriptase with oligo octamers. We performed the reaction following the kit instructions.

4.2.4 RNA quantitation by quantitative real-time PCR (qPCR)

The quantitative PCR (qPCR) is robust technique to measure the gene expression [48]. The product of its amplifications is detected at the reaction progresses in "real-time". To monitor the PCR, we used the SYBR Green I Dye. This dye binds to the dsDNA. At the beginning of the reactions, only the qPCR primers region is dsDNA, therefore, the fluorescent signal is very weak. After several cycles and at the end of the elongation phase, the emitted fluorescence by the intercalated dyes is enough to be measure of the machine at 530 nm. We filled each well with 200 ng of cDNA of interest, 2 µl premixed of qPCR primers (1.5 µM), 5 µl of CyberGreen and until 10 µl with H_2O, between 2 and 2.8 µl depending on cDNA concentration. Then we span the plate of 1 min at 1000 rpm. To avoid errors in the quantifications, we chose two genes as reference: TFC1 and UBC6. TFC1 is one of six subunit of RNA polymerase III transcription initiation factor complex; and UBC6 is an ubiquitin-conjugating enzyme involved in endoplasmic reticulum-associated degradation. These genes are known as *house-keeping* genes due to constant level of expression. As the qPCR is an exponential reaction, the PCR product is double each cycle if the PCR is 100% efficient. To test if that was our case, we measured the efficiency of qPCR primers. We prepared 6, 10-fold serial dilution from cDNA and performed the qPCR. (Appendix: Oligos)

4.2.5 Harvesting cell culture for protein and RNA analysis

We prepared a 5 ml overnight culture of SD –CSM 2% raffinose +0.5% galactose (0.005% glucose) medium at 30°. We refreshed next morning at OD_{600}~0.1 in 60 ml of the same raffinose medium and we let the cells grow until OD_{600}~0.5 at 30°. We took 2 samples before induce the decay and 10 samples at different time during time course (1.5, 3, 4.5, 6, 7.5, 9, 10.5, 12, 13.5 and 24 hours). 10 ml culture was collected at each indicated time point (5ml for MS/MS and 5ml for RNA). The

cell density was maintained to prevent reaching OD_{600} of 1.0 throughout the time course by dilutions during sample taking. For RNA and protein analysis, the cells were collected with dry ice cooled at 50% methanol similar to sample preparations for galactose consumption measurements (section 4.3.3); where the cells were pelleted at 4 C°, 4000 rpm for 5 mins. Then cells were stored at -80 C° until further measurements. Further samples were processed for both RNA (section 4.2.2) and protein analysis.

4.2.6 Sample preparation for protein quantification

Protein quantification was performed by mass spectrometry as previously described, with minor modifications.[76] Cell pellets were resuspended in 100µl lysis buffer (100 mM ammoniumbicarbonate, 8M urea, 0.1% RapiGest™). The cells were disrupted by vortexing for 3 x 30 seconds followed by sonication (100% amplitude, 0.5 cycle, 3 × 10 s) in a VialTweeter (Hielscher). 10 µl aliquot of the supernatant was taken to determine the protein concentration of each sample using a BCA assay (Thermo Fisher Scientific). Proteins obtained from the different samples were reduced with 5mM TCEP for 60min at 37°C and alkylated with 10mM 18 iodoacetamide for 30min in the dark at 25°C. After quenching the reaction with 12 mM N-acetylcysteine, the proteins were proteolyzed for 4h at 37°C using sequencing-grade Lys-C (Wako Chemicals) at 1/200 w/w. Then, the samples were diluted with 100mM ammoniumbicarbonate buffer to a final urea concentration of 1.6M and further digested by incubation with s quencinggrade modified trypsin (1/50, w/w; Promega, Madison, Wisconsin) over night at 37°C. The samples were acidified with 2M HCl to a final concentration of 50mM, incubated for 45min at 37°C and the cleaved detergent removed by centrifugation at 14,000g for 5min. Subsequently, an aliquot of the heavy reference peptide mix were spiked into each sample at a concentration of 200 fmol of heavy reference peptides per 1µg of total endogenous protein mass. All peptide samples were then desalted by C18 reversed-phase spin columns according to the manufacturer's instructions (Macrospin, Harvard Apparatus), separated in aliquots of 150 µg peptides, dried under vacuum and stored at -80°C until further use. For LC-

MS analysis, samples were solubilized in solvent A (98% water, 2% acetonitrile, 0.15% formic acid) at a concentration of 0.5 µg/µl and 3 µl were injected per LC-MS run.

4.2.7 Absolute quantification of protein concentration by targeted LC-MS

For absolute quantification of rtTA, heavy reference peptides were selected matching the sequence of the endogenous peptide with the highest precursor ion MS-intensity determined in the label-free quantification experiment. Peptides containing missed cleavages or a glutamine at the N-terminus were excluded. Endogenous peptides were detected after scan run for the full spectrum. To synthesize heavy peptides, five peptide sequences were selected that had the highest peaks. (Table 4.5) To generate the SRM assays, a mixture containing 500 fmol of each reference peptide was analysed by shotgun LC MS/MS using HCD fragmentation, database searched by Mascot applying the same settings as above with two changes; isotopically labelled arginine (+10 Da) and lysine (+8 Da) were added as variable modifications and the mass tolerance for MS2 fragments was set to 0.02 Da. The resulting dat-file was imported to skyline version 1.4 (https://brendanx-uw1.gs.washinton.edu/labkey/project/home/sofware/Skyline/begin.view) to generate a spectral library and select the best transitions for each peptide. After collusion energy optimization, the final transition list were imported to a triple quadrupole mass spectrometer (TSQ Vantage) connected to an electrospray ion source (both ThermoFisher Scientific). Peptide separation was carried out using an Easy-LC systems (ThermoFisher Scientific) equipped with a RP-HPLC column (75 µm x 20 cm) packed in-house with C18 resin (Magic C18 AQ 3 µm; Michrom BioResources) using a linear gradient from 95% solvent A (0.15% formic acid, 2% acetonitrile) and 5% solvent B (98% acetonitrile, 0.15% formic acid) to 35% solvent B over 90 minutes at a flow rate of 0.2 µl/min. Each sample was analysed in duplicate. All raw-files were imported into Skyline for protein quantification.

Based on the number of cells counted for each sample, absolute abundances for the selected proteins (in copies/cell) were calculated across all samples.

4.2.8 Flow cytometry

GFP fluorescence was measured by BD FACSCanto™ II Flow Cytometer using the 488 nm laser and the 530/30 nm band pass emission filter, coupled to a 502 nm long pass dichroic mirror. Gating based on the forward- and side-scatter signal was performed to omit the cell debris and clusters. At least 5,000 cell events were recorded for a single measurement.

4.3 Data analysis

4.3.1 Protein analysis

4.3.1.1 Absolute quantification of protein concentration by targeted LC-MS

4.3.1.1.1 Introduction to selected reaction monitoring (SRM)

Absolute quantification using SRM (selected reaction monitoring) is solemnly dependent on the ratio between selected standard heavy peptides and their endogenous counterparts. In SRM peptides are targeted using a triple quadrupole mass spectrometer (QQQ).

4.3.1.1.2 Basic workflow for SRM analysis

Step 0: Successfully solubilize lyophilized peptide standards. Recommend stepwise resuspension.

Step 1: Determine strongest transitions for each peptide (start with 5/peptide; method can be trimmed down to 3/peptide later on). If your instrument has an ion trap, this process is easier.

Step 2: Optimize collision energy (CE). This must be performed for every single transitions.

Step 3: Determine retention time of peptide. Using scheduled SRM methods significantly improves multiplexing capability.

Step 4: Look for endogenous peptides. Determine necessary pre-fractionation steps.

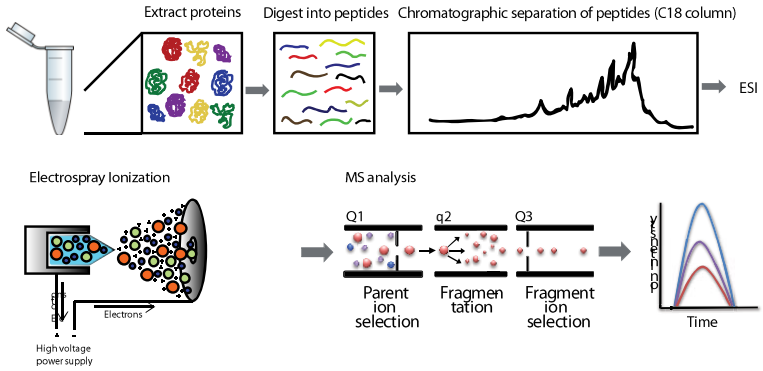

Figure 4.9 Targeted mass spectrometry work flow.

In selected reaction monitoring peptides are quantified using stable isotope labelled peptide standards. Quantitation is achieved by measuring area under extracted-ion chromatogram (XIC) curve.[77] In XIC curves one or more m/z values represent one or more analytes of interest that are recovered from the entire data set for a chromatographic run. The total intensity or base peak intensity within a mass tolerance window around a particular analyte's mass-to-charge ratio is plotted at every point in the analysis. The size of the mass tolerance window typically depends on the mass accuracy and mass resolution of the instrument collecting the data. This is useful for re-examining data to detect previously-unsuspected analytes, to highlight potential isomers, resolve suspected co-eluting substances, or to provide clean chromatograms of compounds of interest. When selecting peptides for SRM analysis one needs to consider the feasibility of chemical synthesis. Peptide length should be less than 24 A.A. It is also important to consider the post translational modifications and the physiochemical properties of the peptides to be programmed in the transition lists and the

HPLC programming gradient programming. Peptide should be unique and should not be proned to trypsin miscleavage.[78]

$$Endogenous\ peptide\ concentration = Heavy\ peptide\ concentration \frac{Endogenous\ peptide\ chromatographic\ peak\ area}{Heavy\ peptide\ chromatographic\ peak\ area}$$

4.3.1.1.2.1 Actin Normalization and absolute quantification

When we are using mass spectrometry there are few key issues we need to take into account. Since we are aiming to obtain absolute protein amounts in cells it is very important to include control measurements in our MS/MS data.

There are three key points where we may lose some our peptides whilst preparing our samples using MS/MS which are cell lysis, tryptic digestion and C-18 column purification.

The control for the C-18 column purification is straight forward. All we need to check is the heavy peptide fragments peak areas of the samples since the heavy peptide is added after the lysis and it's already digested (Figure 4.12). However the control for the cell lysis efficiency and the tryptic digestion is more ambiguous. One of the very first control experiment we have done was to check the linearity of a protein quantification in a dilution series. Where we had two strains one expressing high levels of *GAL1* protein (Figure 4.10) and one a Δ*GAL1* strain.

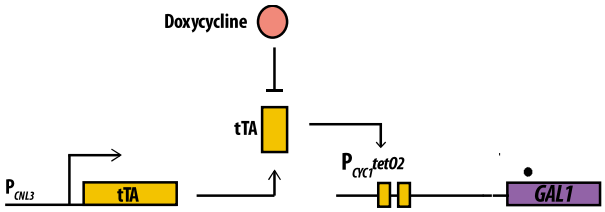

Figure 4.10: Control of expression in GAL1 gene using tet OFF system.

Results showed us that the measurement gives a scattered data instead of a linear reduction of GAL1 protein over dilution (Figure 4.11). This pointed out the fact that we need to design another control for our protein measurements.

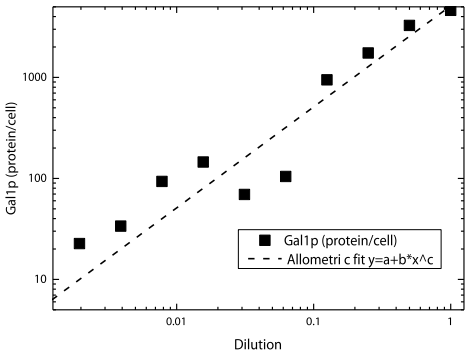

Figure 4.11: GAL1 protein number per cell in a dilution series. Cells have been grown overnight and refreshed in the morning afterwards a dilution series been made with a ΔGAL1 strain to check the precision of mass spectrometry. Data is fit with an allometric equation where c is 0.891 and Adj. R-square is 0.751.

After the absolute number detection problems we had with the dilution calibration we checked the actin values which somewhat should be similar for every sample injected since actin is highly abundant and constitutively expressed. When we analysed the mass spec data carefully we saw that the actin amount was scattered quite similar to the GAL1 protein (Figure 4.12).

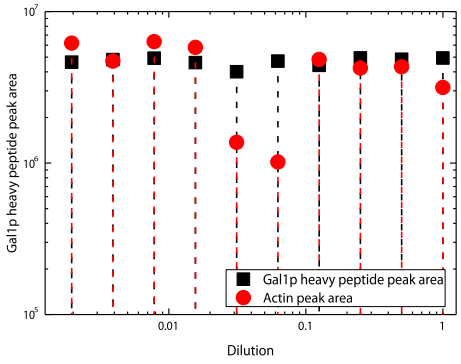

Figure 4.12: GAL1 heavy peptide fragments peak area (A.U) average compared to Actin peptide fragments peak area average (A.U). Cells have been grown overnight and refreshed in the morning afterwards a dilution series been made with a ΔGAL1 strain to check the precision of mass spectrometry.

In order to avoid the issue of different endogenous protein amount injection we have decided to make a calibration where we know the actin peptide fragments peak area corresponding to the number of cells and the amount of protein.

For this purpose we first counted the cells with flow cytometer and measured the total amount of protein we have in the lysate using BCA assay. It is important to note that the cells were checked under the microscope before and after the lysis to ensure the >95% cell lysing (Figure 4.13).

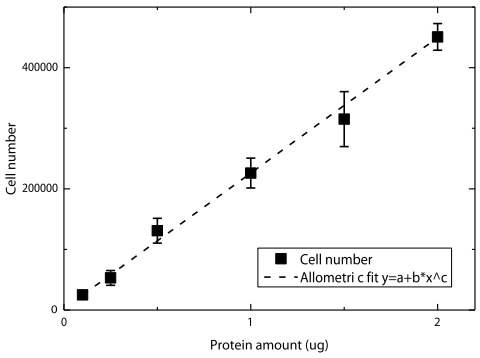

Figure 4.13: Cell number measured with flow cytometry compared to the amount of protein measured by BCA assay. Cells have been grown overnight and refreshed in the morning afterwards a dilution series been made with HPLC grade water. Data has been fit with allometrically where c is 0.99 and Adj. R-square is 0.998.

After measuring the cell number corresponding to the total protein amount the next step was to correlate the amount of protein injected to the actin peptide fragments area. We added a GFP heavy peptide to ensure that we do not lose any protein during C-18 column purification where we used a macro column not to saturate the column and not to lose any protein at any HPLC elution range (Figure 4.14). By using BCA assay we get the following correlation:

injected cell number	5.26E+07
injected protein concentration (ug/ul)	0.5
total amount of protein per yeast (ug)	9.50E-09

Which means we can calculate the number of cell injected in each measurement. Using heavy to endogenous ratio we can calculate the number of protein molecules in cell:

$$P_{conc} = H_{conc} \frac{P_{peak\ area}}{H_{peak\ area}}$$

$$Protein_{number/cell} = N_{injected\ cell\ number} N_{avogadro} H_{conc} \frac{P_{peak\ area}}{H_{peak\ area}}$$

As described at the beginning of this section we can also use this method to reduce the errors that maybe introduced during digestion or column purification by a method we developed named actin normalization. Where calculate the amount of actin that should be in cell using a reference curve and normalize the amount of endogenous protein according to this graph. This dramatically increases the consistency of our measurements.

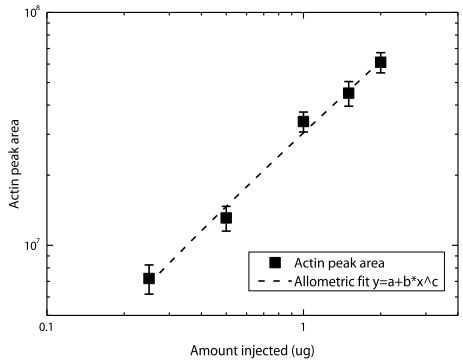

Figure 4.14: Actin peptide fragments peak area (A.U) compared to the injected amount of protein (µg). Cells have been grown overnight and refreshed in the morning afterwards a dilution series been made with HPLC grade water.

After having our correlation between actin peptide fragments peak area and the amount of injected protein. Now we can calculate back the amount of protein that was lost during the sample preparation (Figure 4.15).

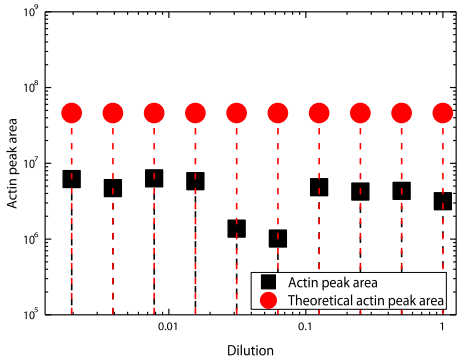

Figure 4.15: Actin peptide fragments peak area (A.U) compared to theoretical actin peptide peak area (A.U) calculated from the injected sample amount. Cells have been grown overnight and refreshed in the morning afterwards a dilution series been made.

Once we have the amount of peptides lost during lysis and tryptic digestion we can normalize the initial GAL1 protein dilution results we had (Figure 4.11) and update them (Figure 4.16).

We see that instead of the scattered results we previously had now our dilution shows a linear decrease over the series. This graph also gives us a guideline in what range we can trust our results. For GAL1 protein we see that the dynamic range of linearity is from 100 to 100000 proteins per cell. The linearity of the measurement of course doesn't only depend on the effective way to normalize our peptide loses during sample preparation it also depends on the signal intensity of the peptides, their elution states, their m/z ratios etc.

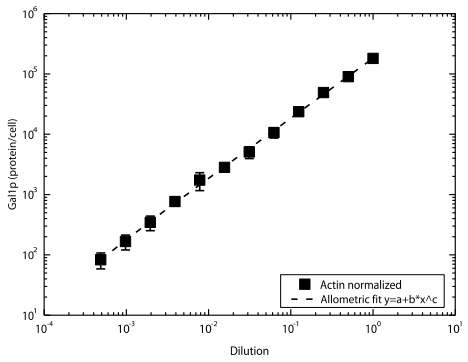

Figure 4.16: Actin normalized dilution series results of GAL1 protein (protein/cell). Cells have been grown overnight and refreshed in the morning afterwards a dilution series been made with a ΔGAL1 strain to check the precision of mass spectrometry.

When we apply this method for other Galactose network regulatory proteins we that our measurements show a linear range until 50-200 proteins per cell which is more than enough for us to proceed with our decay and binding experiments.

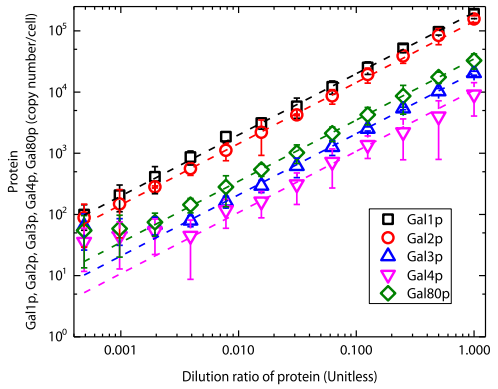

Figure 4.17: Actin normalized dilution series results for Galactose network proteins (protein/cell). Cells have been grown overnight and refreshed in the morning afterwards a dilution series been made with their deletion strains to check the precision of mass spectrometry.

Table 4.4: Coefficient of determination of MS/MS titration curves non-linear fitting using allometric $y=Ax^n$ where the power n is fixed to 1.

	Adj. R-Square
Gal1p	0.9957
Gal2p	0.9922
Gal3p	0.9922
Gal4p	0.7839
Gal80p	0.9858

4.3.1.1.3 Peptide selection and SRM development for Galactose regulatory genes

Things to take into account to choose best possible peptides for SRM; Number of hits, Best flyer peptides, Signal intensity, AP sequence tends to give nice signals, Post-translational modifications, Avoid M (oxidation).

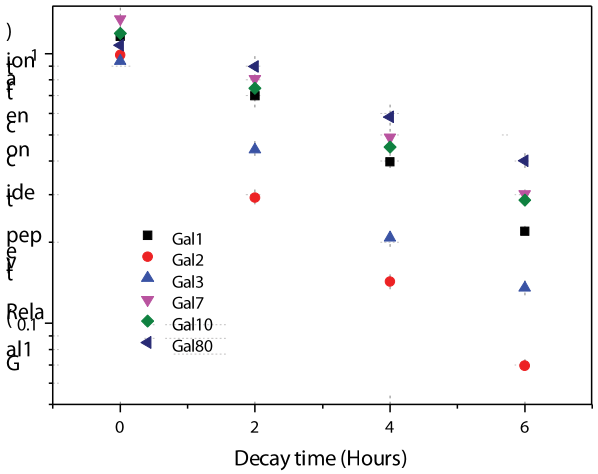

Figure 4.18: Relative peptide concentrations of GAL regulatory genes over time after glucose shut off at t=0.

Upper figure is the first decay measurement we have done using shotgun proteomics. We could not detect Gal4p which confirms the power of SRM measurements.

Table 4.5: Selected peptides from GAL regulatory genes to perform selected reaction monitoring MS/MS. Heavy aqua peptides have been ordered to measure absolute concentrations of GAL proteins.

Protein name	*Peptide sequence*	*Peptide length*
Gal1p	DYLTTSPVR	9
Gal1p	EALANEFYK	9
Gal1p	ICSIALSNGSYGSR	14
Gal1p	NPSITLINADPK	12
Gal1p	SHSEEVIVPEFNSSAK	16
Gal3p	DYLTTFPVR	9
Gal3p	NHEISFVIANTLVK	14
Gal3p	NPSITLTNADPK	12
Gal3p	SGFTVHEASTALNCSR	16
Gal3p	YPDLTDEELK	10
Gal4p	ISATSSSEESSNK	13
Gal4p	SQLEQDQNDHQSYEVK	16
Gal4p	VFESGSIILVTALHLLSR	18
Gal4p	ALLTGLFVQDNVNK	14
Gal4p	LLSSIEQACDICR	13
Gal80p	LYQSISDFHFNTK	13
Gal80p	NLVIDIHGTK	10
Gal80p	SSVSTVPNAAPIR	13
Gal80p	IETSIATIQR	10
Gal80p	NYNAIVGNIHR	11

We have selected the peptides in the upper table to measure in SRM after our shotgun measurement. The following subsections show the detected peptides for each regulatory GAL protein.

4.3.1.1.3.1 Gal1p

We have identified 30 unique Gal1p peptides using shotgun proteomics. We have covered 71% of the endogenous protein sequence.

Figure 4.19: Sequence coverage of Gal1p. Yellow highlighted peptides are the hits (identified peptides) using shotgun proteomics. Green highlighted aminoacids are candidates for posttranslational modification (Methylation, oxidation etc.).

4.3.1.1.3.2 Gal3p

We have identified 14 unique Gal1p peptides using shotgun proteomics. We have covered 43% of the endogenous protein sequence.

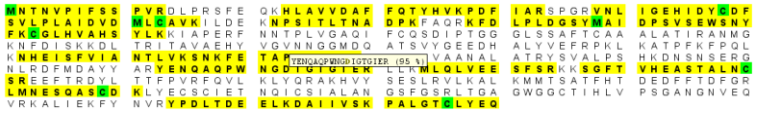

Figure 4.20: Sequence coverage of Gal3p. Yellow highlighted peptides are the hits (identified peptides) using shotgun proteomics. Green highlighted aminoacids are candidates for posttranslational modification (Methylation, oxidation etc.).

4.3.1.1.3.3 Gal4p

We have identified 5 unique Gal1p peptides using shotgun proteomics. We have covered 10% of the endogenous protein sequence. Gal4p peptide hit is much lower compared to Gal1p and Gal3p. This low number of coverage is not surprising since the endogenous Gal4p level is much lower than Gal1p and Gal3p.

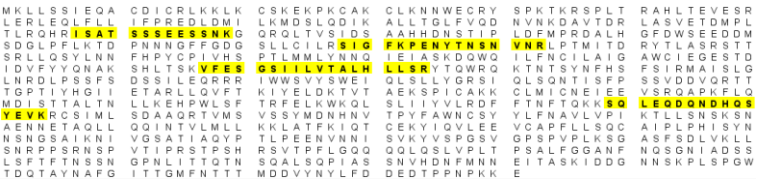

Figure 4.21: Sequence coverage of Gal1p. Yellow highlighted peptides are the hits (identified peptides) using shotgun proteomics.

4.3.1.1.3.4 Gal80p

We have identified 7 unique Gal1p peptides using shotgun proteomics. We have covered 17% of the endogenous protein sequence. Gal80p peptide hit, much like Gal4p, is much lower compared to Gal1p and Gal3p. This low number of coverage is not surprising since the endogenous Gal80p level is, similar to Gal4p, much lower than Gal1p and Gal3p.

Figure 4.22: Sequence coverage of Gal1p. Yellow highlighted peptides are the hits (identified peptides) using shotgun proteomics.

4.3.1.2 Flow cytometric measurements of fluorescence proteins

4.3.1.2.1 Using GFP fluorescent protein and measuring growth during decay experiments

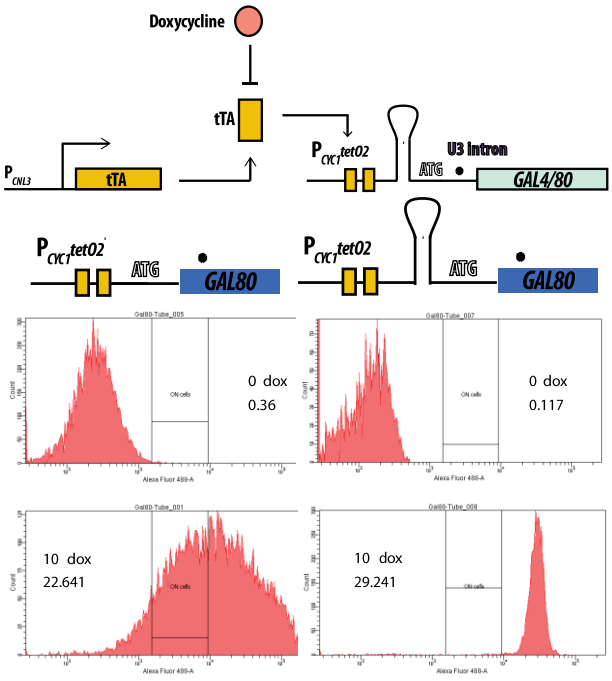

Figure 4.23: Efficient regulation of the proteins were achieved through synthetic regulation using a Tet OFF system. All the strains and plasmids were optimized for GAL regulatory proteins to get the largest dynamic range using tet OFF system.

We also used GFP fluorescence to measure if our decay experiments are working well. If the regulatory proteins decay we see a decrease in GFP fluorescence over time. This enables us to make sure that the experiments is working before we spend weeks to analyse respective RNA, LC-MS, and metabolic data.

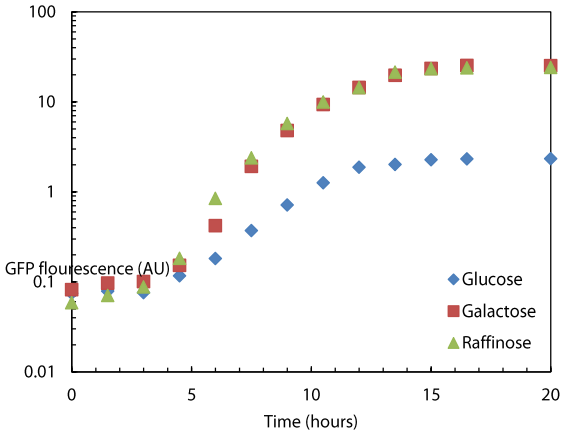

Figure 4.24: Increase in GAL network activity (GFP fluorescence) during Gal80p decay over time.

We have also checked the cell division time in order to make sure that the cells are growing.

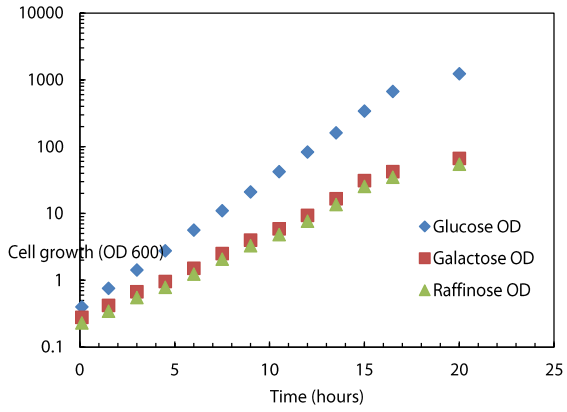

Figure 4.25: Increase in OD600 during Gal80p decay over time. Initial OD 600 was 0.4 we have diluted the samples every 1.5 hours (during sample taking) keeping the cell concentration lower than OD600=1 over the course of the whole experiment. For the figure cell growth value on the y-axis was determined by multiplying the new OD600 at each sample taking point by the dilution factor to determine the cell growth. The actual OD600 during the measurement was kept between 0.4 (after dilution $t=t_0$) and 0.8 (before dilution $t=t_0 + 1.5$ hours).

4.3.1.2.2 Input output methods and analysis

We have used flow cytometry to optimize our input output measurements (in section 2.4-GAL network analysis by using input/output matching).

4.3.1.2.2.1 Double colour for IO and ID strains

We have controlled the whether we can use fluorescence to measure the relative mRNA amount in the cell in order to optimize and rougly detect the bistability boundaries before measuring the mRNA responses.

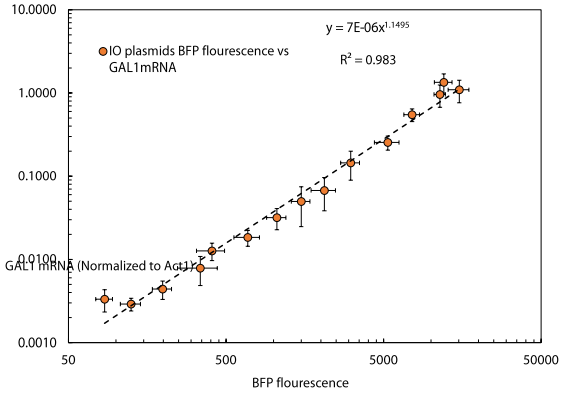

Figure 4.26: Relation between Gal1 mRNA and BFP using double colour flourescent method.

4.3.1.2.2.2 IO and ID measurements

Following figures show the day to day variation of the IO measurements that has been shown in Figure 2.40: Mapping of ΔGAL2ΔGAL3 strain steady states using Gal1p feedback opening. Cells grown for 24 hours at different Galactose concentrations and in a GAL1 mRNA gradient. There is no day to day variation which means the input output response reaches steady state after 24 hours.

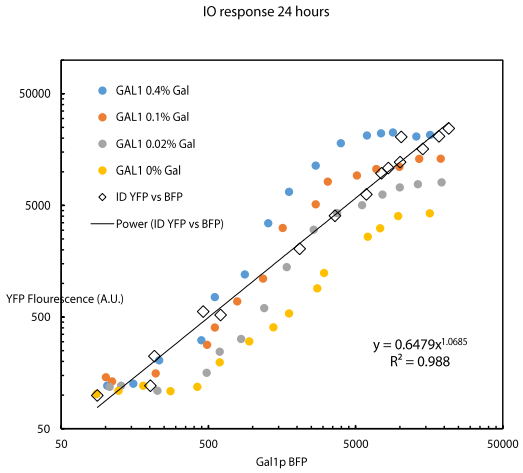

Figure 4.27: Input output response using dooble colour flourscence method (described in section 2.4.1). Cell were grown in a galactose and doxycycline gradient (Gal1p gradient) for 24 hours before measurement. OD600 was kept below 1 at all times.

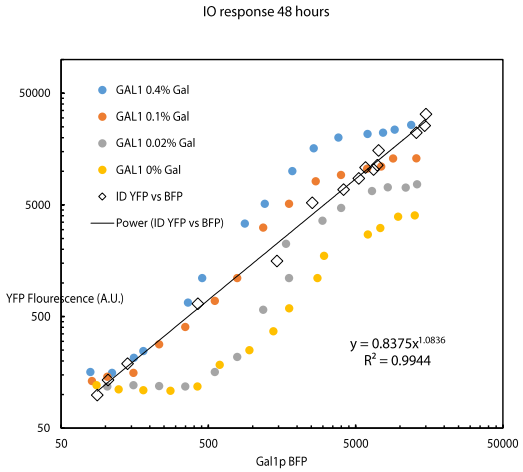

Figure 4.28: Input output response using dooble colour flourscence method (described in section 2.4.1). Cell were grown in a galactose and doxycycline gradient (Gal1p gradient) for 48 hours before measurement. OD600 was kept below 1 at all times.

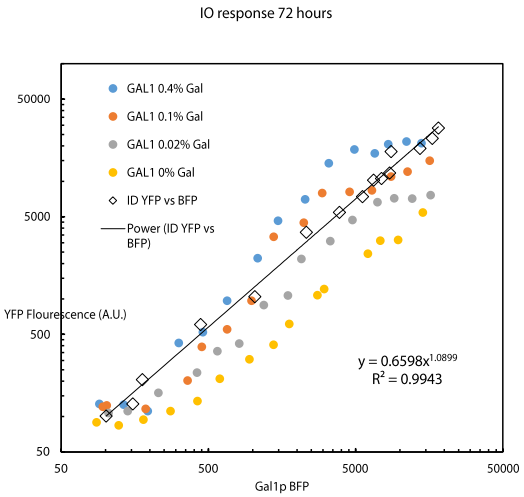

Figure 4.29: Input output response using dooble colour flourscence method (described in section 2.4.1). Cell were grown in a galactose and doxycycline gradient (Gal1p gradient) for 72 hours before measurement. OD600 was kept below 1 at all times.

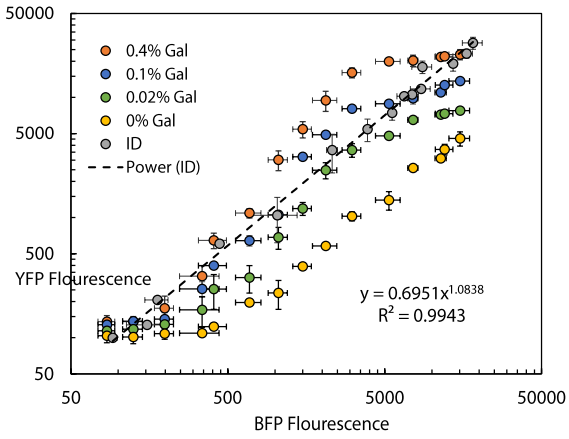

Figure 4.30: The average input output response using dooble colour flourscence method over 72 hours (described in section 2.4.1). Measurements have been done every 24 hours and OD600 was kept below 1 at all times.

4.3.2 RNA analysis

4.3.2.1 RNA isolation

RNA was isolated from each time point using RNeasy ® Mini-kit of QIAGEN ® with DNase I treatment (Qiagen). We included an optional DNase digestion step because the qPCR is a sensitive application and we wanted to avoid any genomic DNA.

4.3.2.2 Reverse transcription

The reverse transcription is a technique to synthetize cDNA using RNA as template. In the market there are several kits to performer the cDNA synthesis. We tested three of them to see which one gave us better results. We tested the QuantiTect Reverse Transcription Kit and SuperScript® Reverse Transcriptase with oligo octamers. We performed the reaction following the kit instructions.

4.3.2.3 RNA quantitation by quantitative real-time PCR (qPCR)

The quantitative PCR (qPCR) is robust technique to measure the gene expression [48]. The product of its amplifications is detected at the reaction progresses in "real-time". To monitor the PCR, we used the SYBR Green I Dye. This dye binds to the dsDNA. At the beginning of the reactions, only the qPCR primers region is dsDNA, therefore, the fluorescent signal is very weak. After several cycles and at the end of the elongation phase, the emitted fluorescence by the intercalated dyes is enough to be measure of the machine at 530 nm. We filled each well with 200 ng of cDNA of interest, 2 µl premixed of qPCR primers (1.5 µM), 5 µl of CyberGreen and until 10 µl with H_2O, between 2 and 2.8 µl depending on cDNA concentration. Then we span the plate of 1 min at 1000 rpm. To avoid errors in the quantifications, we chose two genes as reference: TFC1 and UBC6. TFC1 is one of six subunit of RNA polymerase III transcription initiation factor complex; and UBC6 is an ubiquitin-conjugating enzyme involved in endoplasmic reticulum-associated degradation. These genes are known as *house-keeping* genes due to constant level of expression. As the qPCR is an exponential reaction, the PCR product is double each cycle if the PCR is 100% efficient. To test if that was our case, we measured the efficiency of qPCR primers. We prepared 6, 10-fold serial dilution from cDNA and performed the qPCR. (Appendix: Oligos)

4.3.3 Metabolic measurements

One of the critical measurements we use in our transport and galactose sugar related experiments is to be able to measure the intracellular galactose concentration. We have used megazymes Raffinose/D-Galactose assay kit for our meas-

urements: https://secure.megazyme.com/Raffinose-D-Galactose-Assay-Kit. In our tests we were satisfied with the precision and the dynamic range of the assay.

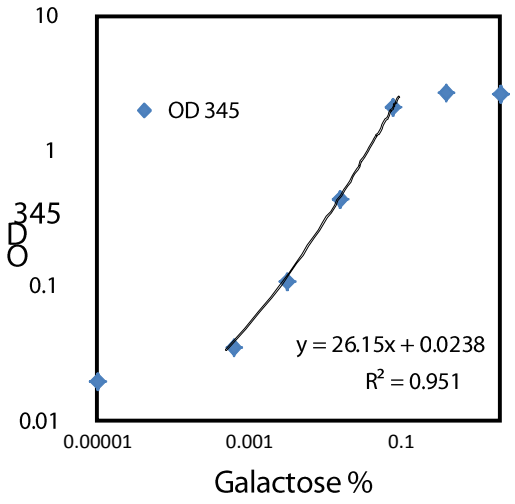

Figure 4.31: Samples containing different concentrations of galactose have been used to determine the dynamic range that we can measure by enzymatic reactions.

4.3.3.1 Sample preparation for intracellular galactose concentration measurements

Cells have been grown over night in 2% raffinose then 2% galactose have been added to the media and the change in the intracellular concentration has been measured over time.

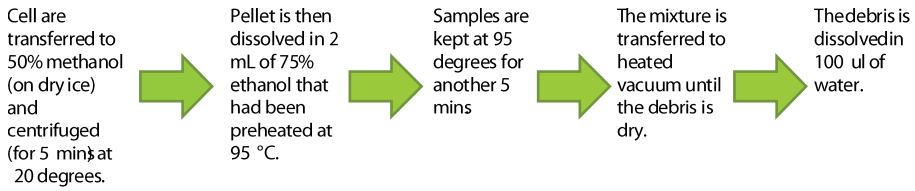

Figure 4.32: Scheme representing the sample preparation to measure intracellular galactose concentration.

Some of the limitations of the metabolic measurements are:

Metabolic reactions are extremely fast, so we should be very careful whilst treating the samples since the metabolic measurements unlike the protein decay are extremely fast.

The pellet size of the media is roughly 0.1% of the total culture at OD 1. We ought to work always with big volumes (roughly 50 ml) in order to get a pellet of 10-20ul.

There is always a danger of working with different sample sizes. We use different growing containers for our measurements. Although we have checked that growing in 96 well and Erlenmeyer does not affect the activation time so much one has to be careful and take the risk into consideration.

4.4 Data fitting

One big potential problem. Algebraic constrains not only makes the equations complicated but also makes the parameters even more correlated.

For our binding fitting we have used global fitting where we fit the parameters with both mRNA responses decay of the proteins.

Data fitting has been done with MathWorks® product SimBiology software and Global Optimization Toolbox. The global minima in our models has been found using the genetic algorithm. The algorithm repeatedly modifies a population of individual solutions. At each step, the genetic algorithm (GA) randomly selects individuals from the current population and uses them as parents to produce the children for the next generation. Over successive generations, the population "evolves" toward an optimal solution. GA is preferred in highly non-linear problems.

4.4.1 *GAL* network mRNA decay

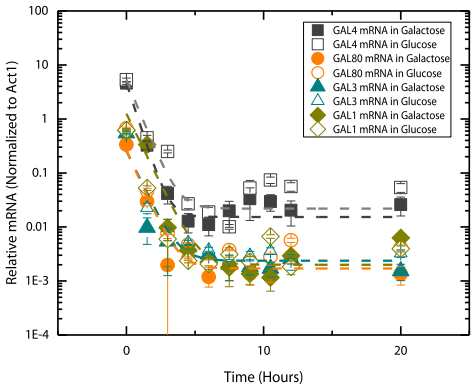

Figure 4.33 GAL mRNA decay over time after addition of 10 ug/ul of doxycycline. Half-life gal4 mRNA: 7.55 min.

Equation 4.1: $\frac{d}{dt} GAL_{mRNA}(t) = b_{GAL\,mRNA} - \gamma_{GAL\,mRNA}\, GAL_{mRNA}(t),\ GAL_{mRNA}(0) = GAL\ mRNA_0.$

4.4.2 *GAL* regulatory protein decay rates

4.4.2.1 Gal4p decay

We assume that Gal80p is produced at a basal rate of b_{804} and is degraded at the rate of γ_{G4}. The production and decay process for the total concentration of Gal4p ($G4_{PT}$) is simply modelled by the following differential equation,

Equation 4.2: $$\frac{d}{dt} G4_{PT}(t) = b_{G4} - \gamma_{G4}\, G4_{PT}(t),$$

$$G4_{PT}(0) = G4_0.$$

The exact solution of system the is given by the following function of time

Equation 4.3: $$G4_{PT}(t) = Y_0 + A\, e^{R_0 t},$$

Where

Equation 4.4: $R_0 = -\gamma_{G4},\ A = G4_0 - \frac{b_{G4}}{\gamma_{G4}},\ Y_0 = \frac{b_{G4}}{\gamma_{G4}}.$

In what follows, we perform the nonlinear regression using equation above and estimate the parameter values given in equations. We first investigate the raw data measured by proteomics.

4.4.2.2 Gal80p decay

We assume that Gal80p is produced at a basal rate of b_{804} and is degraded at the rate of γ_{G80}. The production and decay process for the total concentration of Gal80p ($G80_{PT}$) is simply modelled by the following differential equation,

Equation 4.5: $$\frac{d}{dt}G80_{PT}(t) = b_{G80} - \gamma_{G80}\, G80_{PT}(t),$$
$$G80_{PT}(0) = G80_0.$$

The exact solution of the system is given by the following function of time

Equation 4.6: $$G80_{PT}(t) = Y_0 + A\, e^{R_0 t},$$

Where

Equation 4.7: $$R_0 = -\gamma_{G4},\ A = G80_0 - \frac{b_{G80}}{\gamma_{G80}},\ Y_0 = \frac{b_{G80}}{\gamma_{G80}}.$$

In what follows, we perform the nonlinear regression using equation above and estimate the parameter values given in the equations. We first investigate the raw data measured by proteomics.

4.4.2.3 Gal3p decay

Efficient regulation of the key transcription factor Gal3p is reached by synthetic Tet-OFF system. Addition of doxycycline stops the expression of the transcriptional repressor (Gal80p) and permits us to determine its decay rate. Translational interference due to a stable remaining mRNA could impact on the Gal3p protein decay rate. Indeed the decay rate of *gal3* mRNA is quite fast compared to the protein data.

Equation 4.8: $\frac{d}{dt}G3_{PT}(t) = b_{G3} - \gamma_{G3}\, G3_{PT}(t),\ G3_{PT}(0) = G3_0.$

The exact solution of the system is given by the following function of time

Equation 4.9: $G3_{PT}(t) = Y_0 + A\, e^{R_0 t},$

Where

Equation 4.10: $R_0 = -\gamma_{G3},\ A = G3_0 - \frac{b_{G3}}{\gamma_{G3}},\ Y_0 = \frac{b_{G3}}{\gamma_{G3}}.$

In what follows, we perform the nonlinear regression using equations above and estimate the parameter values.

4.4.2.4 Gal1p decay

We assume that Gal1p is produced at a basal rate of b_{G1} and is degraded at the rate of γ_{G1}. The production and decay process for the total concentration of Gal4p ($G1_{PT}$) is simply modelled by the following differential equation,

Equation 4.11: $\frac{d}{dt}G1_{PT}(t) = b_{G1} - \gamma_{G1}\, G80_{PT}(t)$,

$$G1_{PT}(0) = G1_0.$$

The exact solution of the system is given by the following function of time

Equation 4.12: $G1_{PT}(t) = Y_0 + A\, e^{R_0 t}$,

Where

Equation 4.13: $R_0 = -\gamma_{G80},\ A = G1_0 - \frac{b_{G1}}{\gamma_{G1}},\ Y_0 = \frac{b_{G1}}{\gamma_{G1}}$.

In what follows, we perform the nonlinear regression using equations above and estimate the parameter values.

4.4.3 Gal4p homodimerization and Gal4p$_{Homodimer}$-DNA dissociation constant

Following table shows the parameter estimation for Gal4p binding to DNA in galactose. Proteomics data was fit against the mRNA data to determine the 1st layer parameters using equations in section 4.4.3.1, 4.4.3.2, and 4.4.3.3.

Table 4.6: Parameter estimation of the 1st layer fitting in galactose.

Parameter name	Estimate	Standard error
'Vyfp'	0.947993231	13.82178725
'vyfp'	0.898146687	12.59202608
'byfp'	0.00139512	1.024283535
'kon'	4.28915E-05	0.122874865
'koff'	0.596398803	39.03034441
'b7'	0.010122674	1.366286751
'v7'	1.615104737	48.43049858
'V7'	1.72945652	55.81973967
'Kd4'	1.09080073	92.42985894
'v4'	0.502846205	0.024892962
'b4'	1.004535421	0.230762053
'bgcy1'	0.029066093	1.013873751
'Vgcy1'	0.303410879	9.408027925
'vgcy1'	0.814583675	20.28989084
'c'	35.43154674	63.77494018
'b'	0.334082329	38.32345536

Following table shows the parameter estimation for Gal4p binding to DNA in glucose.

Table 4.7: Parameter estimation of the 1st layer fitting in glucose.

Parameter name	Estimate	Standard error
'Vyfp'	0.511322059	125.831
'vyfp'	1.13195172	279.777
'byfp'	0.000572028	2.63922
'kon'	4.91099E-05	0.71549
'koff'	0.794355163	223.679
'b7'	0.003371428	2.95328
'v7'	1.422315909	519.153
'V7'	1.13211311	410.869
'Kd4'	1.332891213	1385.27
'v4'	0.494680296	0.07509
'b4'	0.910851663	0.75192
'bgcy1'	0.034486831	4.00269
'Vgcy1'	0.489876277	77.0774
'vgcy1'	0.816176213	89.94
'c'	36.72189392	280.047
'b'	0.402750311	82.2171

4.4.3.1 Algebraic constrains

$$Gal4p_{total} = Gal4p_{free} + 2\,C4p_{complex-homodimer}$$

4.4.3.2 Set of ODE equations for protein levels

$$\frac{dGal4p_{free}}{dt} = \text{basal}_{G4pfree} - 2G4p_{\text{free}}{}^{2} kon_{\text{G4pG4p}} + 2C4p_{complex}\, koff_{\text{G4pG4p}} - {}^{\gamma}{}_{G4pfree}\,\text{G4p}_{\text{free}}$$

$$\frac{dC4p_{complex-homodimer}}{dt} = \text{basal}_{C4pcomplex} - 2C4p_{\text{free}}\, kon_{\text{G4pG4p}} + 2C4p_{complex}\, koff_{\text{G4pG4p}} - {}^{\gamma}{}_{C4pcomplex}\,\text{C4p}_{complex}$$

4.4.3.3 Set of ODE equations for mRNA responses

4.4.3.3.1 Fitting mRNA response using Hill function

In our earlier modelswe have tried different options. We have used Hill function to write the promoter saturation.

$$\frac{dGCY1_{mRNA}}{dt} = \text{basal}_{GCY1mRNA} - V_{max}\frac{C4p_{complex}{}^{nGCY1}}{C4p_{complex}{}^{nGCY1} + Kd_{C4p-DNA}{}^{nGCY1}} - \gamma_{GCY1mRNA}\,\text{GCY1}_{\text{mRNA}}$$

$$\frac{dGAL7_{mRNA}}{dt} = \text{basal}_{GAL7mRNA} - V_{max}\frac{C4p_{complex}{}^{nGAL7}}{C4p_{complex}{}^{nGAL7} + Kd_{C4p-DNA}{}^{nGAL7}} - \gamma_{GAL7mRNA}\text{GAL7}_{\text{mRNA}}$$

$$\frac{dGFP_{mRNA}}{dt} = \text{basal}_{GFPmRNA} - V_{max}\frac{C4p_{complex}{}^{nGAL1}}{C4p_{complex}{}^{nGAL1} + Kd_{C4p-DNA}{}^{nGAL1}} - \gamma_{GFPmRNA}\,\text{GFP}_{\text{mRNA}}$$

When we were deciding on the homodimerization and DNA-Gal4p fitting. One thing for sure was to fit with GCY1 promoter. Since GCY1 has one binding site its Hill coefficient should be one. This gave us the range that we can expect for both homodimerization and the Gal4p DNA binding.

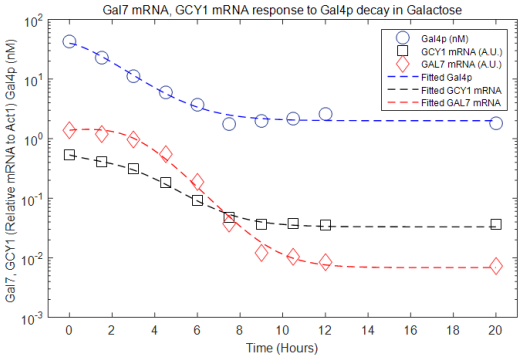

Figure 4.34: Global fit for GCY1 and GAL7 relative mRNA level. GCY1 hill coefficient: 0.995 and GAL7 hill coefficient: 1.238. Gal4p homodimerization: 7.339 µM and Gal4p$_{\text{homodimer}}$-DNA binding: 1.256.

One of the disadvantage of this model was the fact that in the upper layers we would have had problems taking the competitive inhibitor (Gal80p) binding. For GCY1 we would not have had problems to write the saturation function but with multiple binding sites of GAL7 and GFP (controlled by GAL1 promoter) adding the competitive inhibitor to the denominator was a challenge.

4.4.3.3.2 Fitting mRNA response using Adair equation

We decided to use adair equation to write the promoter saturation functions where we with different promoter binding states we can clearly define the Gal80p binding to multiple sites.

$$\frac{dGCY1_{mRNA}}{dt} = \text{basal}_{GCY1mRNA} - V_{max}\frac{C4p_{complex}\,/\,Kd_{C4p-DNA}}{1 + C4p_{complex}\,/\,Kd_{C4p-DNA}} - \gamma_{GCY1mRNA}\,\text{GCY1}_{\text{mRNA}}$$

For a single binding site the GCY1 ODE looks almost the same if we assume n_{GCY1}=1.

4.4.3.3.2.1 Introducing the b factor

When we have written the GAL7 promoter saturation function we have added a b factor. Since the activation in multiple binding site promoter vary with different numbers of bount protein we have introduced a b factor where we reduce the Vmax in case only one protein binds to the promoter instead of multiple.

$$\frac{dGAL7_{mRNA}}{dt} = \text{basal}_{GAL71mRNA} - V_{max}\frac{2b\frac{C4p_{complex}}{Kd_{C4p-DNA}} + c(\frac{C4p_{complex}}{Kd_{C4p-DNA}})^2}{1 + 2\frac{C4p_{complex}}{Kd_{C4p-DNA}} + c(\frac{C4p_{complex}}{Kd_{C4p-DNA}})^2} - \gamma_{GAL7mRNA}\text{GAL7}_{\text{mRNA}}$$

$$\frac{dGAL1/GFP_{mRNA}}{dt} = \text{basal}_{GAL71mRNA} - V_{max}\frac{4b\frac{C4p_{complex}}{Kd_{C4p-DNA}} + 2c(\frac{C4p_{complex}}{Kd_{C4p-DNA}})^2 + c^2(\frac{C4p_{complex}}{Kd_{C4p-DNA}})^3 + c^3(\frac{C4p_{complex}}{Kd_{C4p-DNA}})^4}{1 + 4\frac{C4p_{complex}}{Kd_{C4p-DNA}} + 2c(\frac{C4p_{complex}}{Kd_{C4p-DNA}})^2 + c^2(\frac{C4p_{complex}}{Kd_{C4p-DNA}})^3 + c^3(\frac{C4p_{complex}}{Kd_{C4p-DNA}})^4} - \gamma_{GAL7mRNA}\text{GAL1/GFP}_{\text{mRNA}}$$

We have written the promoter states and the cooperative binding of Gal4p to GAL1 promoter.

4.4.3.3.3 Comparing models using Akaike's Information Criterion (AIC)

The Akaike information criterion (AIC) is a measure of the relative quality of statistical models for a given set of data. Given a collection of models for the data, AIC estimates the quality of each model, relative to each of the other models. Hence, AIC provides a means for model selection. AIC is founded on information theory: it offers a relative estimate of the information lost when a given model is used to represent the process that generates the data. In doing so, it deals with the trade-off between the goodness of fit of the model and the complexity of the model. The following formula is used to calculate AIC:

Equation 4.14: Akaike's Information Criterion

$$AIC = N.ln\left(\frac{RSS}{N}\right) + 2K$$

Where N is the number of observations, K is the number of free parameters, and RSS is the sum of the squares of the vertical distances of the points from the

fitted data. In biological samples N is generally small. When this is the case the corrected AIC is more accurate.

Equation 4.15: A second order (corrected) AIC

$$AIC_{corrected} = AIC + \frac{2K(K+1)}{N-K-1}$$

The change in AIC_c tells you the likelihood that a model is correct. The model with the lower AIC is more likely to be correct and we calculate how likely by using the following equation:

Equation 4.16: The relative likelihood or the evidence ratio for model selection using $AIC_{corrected}$.

$$Evidence\ Ratio = \frac{Probability\ that\ model\ 1\ is\ correct}{Probability\ that\ model\ 2\ is\ correct} = \frac{1}{e^{-0.5.\Delta AIC_c}}$$

The evidence ratio is based on the absolute difference between AIC_c scores, not the relative difference. We have compared the Adair model (Model 1, 4.4.3.3.2) and Hill model (Model 2, 4.4.3.3.1) using AIC. Leaving all parameters free in our fit, we found that Adair model is more likely to be correct compared to Hill model.

Table 4.8: AIC values for hill and adair model leaving all the parameters free.

$AIC^1_{corrected}$	166.62
$AIC^2_{corrected}$	176.09
ΔAIC	9.47

Using Table 4.8 and Equation 4.16 we calculated the evidence ratio to be 113.62. This means that Adair model (Model 1) is 113.62 times more likely to be correct than the Hill model (Model 2).

4.4.4 Gal80p homodimerization and $Gal80p_{Homodimer}$-$Gal4p_{Homodimer}$ dissociation constant

One main reason for the emergence of high ultra-sensitivity is the inappropriate choice of parameter values (variations in the value of Kd4 and Kd80). In the following, I will reproduce all the above results for another set of parameter values. These new parameter values are achieved by performing the nonlinear regression on the data set for Gal80p total concentration and GAL7mRNA using the Hill-like response function. The following diagrams have been constructed for the Hill-like function with n=1 and n=2 and the Adair equation for different values of Kd80.

The new parameter set reduces the ultra-sensitivity significantly. Again, as is clear, the Adair response is less steep for different values of alpha.

Any decrease in the value of Kd80 will increase the sensitivity of the output with respect to the input. Sensitivity of the response to this parameter is very high. Likewise, sensitivity will go up as the value of Kd4 goes down. I think the reason is that the complex G4-G80 binds with the same dissociation constant (Kd4) to the promoter as the single protein G4; however, the sensitivity of the response to this parameter is very low. Proteomics data was fit against the mRNA data to determine the 1st layer parameters using equations in section 4.4.4.1, 4.4.4.2, and 4.4.4.3. Following table shows the parameter estimation for Gal80p binding to Gal4p in galactose.

Table 4.9: Parameter estimation of the 2nd layer fitting in galactose.

	Parameter estimation	SE
'kon480'	1.98873747	9.59729
'koff480'	2.367879441	1.48401
'kon80'	1.284025417	9.14862
'koff80'	8.678683632	7.94927
'v80'	0.515054684	0.05305
'alpha'	0.006065307	476.181
'b'	0.516890377	8186.59
'c'	12.01689608	11.2274
'b2'	0.757738391	34.8942
'c2'	31.93483377	22.281
'alpha2'	0.224084454	23.2057
'Kd480'	0.155760157	67.6772

Following table shows the parameter estimation for Gal80p binding to Gal4p in glucose.

Table 4.10: Parameter estimation of the 2nd layer fitting in glucose.

	Parameter estimation	SE
'kon480'	2.18761	10.557
'koff480'	3.09543	1.63242
'kon80'	1.55235	10.0635
'koff80'	15.2343	8.74419
'v80'	0.47518	0.05835
'alpha'	0.00945	523.799
'b'	0.3154	9005.24
'c'	21.568	12.3501
'b2'	0.4956	38.3837
'c2'	39.5184	24.5091
'alpha2'	0.24649	25.5262
'Kd480'	0.35143	74.4449

4.4.4.1 Algebraic constrains in the 2nd layer

$$Gal4p_{total} = Gal4p_{free} + 2\,C4p_{complex-homodimer} + 2\,C480p_{complex-heterodimer}$$

$$Gal80p_{total} = Gal80p_{free} + 2\,C80p_{complex-homodimer} + 2\,C480p_{complex-heterodimer}$$

4.4.4.2 Set of ODE equations for protein levels

$$\frac{dGal4p_{free}}{dt} = \text{basal}_{G4pfree} - 2G4p_{\text{free}}{}^{2} kon_{\text{G4pG4p}} + 2C4p_{complex}\, koff_{\text{G4pG4p}} - \gamma_{G4pfree}\,\text{G4p}_{\text{free}}$$

$$\frac{dC4p_{complex-homodimer}}{dt} = \text{basal}_{C4pcomplex} - 2C4p_{\text{free}}\, kon_{\text{G4pG4p}} + 2C4p_{complex}\, koff_{\text{G4pG4p}} - \gamma_{C4pcomplex}\,\text{C4p}_{complex}$$

$$\frac{dGal80p_{free}}{dt} = \text{basal}_{G80pfree} - 2G80p_{\text{free}}{}^{2} kon_{\text{G4pG4p}} + 2C80p_{complex}\, koff_{\text{G4pG4p}} - \gamma_{G80pfree}\,\text{G4p}_{\text{free}}$$

$$\frac{dC80p_{complex-homodimer}}{dt} = G80p_{\text{free}}{}^{2} kon_{\text{G4pG4p}} - C80p_{complex} koff_{\text{G4pG4p}} - \gamma_{G80pfree}\,\text{G4p}_{\text{free}} - \gamma_{C4pcomplex}\,\text{C4p}_{complex}$$

$$\frac{dC480p_{complex-quadromer}}{dt} = C80p_{complex-homodimer}\, C4p_{complex-homodimer}\; kon_{\text{C4pC80p}} - C480p_{complex-quadromer}\, koff_{\text{C4pC80p}} - \gamma_{C4pcomplex}\,\text{C480p}_{complex-quadromer}$$

4.4.4.3 Set of ODE equations for mRNA responses

$$\frac{dGCY1_{mRNA}}{dt} = \text{basal}_{GCY1mRNA} - V_{max}\,\frac{C4p_{complex}/Kd_{C4p-DNA}}{1 + C4p_{complex}/Kd_{C4p-DNA} + C480p_{complex}/Kd_{C4p-80p-DNA}} - \gamma_{GCY1mRNA}\,\text{GCY1}_{\text{mRNA}}$$

4.4.4.3.1 Introducing the α factor

For GAL7 we need consider the fact that there will be an incomplete repression when two Gal4p homodimers and a one Gal80p homodimer is bount to the promoter. We have introduced the term α in order to take the incomplete repression in promoters with multiple binding sites into account. For GAL7 promoter we can write the following states:

G4 + D00 = D01
G4 + D00 = D10
G4 + D01 = D11
G4 + D10 = D11
G80 + D11= D12
G80 + D11 = D21
G80 + D12 = D22
G80 + D21 = D22

D represents the DNA, and the digits (0, 1, and 2) show the number of proteins (G4, G80) bound to either of the binding sites. The fractional saturation function will then be given by the following expression (DT denotes the total DNA).

$$DT\,\frac{\left(\frac{C4}{Kd4}\right)^2\left(1+2\frac{C480}{Kd80}\right)}{1+2\frac{C4}{Kd4}+\left(\frac{C4}{Kd4}\right)^2+2\left(\frac{C4}{Kd4}\right)^2\frac{C480}{Kd80}+\left(\frac{C480}{Kd80}\right)^2}$$

The response function for *GAL7mRNA* (with an extra factor $\boldsymbol{\alpha}$) will be as follows

$$b+V\,\frac{\left(\frac{C4}{Kd4}\right)^2\left(1+2\,\boldsymbol{\alpha}\frac{C480}{Kd480}\right)}{1+2\frac{C4}{Kd4}+\left(\frac{C4}{Kd4}\right)^2+2\left(\frac{C4}{Kd4}\right)^2\frac{C480}{KdC480}+\left(\frac{C480}{Kd480}\right)^2}$$

So we can write the ODE function for GAL7 as follows:

$$\frac{dGAL7_{mRNA}}{dt}=\text{basal}_{GAL71mRNA}-V_{max}\,\frac{2b\frac{C4p_{complex}}{Kd_{C4p-DNA}}+c(\frac{C4p_{complex}}{Kd_{C4p-DNA}})^2+2\boldsymbol{\alpha}(\frac{C4p_{complex}}{Kd_{C4p-DNA}})^2\frac{C480p_{complex}}{Kd_{C480p-DNA}}}{1+2\frac{C4p_{complex}}{Kd_{C4p-DNA}}+c(\frac{C4p_{complex}}{Kd_{C4p-DNA}})^2}-{}^{\gamma}{}_{GAL7mRNA}\,\text{GAL7}_{\text{mRNA}}$$

4.4.4.3.2 Selecting the promoter function for GAL1 promoter

Gal1 promoter function brings us with a tricky question since it has 4 binding sites how are we going to write the partial repression and different Vmax for different numbers of protein bound.

In the first layer we have used either Hill function or Adair's with c enhancement factor. Although including the b factor in the equation was not straightforward since GAL1 has different strengths of binding sites. GAL1's high binding sites created a large equation we were able to fit it without any problems since the binding was straight forward. Now we have to also address the incomplete re-pression.

$$\frac{dGAL1/GFP_{mRNA}}{dt}=\text{basal}_{GAL71mRNA}-V_{max}\,\frac{4b\frac{C4p_{complex}}{Kd_{C4p-DNA}}+2c(\frac{C4p_{complex}}{Kd_{C4p-DNA}})^2+c^2(\frac{C4p_{complex}}{Kd_{C4p-DNA}})^3+c^3(\frac{C4p_{complex}}{Kd_{C4p-DNA}})^4}{1+4\frac{C4p_{complex}}{Kd_{C4p-DNA}}+2c(\frac{C4p_{complex}}{Kd_{C4p-DNA}})^2+c^2(\frac{C4p_{complex}}{Kd_{C4p-DNA}})^3+c^3(\frac{C4p_{complex}}{Kd_{C4p-DNA}})^4}-{}^{\gamma}{}_{GAL7mRNA}\,\text{GAL1/GFP}_{\text{mRNA}}$$

Since GAL1 and GAL7 has a similar dynamic range and their response is quite often is quite often same we can perhaps modify the GAL7 equation we have

and write it for GAL1 with different enhancement factor and an incomplete repression factor.

$$\frac{dGAL1_{mRNA}}{dt} = \text{basal}_{GAL71mRNA} - V_{max}\frac{2b_{GAL1}\frac{C4p_{complex}}{Kd_{C4p-DNA}} + c_{GAL1}(\frac{C4p_{complex}}{Kd_{C4p-DNA}})^2 + 2\boldsymbol{\alpha_{GAL1}}(\frac{C4p_{complex}}{Kd_{C4p-DNA}})^2\frac{C480p_{complex}}{Kd_{C480p-DNA}}}{1 + 2\frac{C4p_{complex}}{Kd_{C4p-DNA}} + c_{GAL1}(\frac{C4p_{complex}}{Kd_{C4p-DNA}})^2 + 2(\frac{C4p_{complex}}{Kd_{C4p-DNA}})^2\frac{C480p_{complex}}{Kd_{C480p-DNA}} + (\frac{C480p_{complex}}{Kd_{C480p-DNA}})^2} - {}^{\gamma}{}_{GAL7mRNA}\text{GAL1}_{\text{mRNA}}$$

4.4.4.3.3 Cooperative binding of the Gal80p to Gal4p

We have also integrated enhancement factor d for a possible cooperative binding of Gal80p to Gal4p.

$$\frac{2\,b_{GAL1}\frac{C4p_{complex}}{Kd_{C4p-DNA}} + c_{GAL1}(\frac{C4p_{complex}}{Kd_{C4p-DNA}})^2 + 2\boldsymbol{\alpha_{GAL1}}(\frac{C4p_{complex}}{Kd_{C4p-DNA}})^2\frac{C480p_{complex}}{Kd_{C480p-DNA}}}{1 + 2\frac{C4p_{complex}}{Kd_{C4p-DNA}} + c_{GAL1}(\frac{C4p_{complex}}{Kd_{C4p-DNA}})^2 + 2(\frac{C4p_{complex}}{Kd_{C4p-DNA}})^2\frac{C480p_{complex}}{Kd_{C480p-DNA}} + d_{GAL1}(\frac{C480p_{complex}}{Kd_{C480p-DNA}})^2}$$

In our fits we have found d to be 1.

4.4.5 Gal3p-Gal80p dissociation constant

Following table shows the parameter estimation for Gal3p binding rates to both Gal80p and galactose.

Table 4.11: Fitted parameters of mRNA response to Gal3p gradient at different galactose concentrations. The measurement was performed at steady state after 24 hours of Galactose addition to the media.

	Parameter estimation	std error
kon380a	7.70162	44133.1
koff380a	1.99969	38177.4
kon3a	3.96E-08	1.6E-09
koff3a	0.60821	31172.2
kon380	0.23674	0.0373
koff380	2.8618	713.177

4.4.5.1.1 Algebraic constrains

$$Gal4p_{total} = Gal4p_{free} + 2\,C4p_{complex-homodimer} + 2\,C480p_{complex-heterodimer}$$

$$Gal80p_{total} = Gal80p_{free} + 2\,C80p_{complex-homodimer} + 2\,C480p_{complex-quadromer} + C380p_{complex-heterodimer}$$

$$Gal3p_{total} = Gal3p_{free} + C380p_{complex-heterodimer}$$

4.4.5.2 Set of ODE equations for protein levels

$$\frac{dGal4p_{free}}{dt} = \text{basal}_{G4pfree} - 2G4p_{\text{free}}{}^{2}kon_{\text{G4pG4p}} + 2C4p_{complex}koff_{\text{G4pG4p}} - \gamma_{G4pfree}\,\text{G4p}_{\text{free}}$$

$$\frac{dC4p_{complex-homodimer}}{dt} = \text{basal}_{C4pcomplex} - 2C4p_{\text{free}}kon_{\text{G4pG4p}} + 2C4p_{complex}koff_{\text{G4pG4p}} - \gamma_{C4pcomplex}\,\text{C4p}_{complex}$$

$$\frac{dGal80p_{free}}{dt} = \text{basal}_{G80pfree} - 2G80p_{\text{free}}{}^{2}kon_{\text{G4pG4p}} + 2C80p_{complex}koff_{\text{G4pG4p}} - G80p_{\text{free}}\,G3p_{\text{free}}kon_{\text{G3pG80p}} + C380p_{complex}koff_{\text{G3pG80p}} - \gamma_{G80pfree}\,\text{G4p}_{\text{free}}$$

$$\frac{dC80p_{complex-homodimer}}{dt} = G80p_{\text{free}}{}^{2}kon_{\text{G4pG4p}} - C80p_{complex}koff_{\text{G4pG4p}} - \gamma_{G80pfree}\,\text{G4p}_{\text{free}} - \gamma_{C4pcomplex}\,\text{C4p}_{complex}$$

$$\frac{dC480p_{complex-quadromer}}{dt} = C80p_{complex-homodimer}\,C4p_{complex-homodimer}\;\; kon_{\text{C4pC80p}} - C480p_{complex-quadromer}\,koff_{\text{C4pC80p}} - \gamma_{C4pcomplex}\,\text{C480p}_{complex-quadromer}$$

$$\frac{dC380p_{complex-heterodimer}}{dt} = G80p_{free}G3p_{free}\,kon_{\text{G3pG80p}} - C380p_{complex-heterodimer}\,koff_{\text{G3pG80p}} - \gamma_{C4pcomplex}\,\text{C380p}_{complex-heterodimer}$$

4.4.6 Gal1p-Gal80p dissociation constant

For Gal1p the set of ODE equations are exactly the same as Gal3p (see section 4.4.5). Following table shows the parameter estimation for Gal1p binding rates to both Gal80p and galactose.

Table 4.12: Fitted parameters of mRNA response to Gal1p gradient at different galactose concentrations. The measurement was performed at steady state after 24 hours of Galactose addition to the media.

	Parameter estimation	std error
kon180a	2.90665	2427320
koff180a	3.32709	2099757
kon1a	1.07E-08	8.65E-08
koff1a	0.30657	1714473
kon180	2.32E-04	2.05156
koff180	0.02215	39224.7

4.4.7 Fitting of the GAL1 input output data

Table 4.13: Parameter estimation of input output response in ΔGAL2ΔGAL3 strain steady states using Gal1p feedback opening.

	Parameter Est	Std Error		
kon180a	450.93	1259.16	Kd_{1a80} (nM)	1.529
koff180a	702.44	1157.42		
kon1a	0.70	10.85	K_{d1a} (μM)	38.94
koff1a	30705.56	1150113.15		
kon180	20110.05	12101.16	Kd_{180} (nM)	73.14
koff180	1470907.15	129452.15		

Input output equations are quite similar to 3rd layer fittings but here we need to add the translation rates to our equations. Since we measure mRNA as our input and output.

$$\frac{dGal4p_{free}}{dt} = \Gamma_{G80\ translation\ rate} G4_{mRNA} - 2G4p_{\text{free}}{}^{2} kon_{\text{G4pG4p}} + 2C4p_{complex}\, koff_{\text{G4pG4p}} - \gamma_{G4pfree}\, \text{G4p}_{\text{free}}$$

$$\frac{dC4p_{complex-homodimer}}{dt} = 2G4p_{\text{free}}{}^{2} kon_{\text{G4pG4p}} - 2C4p_{complex}\, koff_{\text{G4pG4p}} - \gamma_{C4pcomplex}\, \text{C4p}_{complex}$$

$$\frac{dGal80p_{free}}{dt} = \Gamma_{G80\ translation\ rate} G80_{mRNA} - 2G80p_{\text{free}}{}^{2} kon_{\text{G80pG80p}} + 2C80p_{complex} koff_{\text{G80pG80p}} - G80p_{\text{free}}\, G1p_{\text{free}} kon_{\text{G1pG80p}} + C180p_{complex} koff_{\text{G1pG80p}} - \gamma_{G80pfree}\, \text{G80p}_{\text{free}}$$

$$\frac{dC80p_{complex-homodimer}}{dt} = G80p_{\text{free}}{}^{2} kon_{\text{G80pG80p}} - C80p_{complex} koff_{\text{G80pG80p}} - \gamma_{G80pfree}\, \text{G80p}_{\text{free}} - \gamma_{C80pcomplex}\, \text{C80p}_{complex}$$

$$\frac{dC480p_{complex-quadromer}}{dt} = C80p_{complex-homodimer}\, C4p_{complex-homodimer}\; kon_{\mathrm{C4pC80p}} - C480p_{complex-quadromer}\; koff_{\mathrm{C4pC80p}} - \gamma_{C4pcomplex}\,\mathrm{C480p}_{complex-quadromer}$$

$$\frac{dG1p_{free}}{dt} = \Gamma_{G1\ translation\ rate}\, G1_{mRNA} - \gamma_{G1pfree}\,\mathrm{G1p}_{free} - G1p_{free} Galactose_{intracellular}\; kon_{\mathrm{G1pGalactose}} + C1Ap_{complex}\, koff_{\mathrm{G1pGalactose}} - G1p_{free} G80p_{free}\, kon_{\mathrm{G1pG80p}} + C180p_{complex-heterodimer}\, koff_{\mathrm{G1pG80p}}$$

$$\frac{dC1Ap_{complex}}{dt} = G1p_{free} Galactose_{intracellular}\; kon_{\mathrm{G1pGalactose}} - C1Ap_{complex}\, koff_{\mathrm{G1pGalactose}}$$

$$\frac{dC1A80p_{complex-heterodimer}}{dt} = C1Ap_{G1p-galactose}\, G80p_{free}\, kon_{\mathrm{C1ApG80p}} - C1A80p_{complex}\, koff_{\mathrm{C1ApG80p}}$$

$$\frac{dDox_{doxycycline\ concentration}}{dt} = Dox_{conc}\,\gamma_{Doxycycline\ decay\ rate}$$

$$\frac{dC180p_{complex-heterodimer}}{dt} = G1p_{free} G80p_{free}\, kon_{\mathrm{G1pG80p}} - C180p_{complex-heterodimer}\, koff_{\mathrm{G1pG80p}}$$

$$\frac{dYFP_{mRNA}}{dt} = \mathrm{basal}_{YFPmRNA} - V_{max}\frac{2b_{YFP}\frac{C4p_{complex}}{Kd_{C4p-DNA}} + c_{YFP}(\frac{C4p_{complex}}{Kd_{C4p-DNA}})^2 + 2\boldsymbol{\alpha_{YFP}}(\frac{C4p_{complex}}{Kd_{C4p-DNA}})^2\frac{C480p_{complex}}{Kd_{C480p-DNA}}}{1 + 2\frac{C4p_{complex}}{Kd_{C4p-DNA}} + c_{GAL1}(\frac{C4p_{complex}}{Kd_{C4p-DNA}})^2 + 2(\frac{C4p_{complex}}{Kd_{C4p-DNA}})^2\frac{C480p_{complex}}{Kd_{C480p-DNA}} + (\frac{C480p_{complex}}{Kd_{C480p-DNA}})^2} - \gamma_{YFPmRNA}\,\mathrm{YFP}_{\mathrm{mRNA}}$$

$$\frac{dGAL4p_{mRNA}}{dt} = \mathrm{basal}_{G4mRNA} - \gamma_{GAL4pmRNA}\,\mathrm{GAL4}_{\mathrm{mRNA}}$$

$$\frac{dGAL80_{mRNA}}{dt} = \mathrm{basal}_{GAL80mRNA} - V_{max}\frac{C4p_{complex}/Kd_{C4p-DNA}}{1 + C4p_{complex}/Kd_{C4p-DNA} + C480p_{complex}/Kd_{C4p-80p-DNA}} - \gamma_{GAL80mRNA}\,\mathrm{GAL80}_{\mathrm{mRNA}}$$

$$\frac{dGAL1_{mRNA}}{dt} = \mathrm{basal}_{GAL1mRNA} - V_{max}\frac{Dox_{intracellular}^{\ nDox}}{Dox_{intracellular}^{\ nDox} + Kd_{tTA-DNA}^{\ nDox}} - \gamma_{GAL1mRNA}\,\mathrm{GAL1}_{\mathrm{mRNA}}$$

$$Gal4p_{total} = Gal4p_{free} + 2\,C4p_{complex-homodimer} + 2\,C480p_{complex-heterodimer}$$

$$Gal80p_{total} = Gal80p_{free} + 2\,C80p_{complex-homodimer} + 2\,C480p_{complex-quadromer} + C180p_{complex-heterodimer} + C1A80p_{complex-heterodimer}$$

$$Gal1p_{total} = Gal1p_{free} + C180p_{complex-heterodimer} + C1Ap_{complex-galactose} + C1A80p_{complex}$$

4.4.7.1 *GAL* protein translation rates

We integrated the translation rates in our final input output model using our MS and qPCR measurements.

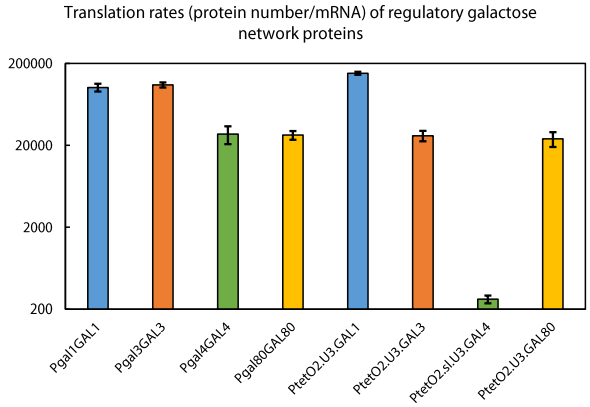

Figure 4.35: Translation rates of GAL regulatory proteins.

Table 4.14: Peptide selection for the targeted mass spectrometry.

	Protein number per cell/Relative mRNA	Protein concentration (nM)/Relative mRNA
Pgal1GAL1	101650	4085.62
Pgal3GAL3	109271	4391.9
Pgal4GAL4	27410	1101.7
Pgal80GAL80	26646	1070.97
PtetO2.U3.GAL1	151605	6093.45
PtetO2.U3.GAL3	26204	1053.2
PtetO2.sl.U3.GAL4	264	10.6242
PtetO2.U3.GAL80	23977	963.704

4.4.8 Fitting of transition rates

The transition rate, which represents the probability that cell switches from its current state of activity to the other one, is used to characterize the stochastic stability of a bistable system.

The ON and OFF cell population was separated by a threshold value. The threshold was set equal to the geometric mean of the fluorescence of the non-induced and maximally induced cell populations, measured at 96 hours 0.4% galactose.

When the noise of the system is high, transitions occur in both directions. Consequently, the percentage of ON cells stays between 4% and 96%. In these cases, we performed fitting with equations describing bi-directional transitions.

For the low initial condition: $r(t) = \frac{k_{up} - k_{up}\, e^{-t(k_{up}+k_{down})}}{k_{up}+k_{down}}$

For the high initial condition: $r(t) = \frac{k_{up}+k_{down}\, e^{-t(k_{up}+k_{down})}}{k_{up}+k_{down}}$

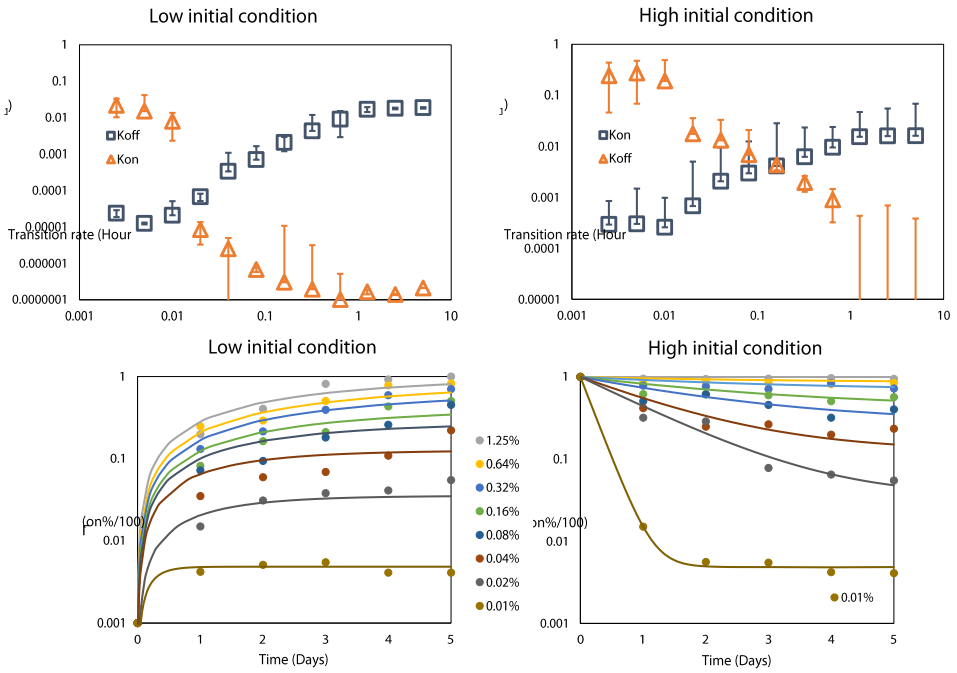

Figure 4.36: Transition rates of reduced GAL network over 5 days at different galactose concentrations.

In the upper figure the transition rates have been fit for both LOW initial condition and HIGH initial condition. Results are compatible though different. In order to reduce the standard error we did a global fit of transition rates using both data set.

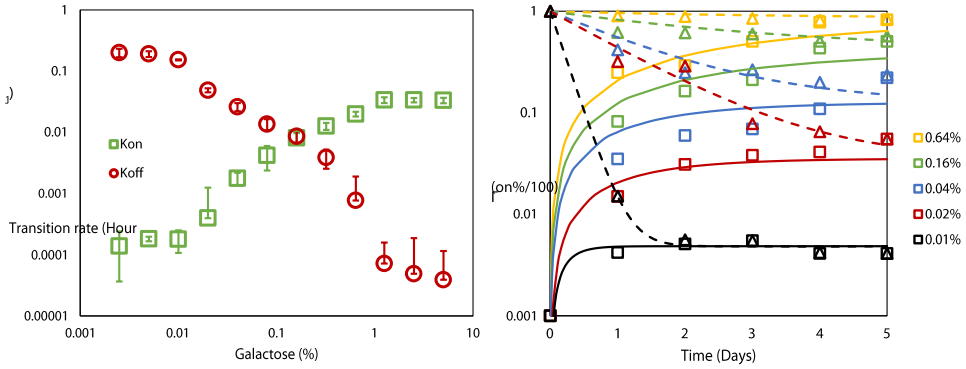

Figure 4.37: Global fit of the transition rates of reduced GAL network over 5 days at different galactose concentrations.

4.4.9 Galactose consumption

$$k_{cat} = \frac{V_{max}}{E_0}$$

K_m=0.25mM, K_{cat}=20s^{-1}=1200min^{-1}

$$\frac{dx}{dy} = -k_{cat} E_0 \frac{x}{K_m + x}$$

Galactose intracellular

1mM=0.18 g/l

X (0) =2mM

Assume intracellular and extracellular galactose concentration reaches steady state fast and is the same. The intracellular enzyme concentration: 0.01mM

Cell fraction in a yeast culture where at OD600 1 is 0.1% this makes total enzyme concentration in the medium:

$$0.01mM \times \frac{0.1}{100} = 0.00001mM$$

Under saturating conditions:

$$\frac{dx}{dt} = -0.00001 * 1200 = -0.012 {}^{mM}/_{min}$$

A galactose induced wild type cell should consume roughly 1mM of galactose per hour.

4.4.10 Galactose transport

We came to the final transport equation by using the proof of Widda's formula:

$$S + E \underset{k-}{\overset{k+}{\longleftrightarrow}} Y$$

Carrier is not the rate limiting step in the transport progress

Equation 4.17: $0 = k_+ SE + k\_ Y$

The number of carriers are constant since they are on the membrane.

Equation 4.18: $E + Y = E_0$

Equation 4.19: $K_d == {k_+}/{k\_} = {SE}/{Y}$

Equation 4.20: $K_d = {E_0 S}/{(K_d + S)}$

We assume that the current density considered positive in the inward direction and by using the integrated version of the Fick's law,

Equation 4.21: $\mathrm{J} = \left({D_y}/{L}\right)(Y_{external} - Y_{internal})$

By replacing the ligand we get Widda's formula:

Equation 4.22: $\mathrm{J} = \frac{D_y E_0}{L}\left(\frac{S_{external}}{K_d + S_{external}} - \frac{S_{internal}}{K_d + S_{internal}}\right)$

Chapter 5 Supplementary documents

5.1 Raw data

5.1.1 Isolation of *GAL4*

BY4742 *ΔGAL80 Saccharomyces cerevisiae* strain with pRS306.$P_{CYC1\ (tetO2)}$.Gal4, pRS303.P_{GAL1}.GFP, pRS402.P_{CNL3}.tTA plasmids integrated.

Overnight cultures grown in 0.5% galactose and 0 ug/ul of doxycycline, then they have been refreshed for 3 hours in the morning. Gal4mRNA transcription has been stopped with addition of 10 ug/ul of doxycycline.

Gal4p decay in Galactose		repetition	repetition #2	average	SD		
Time (Hours)	Gal4p number/cell)	(Protein				average nM	SD
0	993	1348	821	1054.0810	219.4056	42.3666	8.8186
1.5	534	703	483	573.4100	93.9904	23.0470	3.7778
3	294	341	201	278.7807	58.2043	11.2050	2.3394
4.5	161	194	93	149.4413	42.0805	6.0065	1.6913
6	100	123	58	93.5000	26.8732	3.7580	1.0801
7.5	59	41	31	43.7800	11.7356	1.7596	0.4717
9	41	39	66	48.7447	12.2354	1.9592	0.4918
10.5	39	69	54	54.1511	12.0629	2.1765	0.4848
12	40	77	73	63.4783	16.3757	2.5514	0.6582
20	38	55	43	45.2400	7.2302	1.8183	0.2906

Relative mRNA in galactose (rt-PCR A.U.)							
Time (Hours)	GFP (4BS)	GAL1 (4BS)	GAL3 (1BS)	GAL4	GAL7 (2BS)	GAL80 (1BS)	GCY1 (1BS)
0	1.1257	0.5288	0.0792	4.5975	1.3859	0.0000	0.5325
1.5	1.1654	0.4866	0.0733	0.3255	1.1817	0.0000	0.4038
3	1.0874	0.4036	0.0634	0.2416	0.9665	0.0000	0.3123
4.5	0.9401	0.3347	0.0617	0.1628	0.5416	0.0000	0.1806
6	0.5073	0.1781	0.0448	0.1104	0.1853	0.0000	0.0918
7.5	0.1594	0.0897	0.0232	0.0699	0.0380	0.0000	0.0474
9	0.0625	0.0401	0.0142	0.0533	0.0121	0.0000	0.0366
10.5	0.0194	0.0223	0.0149	0.0643	0.0104	0.0000	0.0379
12	0.0078	0.0087	0.0115	0.0604	0.0085	0.0000	0.0356
20	0.0046	0.0065	0.0103	0.0560	0.0073	0.0000	0.0360

Overnight cultures grown in 0.5% galactose+0.2% glucose and 0 ug/ul of doxycycline, then they have been refreshed for 3 hours in the morning. Gal4mRNA transcription has been stopped with addition of 10 ug/ul of doxycycline.

Gal4p decay in Glucose		repetition	repetition #2	average	SD		
Time (Hours)	Gal4p (Protein number/cell)					average nM	SD
0	1056	1492	1203	1250.4483	180.9923	50.2592	7.2746
1.5	587	755	603	648.4467	75.6153	26.0630	3.0392
3	280	367	311	319.4475	35.8785	12.8395	1.4421
4.5	140	180	143	154.4103	18.1299	6.2062	0.7287
6	82	94	68	81.1831	10.6176	3.2630	0.4268
7.5	40	59	54	51.1173	7.8812	2.0546	0.3168
9	32	61	66	52.8477	15.2022	2.1241	0.6110
10.5	31	77	39	49.1450	19.9371	1.9753	0.8013
12	45	51	64	53.1888	8.0833	2.1378	0.3249
24	39	44	77	53.2173	16.9580	2.1390	0.6816

Relative mRNA in glucose (rt-PCR A.U.)							
Time (Hours)	GFP (4BS)	Gal1 (4BS)	Gal3 (1BS)	Gal4	Gal7 (2BS)	Gal80 (1BS)	Gcy1 (1BS)
0	0.4092	0.1487	0.0282	5.3179	0.8146	0.0000	0.2778
1.5	0.4572	0.1052	0.0263	0.4478	0.7581	0.0000	0.2357
3	0.4833	0.0975	0.0226	0.2501	0.6834	0.0000	0.1819
4.5	0.3394	0.0689	0.0217	0.2416	0.2390	0.0000	0.0759
6	0.0854	0.0373	0.0115	0.1639	0.0625	0.0000	0.0354
7.5	0.0220	0.0109	0.0051	0.1009	0.0072	0.0000	0.0154
9	0.0063	0.0035	0.0026	0.0526	0.0049	0.0000	0.0100
10.5	0.0025	0.0013	0.0023	0.0739	0.0043	0.0000	0.0121
12	0.0017	0.0003	0.0020	0.0560	0.0030	0.0000	0.0125
24	0.0012	0.0009	0.0020	0.0537	0.0030	0.0000	0.0129

5.1.2 Isolation of *GAL80*

BY *ΔGAL1ΔGAL3 Saccharomyces cerevisiae* strain with pRS306.$P_{CYC1\ (tetO2)}$.Gal80, pRS303.P_{GAL1}.GFP, pRS402.P_{CNL3}.tTA plasmids integrated.

Overnight cultures grown in 0.5% galactose and 0 ug/ul of doxycycline, then they have been refreshed for 3 hours in the morning. Gal80mRNA transcription has been stopped with addition of 10 ug/ul of doxycycline (Following table).

Gal4p decay in Galactose

	Protein/cell		repetition		Average (nM)			
Time (Hours)	Gal4p	Gal80p	Gal4p	Gal80p	Gal4p (nM)	Gal80p (nM)	Gal4p SD	Gal80p SD
0	497	1103	501	1406	20.07	50.42	0.08	6.07
1.5	519	683	582	795	22.12	29.71	1.26	2.25
3	523	402	295	396	16.42	16.03	4.58	0.13
4.5	490	254	603	164	21.96	8.40	2.26	1.81
6	489	143	305	155	15.97	5.99	3.70	0.25
7.5	463	80	398	61	17.30	2.83	1.30	0.40
9	526	51	279	54	16.17	2.10	4.97	0.06
10.5	597	60	425	58	20.54	2.37	3.45	0.04
12	712	52	492	63	24.20	2.31	4.42	0.23

Relative mRNA in galactose (rt-PCR A.U.)

Time (Hours)	GFP (4BS)	GAL1 (4BS)	GAL2 (3BS)	GAL3 (1BS)	GAL4	GAL7 (2BS)	GAL80 (1BS)	GCY1 (1BS)
0	0.0271	0.0000	0.0010	0.0000	0.0132	0.0028	0.0460	0.0173
1.5	0.0392	0.0000	0.0011	0.0000	0.0123	0.0034	0.0030	0.0176
3	0.0655	0.0000	0.0014	0.0000	0.0130	0.0065	0.0020	0.0257
4.5	0.1972	0.0000	0.0041	0.0000	0.0117	0.0246	0.0026	0.0449
6	0.8813	0.0000	0.0193	0.0000	0.0091	0.1077	0.0012	0.0896
7.5	2.2079	0.0000	0.2099	0.0000	0.0152	0.5369	0.0020	0.1951
9	4.4157	0.0000	0.2741	0.0000	0.0129	1.2613	0.0014	0.2937
10.5	5.7863	0.0000	0.3863	0.0000	0.0147	1.6445	0.0015	0.4499
12	9.7314	0.0000	0.6587	0.0000	0.0174	2.6901	0.0016	0.7133

Overnight cultures grown in 0.5% galactose + 0.2% glucose and 0 ug/ul of doxycycline, then they have been refreshed for 3 hours in the morning. Gal80mRNA transcription has been stopped with addition of 10 ug/ul of doxycycline (Following table).

Gal4p decay in Glucose								
	Protein/cell		repetition		Average (nM)			
Time (Hours)	Gal4p	Gal80p	Gal4p	Gal80p	Gal4p (nM)	Gal80p (nM)	Gal4p SD	Gal80p SD
0	192	1250	157	1508	7.02	55.42	0.71	5.18
1.5	232	647	201	705	8.71	27.19	0.63	1.17
3	213	347	146	380	7.20	14.59	1.35	0.67
4.5	161	184	197	130	7.18	6.30	0.72	1.09
6	175	93	246	75	8.46	3.38	1.43	0.35
7.5	156	50	128	38	5.69	1.78	0.56	0.24
9	163	31	284	33	8.97	1.29	2.44	0.06
10.5	204	40	156	67	7.23	2.15	0.97	0.54
12	153	42	188	74	6.85	2.33	0.71	0.65

Relative mRNA in glucose (rt-PCR A.U.)								
Time (Hours)	GFP (4BS)	GAL1 (4BS)	GAL2 (3BS)	GAL3 (1BS)	GAL4	GAL7 (2BS)	GAL80 (1BS)	GCY1 (1BS)
0	0.0096	0.0000	0.0006	0.0000	0.0032	0.0012	0.0666	0.0069
1.5	0.0162	0.0000	0.0008	0.0000	0.0051	0.0014	0.0070	0.0073
3	0.0246	0.0000	0.0008	0.0000	0.0049	0.0024	0.0076	0.0104
4.5	0.0597	0.0000	0.0012	0.0000	0.0036	0.0075	0.0047	0.0208
6	0.2907	0.0000	0.0121	0.0000	0.0040	0.0623	0.0024	0.0428
7.5	0.6849	0.0000	0.0651	0.0000	0.0047	0.1665	0.0037	0.0811
9	1.2607	0.0000	0.0988	0.0000	0.0037	0.3013	0.0024	0.1567
10.5	1.8729	0.0000	0.1218	0.0000	0.0046	0.5187	0.0028	0.1314
12	1.9287	0.0000	0.1305	0.0000	0.0035	0.5332	0.0020	0.1160

5.1.3 Isolation of *GAL3*

5.1.3.1 Gal3p decay

BY *ΔGAL1ΔGAL2 Saccharomyces cerevisiae* strain with pRS306.$P_{CYC1\ (tetO2)}$.Gal3, pRS303.P_{GAL1}.GFP, pRS402.P_{CNL3}.tTA plasmids integrated.

Overnight cultures grown in 0.5% galactose and 0 ug/ul of doxycycline, then they have been refreshed for 3 hours in the morning. Gal3mRNA transcription has been stopped with addition of 10 ug/ul of doxycycline (Following table).

Gal3p decay in Galactose						
	Protein/cell			Protein concentration (nM)		
Time (Hours)	Gal4p	Gal80p	Gal3p	Gal4p	Gal80p	Gal3p
0	692	4719	13059	27.83	189.69	524.87
1.5	757	2964	8918	30.44	119.14	358.43
3	624	2915	5318	25.08	117.17	213.74
4.5	640	3001	2839	25.71	120.62	114.10
6	585	2599	1884	23.53	104.46	75.74
7.5	570	1774	926	22.93	71.29	37.24
9	627	1497	558	25.18	60.19	22.43
10.5	615	1013	284	24.72	40.70	11.43
12	831	721	131	33.40	28.98	5.28
mRNA response to Gal3p decay in Galactose						
Time (Hours)	Gal3	Gal4	Gal7	Gal80	GFP	GCY1
0	0.5471	0.0199	1.0570	0.1780	2.2038	0.5094
1.5	0.0098	0.0167	0.8526	0.1416	2.1287	0.4461
3	0.0054	0.0165	0.2466	0.0723	0.7846	0.1934
4.5	0.0042	0.0176	0.0347	0.0477	0.0910	0.0398
6	0.0031	0.0183	0.0058	0.0361	0.0141	0.0205
7.5	0.0020	0.0158	0.0012	0.0340	0.0103	0.0041
9	0.0018	0.0202	0.0009	0.0427	0.0139	0.0036
10.5	0.0017	0.0176	0.0005	0.0354	0.0108	0.0021
12	0.0026	0.0458	0.0009	0.0377	0.0175	0.0024

Overnight cultures grown in 0.5% galactose + 0.2% glucose and 0 ug/ul of doxycycline, then they have been refreshed for 3 hours in the morning. Gal3mRNA transcription has been stopped with addition of 10 ug/ul of doxycycline (Following table).

Gal3p decay in Glucose						
	Protein/cell			Protein concentration (nM)		
Time (Hours)	Gal4p	Gal80p	Gal3p	Gal4p	Gal80p	Gal3p
0	228	644	16563	9.17	25.90	665.73
1.5	250	307	8819	10.03	12.33	354.47
3	206	245	4923	8.27	9.87	197.88
4.5	211	215	2764	8.48	8.63	111.10
6	193	184	1974	7.76	7.40	79.36
7.5	188	126	985	7.56	5.08	39.58
9	207	123	427	8.30	4.93	17.14
10.5	203	119	202	8.15	4.80	8.14
12	201	110	110	8.10	4.43	4.41
mRNA response to Gal3p decay in Glucose						
Time (Hours)	Gal3	Gal4	Gal7	Gal80	GFP	GCY1
0	0.5804	0.0115	0.6429	0.0242	1.2570	0.2709
1.5	0.0226	0.0092	0.6236	0.0185	1.1810	0.2461
3	0.0097	0.0081	0.3392	0.0155	1.1212	0.1442
4.5	0.0052	0.0070	0.1187	0.0114	0.5744	0.0640
6	0.0038	0.0096	0.0529	0.0094	0.3923	0.0305
7.5	0.0024	0.0097	0.0074	0.0085	0.2643	0.0161
9	0.0030	0.0136	0.0046	0.0055	0.1862	0.0076
10.5	0.0036	0.0205	0.0052	0.0049	0.0472	0.0061
12	0.0021	0.0114	0.0031	0.0061	0.0450	0.0074

5.1.3.2 Gal3p gradient at steady state

BY *ΔGAL1ΔGAL2 Saccharomyces cerevisiae* strain with pRS306.$P_{CYC1\ (tetO2)}$.Gal3, pRS303.P_{GAL1}.GFP, pRS402.P_{CNL3}.tTA plasmids integrated. For 24 hours cultures were grown in 0% and 0.5% galactose and 0 ug/ul of doxycycline, then they have been refreshed for 3 hours in the morning. Gal3mRNA transcription has been regulated with doxycycline (Following table).

YFP Fluorescence Galactose				MS/MS (nM)	RNA 0.40% Galactose				0% Galactose			
0.40%	0.10%	0.02%	0%	Gal3p	GAL3	GAL80	GAL7	GCY1	GAL3	GAL80	GAL7	GCY1
174	134	252	182	0.51	0.0031	0.0389	0.0045	0.0992	0.0048	0.0198	0.0021	0.0603
247	190	299	188	0.75	0.0042	0.0408	0.0035	0.0891	0.0051	0.0206	0.0018	0.0618
212	163	313	220	0.28	0.0025	0.0411	0.0029	0.0954	0.0025	0.0181	0.0018	0.0508
188	144	337	303	1.51	0.0071	0.0395	0.0043	0.0892	0.0082	0.0206	0.0031	0.0517
250	192	278	404	2.02	0.0120	0.0453	0.0065	0.0984	0.0102	0.0225	0.0021	0.0628
689	530	281	511	5.18	0.0201	0.0597	0.0504	0.1191	0.0259	0.0266	0.0020	0.0652
4380	3369	1506	613	15.13	0.0875	0.1207	0.5322	0.2509	0.0928	0.0289	0.0025	0.0754
19400	14923	7037	749	41.18	0.5510	0.3345	2.1666	0.8011	0.5586	0.0374	0.0118	0.1066
29920	23015	16785	1055	98.45	1.2483	0.5322	3.5064	1.3104	1.3519	0.0701	0.0640	0.1446
34980	26908	21659	1405	111.19	1.5637	0.5322	3.5315	1.2968	1.4142	0.0818	0.0918	0.1678
36360	27969	24637	1725	161.42	1.6644	0.4747	3.4943	1.2790	1.6133	0.0888	0.2273	0.1955
35460	27277	24622	1866	179.13	1.9053	0.5396	3.9417	1.4641	1.6818	0.0983	0.3164	0.2726

5.1.4 Isolation of *GAL1*

5.1.4.1 Gal1p decay

BY *ΔGAL2ΔGAL3 Saccharomyces cerevisiae* strain with pRS306.$P_{CYC1\ (tetO2)}$.Gal1, pRS303.P_{GAL1}.GFP, pRS402.P_{CNL3}.tTA plasmids integrated. Data has been combined to reach full dynamic range with and without stemloop constructs. Overnight cultures grown in 0.5% galactose and 0 ug/ul of doxycycline, then they have been refreshed for 3 hours in the morning. Gal1mRNA transcription has been stopped with addition of 10 ug/ul of doxycycline (Following table).

Gal1p decay in Galactose						
	Protein/cell			Protein concentration (nM)		
Time (Hours)	Gal1p	Gal4p	Gal80p	Gal1p	Gal4p	Gal80p
0	96111	433	1534	3862.99	17.39	61.67
1.5	77804	436	1534	3127.18	17.50	61.67
3	41190	408	1227	1655.57	16.41	49.33
4.5	22884	538	1534	919.76	21.62	61.67
6	13730	386	1227	551.86	15.51	49.33
7.5	9153	388	1227	367.90	15.60	49.33
9	4577	547	614	183.95	22.00	24.67
10.5	2244	410	609	90.17	16.46	24.48
12	1287	444	583	51.71	17.86	23.44
13.5	509	504	384	20.47	20.24	15.44

mRNA response						
Time (Hours)	Gal1	Gal4	Gal7	Gal80	GFP	GCY1
0	0.6088	0.0175	0.5236	0.0575	1.6945	0.3617
1.5	0.0337	0.0196	0.4045	0.0548	1.2698	0.3167
3	0.0098	0.0206	0.1514	0.0474	0.4399	0.1373
4.5	0.0037	0.0142	0.0403	0.0379	0.2289	0.0283
6	0.0022	0.0194	0.0096	0.0370	0.0941	0.0146
7.5	0.0018	0.0223	0.0028	0.0285	0.0559	0.0029
9	0.0014	0.0172	0.0011	0.0313	0.0374	0.0025
10.5	0.0012	0.0126	0.0010	0.0315	0.0274	0.0015
12	0.0029	0.0548	0.0011	0.0318	0.1029	0.0017
13.5	0.0063	0.0164	0.0008	0.0306	0.0294	0.0022

Overnight cultures grown in 0.5% galactose + 0.2% glucose and 0 ug/ul of doxycycline, then they have been refreshed for 3 hours in the morning. Gal1mRNA transcription has been stopped with addition of 10 ug/ul of doxycycline (Following table).

Gal1p decay in Glucose	Protein/cell			Protein concentration (nM)		
Time (Hours)	Gal1p	Gal4p	Gal80p	Gal1p	Gal4p	Gal80p
0	90601	151	2033	3641.53	6.05	81.72
1.5	51016	177	1820	2050.48	7.12	73.14
3	35495	117	986	1426.65	4.70	39.64
4.5	21005	148	740	844.27	5.94	29.73
6	14546	142	581	584.64	5.70	23.34
7.5	8902	159	354	357.79	6.40	14.25
9	4009	141	320	161.15	5.67	12.85
10.5	2991	189	314	120.22	7.60	12.62
12	1984	161	355	79.76	6.47	14.28

mRNA response						
Time (Hours)	Gal1	Gal4	Gal7	Gal80	GFP	GCY1
0	0.6234	0.0102	0.7448	0.0634	1.8404	0.2276
1.5	0.0527	0.0094	0.6162	0.0616	1.1212	0.2067
3	0.0060	0.0099	0.6066	0.0548	0.4852	0.1611
4.5	0.0024	0.0070	0.3408	0.0538	0.2335	0.0937
6	0.0021	0.0080	0.2874	0.0459	0.1040	0.0556
7.5	0.0031	0.0073	0.0516	0.0333	0.0805	0.0235
9	0.0023	0.0103	0.0124	0.0289	0.0783	0.0114
10.5	0.0067	0.0095	0.0116	0.0276	0.0715	0.0061
12	0.0018	0.0086	0.0093	0.0243	0.0608	0.0093

5.1.4.2 Gal1p gradient at steady state (input output method)

BY *ΔGAL2ΔGAL3 Saccharomyces cerevisiae* strain with pRS306.$P_{GAL1\ (tetO4)}$.Gal1 (see section 4.1.2.1.1.1), pRS402.P_{CNL3}.rtTA plasmids integrated. For 24 hours cultures were grown in 0% galactose and doxycycline gradient, then they have been refreshed for 3 hours in the morning. Gal1 mRNA transcription has been regulated with doxycycline (Following table).

0% Galactose	RNA				MS/MS			Fluorescence	
Dox	GAL1	GAL80	GAL7	GCY1	Gal1p	Gal4p	Gal80p	BFP	YFP
0.0001	0.0058	0.0285	0.0011	0.0891	8.45	21.05	13.57	423	109
0.0002	0.0085	0.0298	0.0009	0.0974	14.51	26.54	17.37	726	108
0.0005	0.0108	0.0275	0.0011	0.0946	12.54	18.25	16.81	627	118
0.0010	0.0185	0.0309	0.0011	0.1082	19.84	30.82	15.12	992	131
0.0020	0.0354	0.0380	0.0019	0.1255	31.50	23.36	17.54	1575	249
0.0039	0.0528	0.0443	0.0059	0.1943	68.12	28.43	25.48	3406	468
0.0078	0.0972	0.0550	0.0094	0.2373	152.12	29.29	30.71	7606	673
0.0156	0.2245	0.0581	0.0191	0.2852	299.87	17.47	33.41	14994	1253
0.0313	0.6507	0.0601	0.0328	0.3425	785.15	26.34	31.12	39258	2064
0.0625	0.8736	0.0598	0.0431	0.3519	1465.54	29.77	30.15	73277	3167
0.1250	1.1212	0.0665	0.0510	0.3829	1812.45	31.08	32.84	90623	3400
0.2500	1.1461	0.0625	0.0540	0.3993	2167.15	23.66	31.29	108358	3905

BY *ΔGAL2ΔGAL3 Saccharomyces cerevisiae* strain with pRS306.$P_{GAL1\ (tetO4)}$.Gal1 (see section 4.1.2.1.1.1), pRS402.P_{CNL3}.rtTA plasmids integrated. For 24 hours cultures were grown in 0.5% galactose and doxycycline gradient, then they have been refreshed for 3 hours in the morning. Gal1 mRNA transcription has been regulated with doxycycline (Following table).

0.5% Galactose	RNA				MS/MS			Fluorescence	
Dox	GAL1	GAL80	GAL7	GCY1	Gal1p	Gal4p	Gal80p	BFP	YFP
0.0001	0.0038	0.0339	0.0054	0.1128	2.69	30.84	17.51	135	189
0.0002	0.0031	0.0351	0.0057	0.0975	4.28	38.89	22.41	214	201
0.0005	0.0058	0.0398	0.0070	0.1072	6.24	26.74	18.17	312	465
0.0010	0.0180	0.0420	0.0109	0.1384	19.11	45.15	19.59	956	1357
0.0020	0.0325	0.0481	0.0191	0.1735	42.84	34.23	23.09	2142	3391
0.0039	0.0472	0.0513	0.0393	0.2355	62.40	41.65	24.15	3120	7582
0.0078	0.1921	0.0711	0.2333	0.3104	191.10	42.91	34.81	9555	18600
0.0156	0.2842	0.0897	0.4269	0.4909	360.75	54.18	40.75	18038	25000
0.0313	0.6462	0.1191	0.6976	0.6176	741.51	41.07	52.22	37076	26650
0.0625	1.3149	0.1497	0.8645	0.6308	1785.10	49.98	76.51	89255	25600
0.1250	1.5369	0.1523	0.8615	0.6760	1984.54	41.49	74.12	99227	25050
0.2500	1.5263	0.1608	0.9170	0.6586	2184.54	45.01	80.84	109227	25150

5.1.4.3 *ΔGAL2ΔGAL3* hysteresis histograms

Table 5.1: Histograms of *ΔGAL2ΔGAL3* hysteresis with high initial condition.

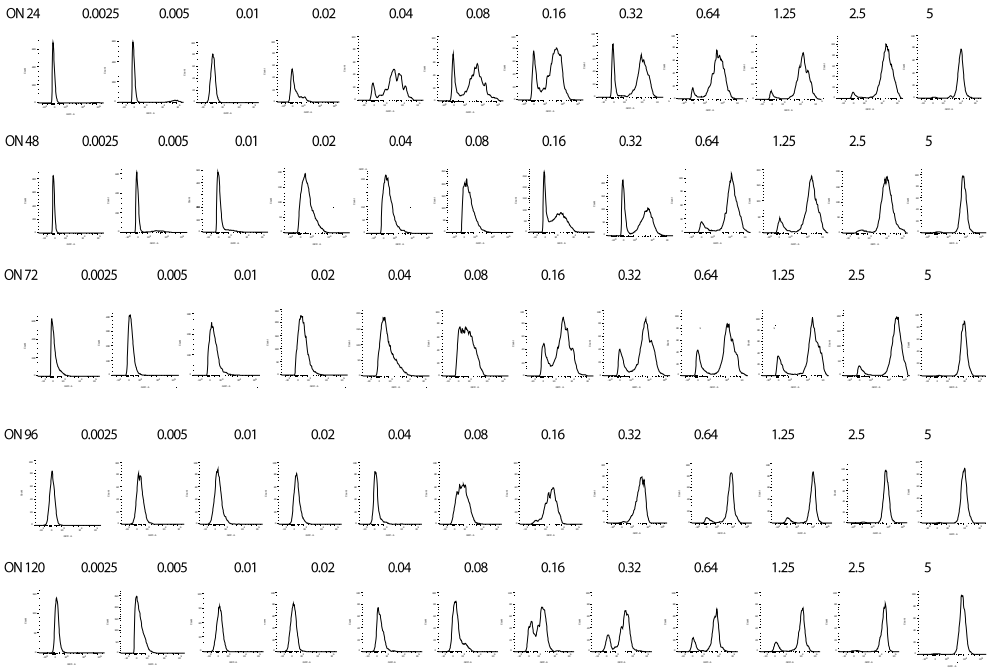

Table 5.2: Histograms of *ΔGAL2ΔGAL3* hysteresis with low initial condition.

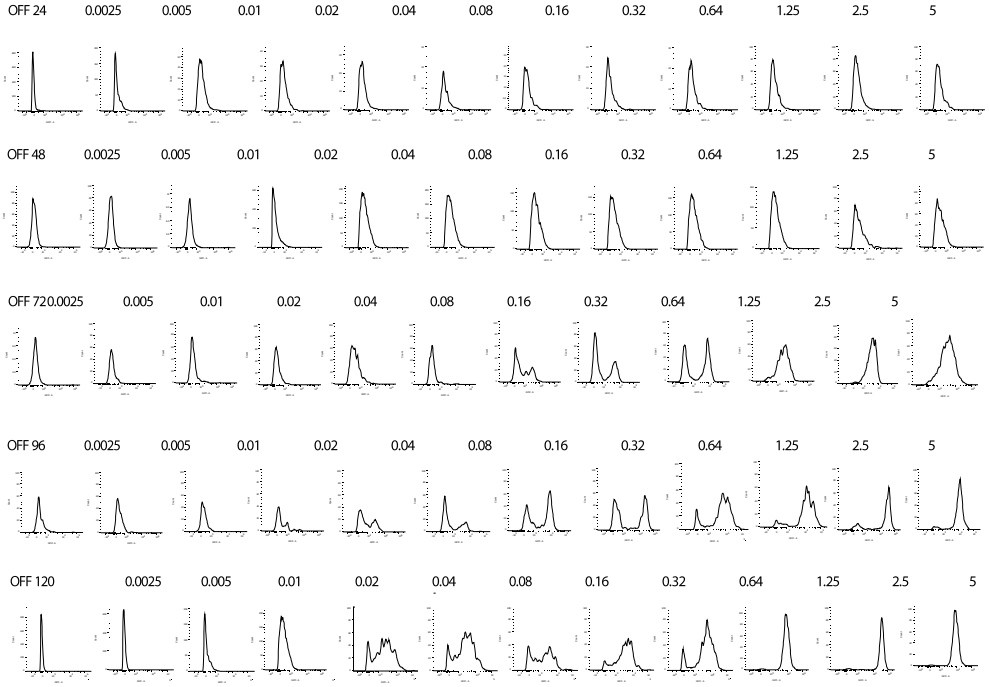

Chapter 6 Bibliography

[1] Cliften P, Sudarsanam P, Desikan A, Fulton L, Fulton B, et al. Finding functional features in Saccharomyces genomes by phylogenetic footprinting. *Science* 2003, 301:71–76.

[2] Bhat PJ. Galactose Regulon of Yeast: From Genetics to System Biology. *Berlin Heidelberg: Springer-Verlag* 2008. 30–31.

[3] Becskei A, Serrano L. Engineering stability in gene networks by autoregulation. *Nature* 2000, 405:590–593.

[4] Lohr D, Venkov P, Zlatanova J. Transcriptional regulation in the yeast GAL gene family: a complex genetic network. *FASEB* 1995, 9:777–787.

[5] Reece RJ. Molecular basis of nutrient-controlled gene expression in *Saccharomyces cerevisiae*. *Cell Mol Life Sci* 2000, 57:1161–1171.

[6] Selleck SB, Majors JE. In vivo DNA-binding properties of a yeast transcription activator protein. *Mol Cell Biol* 1987, 7:3260–3267.

[7] Giniger E, Ptashne M. Cooperative DNA binding of the yeast transcriptional activator GAL4. *Proc Natl Acad Sci USA* 1988, 85:382–386.

[8] Melcher K, Xu HE. Gal80-Gal80 interaction on adjacent Gal4p binding sites is required for complete GAL gene repression. *EMBO J* 2001, 20:841–851.8

[9] Platt A, Reece RJ. The yeast galactose genetic switch is mediated by the formation of a Gal4p-Gal80p-Gal3p complex. *EMBO J* 1998, 17:4086–4091.

[10] Pilauri V, Bewley M, Diep C, Hopper J. Gal80 dimerization and the yeast GAL gene switch. *Genetics* 2005, 169:1903–1914.

[11] Wu Y, Reece RJ, Ptashne M. Quantitation of putative activator-target affinities predicts transcriptional activating potentials. *EMBO J* 1996, 15:3951–3963.

[12] Platt A, Ross HC, Hankin S, Reece RJ. The insertion of two amino acids into a transcriptional inducer converts it into a galactokinase. *Proc Natl Acad Sci USA* 2000, 97:3154–3159.

[13] Schell MA, Wilson DB. Purification and properties of galactokinase from *Saccharomyces cerevisiae*. *J Biol Chem* 1977, 252:1162–1166.

[14] Peng G, Hopper JE. Evidence for Ga13p's cytoplasmic location and Ga180p's dual cytoplasmic- nuclear location implicates new mechanisms for controlling Ga14p activity in *Saccharomyces cerevisiae*. *Mol Cell Biol* 2000, 20:5140–5148.

[15] Klein CJL, Olsson L, Nielsen J. Glucose control in *Saccharomyces cerevisiae*: the role of MIG1 in metabolic functions. *Microbiology* 1998, 144:13–24.

[16] Beaumont HJE, Gallie J, Kost C, Ferguson GC, Rainey PB (2009) Experimental evolution of bet hedging. Nature 462: 90–93.

[17] Ewing JA (1891) Magnetic induction in iron and other metals. London: Van Nostrand. 393.

[18] Mayergoyz ID, Bertotti G, editors. The science of hysteresis. Elsevier (2005). 751.

[19] Xiong, W. & Ferrell, J. E. Jr. A positive-feedback-based bistable 'memory module' that governs a cell fate decision. *Nature* **426**, 460–465 (2003).

[20] Markevich, N. I., Hoek, J. B. & Kholodenko, B. N. Signalling switches and bistability arising from multisite phosphorylation in protein kinase cascades. *J. Cell Biol.* **164**, 353–359 (2004).

[21] Becskei, A., Seraphin, B. & Serrano, L. Positive feedback in eukaryotic gene networks: cell differentiation by graded to binary response conversion. *EMBO J.* **20**, 2528–2535 (2001).

[22] Acar M, Becskei A, van Oudenaarden A. Enhancement of cellular memory by reducing stochastic transitions. *Nature* **435**, 228-232 (2005).

[23] Baldwin M. Protein Identification by Mass Spectrometry. *Molecular & Cellular Proteomics* 2004 3:1-9.

[24] Carr S, Aebersold R, Baldwin M, Burlingame A, Clauser K, Nesvizhskii A. The need for guidelines in publication of peptide and protein identification data: Working Group on Publication Guidelines for Peptide and Protein Identification Data. *Mol Cell Proteomics* 2004. 3:531-3.

[25] Vinzenz Lange, Paola Picotti, Bruno Domon, and Ruedi Aebersold. Selected reaction monitoring for quantitative proteomics: a tutorial. *Mol Syst Biol*. 2008; 4: 222.

[26] Keller A, Nesvizhskii A, Kolker E, Aebersold R. Empirical statistical model to estimate the accuracy of peptide identifications made by MS/MS and database search. *Anal Chem* 2002. 74:5383-92.

[27] Lohr D, Venkov P, Zlatanova J. Transcriptional regulation in the yeast GAL gene family: a complex genetic network. *FASEB J.* 1995. 9:777–787.

[28] Hsu C, Scherrer S, Buetti-Dinh A, Ratna P, Pizzolato J, Jaquet V, Becskei A. Stochastic signalling rewires the interaction map of a multiple feedback network during yeast evolution. *Nat Communication* 2012. 21:3-682.

[29] Hong M, Fitzgerald MX, Harper S, Luo C, Speicher DW, Marmorstein R. Structural basis for dimerization in DNA recognition by Gal4. *Structure* 2008. 16:1019-26.

[30] Keegan L, Gill G, Ptashne M. Separation of DNA binding from the transcription-activating function of a eukaryotic regulatory protein. *Science* 1986. 231:699–704.

[31] Horák J. The role of ubiquitin in down-regulation and intracellular sorting of membrane proteins: insights from yeast. *Biochimica et Biophysica Acta (BBA) - Biomembranes* 2003, 1614:139-155.

[32] Melcher K, Xu H.E. Gal80–Gal80 interaction on adjacent Gal4p binding sites is required for complete *GAL* gene repression. *EMBO J.* 2001, 20: 841–851.

[33] Melcher K, Xu H.E. Gal80–Gal80 interaction on adjacent Gal4p binding sites is required for complete *GAL* gene repression. *EMBO J.* 2001, 20: 841–851.

[34] Bhat P J., Hopper J E. Overproduction of the GAL1 or GAL3 protein causes galactose-independent activation of the GAL4 protein: evidence for a new model of induction for the yeast GAL/MEL regulon. *Mol Cell Biol.* 1992.12(6): 2701–2707.

[35] Horák J. The role of ubiquitin in down-regulation and intracellular sorting of membrane proteins: insights from yeast. *Biochimica et Biophysica Acta (BBA) - Biomembranes* 2003, 1614:139-155.

[36] Bhat PJ, Venkatesh KV. Stochastic variation in the concentration of a repressor activates GAL genetic switch: implications in evolution of regulatory network. *FEBS Lett* 2005, 579:597–603.

[37] Czyz M, Nagiec MM, Dickson RC. Autoregulation of GAL4 transcription is essential for rapid growth of *Kluyveromyces lactis* on lactose and galactose. *Nucleic Acids Res* 1993, 21:4378–4382.

[38] Melcher K, Xu H.E. Gal80–Gal80 interaction on adjacent Gal4p binding sites is required for complete *GAL* gene repression. *EMBO J.* 2001, 20: 841–851.

[39] Bhat P J., Hopper J E. Overproduction of the GAL1 or GAL3 protein causes galactose-independent activation of the GAL4 protein: evidence for a new model of induction for the yeast GAL/MEL regulon. *Mol Cell Biol.* 1992.12(6): 2701–2707.

[40] Vashee S., Xu, H., Johnston, S.A. and Kodadek,T. (1993) How do Zn_2 Cys_6 proteins distinguish between similar upstream activation sites. Comparison of the DNA-binding specificity of the GAL4 protein *in vitro* and *in vivo*. *J. Biol. Chem.*, 268, 24699–24706.

[41] Parthun M.R. and Jaehning, J.A. (1990) Purification and characterization of the yeast transcriptional activator GAL4. J. Biol. Chem., 265, 209–213.

[42] Bhat, Paike Jayadeva. *Galactose Regulon Of Yeast*. Berlin: Springer, 2008. Print.

[43] Lue N.F., Chasman, D.I., Buchman,A.R. and Kornberg,R.D. (1987) Interaction of GAL4 and GAL80 gene regulatory proteins *in vitro*. Mol. Cell. Biol., 7, 3446–3451.

[44] Bhaumik SR, Raha T, Aiello DP, Green MR. In vivo target of a transcriptional activator revealed by fluorescence resonance energy transfer. *Genes Dev* 2004, 18:333–343.

[45] Peng G, Hopper JE. Gene activation by interaction of an inhibitor with a cytoplasmic signaling protein. *Proc Natl Acad Sci U SA* 2002, 99:8548–8553.

[46] Leuther KK, Johnston SA. Nondissociation of GAL4 and GAL80 in vivo after galactose induction. *Science* 1992, 256:1333–1335.

[47] Wightman R, Bell R, Reece RJ. Localization and interaction of the proteins constituting the GAL genetic switch in *Saccharomyces cerevisiae*. *Eukaryot Cell* 2008, 7:2061–2068.

[48] Bhat P J., Hopper J E. Overproduction of the GAL1 or GAL3 protein causes galactose-independent activation of the GAL4 protein: evidence for a new model of induction for the yeast GAL/MEL regulon. *Mol Cell Biol.* 1992.12(6): 2701–2707.

[49] Maier A, Volker B, Boles E, Fuhrman G. Characterisation of glucose transport in Saccharomyces cerevisiae with plasma membrane vesicles (countertransport) and intact cells (initial uptake) with single Hxt1, Hxt2, Hxt3, Hxt4, Hxt6, Hxt7 or Gal2 transporters. *FEMS Yeast Research* 2002, 2:539-555.

[50] Ramos J, Szkutnicka K, Cirillo VP. Characteristics of galactose transport in *Saccharomyces cerevisiae* cells and reconstituted lipid vesicles. *J Bacteriol* 1989, 171:3539–3544.

[51] Reifenberger E, Boles E, Ciriacy M. Kinetic characterization of individual hexose transporters of *Saccharomyces cerevisiae* and their relation to the triggering mechanisms of glucose repression. *Eur J Biochem* 1997, 245:324–333.

[52] Hawkins KM, Smolke CD. The regulatory roles of the galactose permease and kinase in the induction response of the GAL network in *Saccharomyces cerevisiae*. *J Biol Chem* 2006, 281:13485–13492.

[53] Widdas, W.F. Inability of diffusion to account for placental glucose transfer in the sheep and consideration of the kinetics of a possible carrier transfer. *J. Physiol. Lond.* 1952. 118:23-39.

[54] Kulak NA, et al. Minimal, encapsulated proteomic-sample processing applied to copy-number estimation in eukaryotic cells. *Nat Methods* (2014). 11(3):319-24.

[55] Chong YT, et al. Yeast Proteome Dynamics from Single *Cell* Imaging and Automated Analysis. *Cell* (2015). 161(6):1413-24.

[56] Newman JR, et al. Single-cell proteomic analysis of S. cerevisiae reveals the architecture of biological noise. *Nature* (2006). 441(7095):840-6.

[57] Ghaemmaghami S, et al. (2003) Global analysis of protein expression in yeast. *Nature* (2003). 425(6959):737-41.

[58] Broach JR. RAS genes in Saccharomyces cerevisiae: signal transduction in search of a pathway. *Trends Genet* (1991). 7(1):28-33.

[59] Santangelo GM. Glucose signaling in Saccharomyces cerevisiae. *Microbiol Mol Biol Rev* (2006). 70(1):253-82.

[60] Maier A, Volker B, Boles E, Fuhrman G. Characterisation of glucose transport in Saccharomyces cerevisiae with plasma membrane vesicles (countertransport) and intact cells (initial uptake) with single Hxt1, Hxt2, Hxt3, Hxt4, Hxt6, Hxt7 or Gal2 transporters. *FEMS Yeast Research* 2002, 2:539-555.

[61] Ramos J, Szkutnicka K, Cirillo VP. Characteristics of galactose transport in *Saccharomyces cerevisiae* cells and reconstituted lipid vesicles. *J Bacteriol* 1989, 171:3539–3544.

[62] Reifenberger E, Boles E, Ciriacy M. Kinetic characterization of individual hexose transporters of *Saccharomyces cerevisiae* and their relation to the triggering mechanisms of glucose repression. *Eur J Biochem* 1997, 245:324–333.

[63] Hawkins KM, Smolke CD. The regulatory roles of the galactose permease and kinase in the induction response of the GAL network in *Saccharomyces cerevisiae*. *J Biol Chem* 2006, 281:13485–13492.

[64] Sellick CA, Jowitt TA, Reece RJ. The effect of ligand binding on the galactokinase activity of yeast Gal1p and its ability to activate transcription. *J Biol Chem*. 2009. 284:229-36.

[65] de Jongh WA, et al. The roles of galactitol, galactose-1-phosphate, and phosphoglucomutase in galactose-induced toxicity in Saccharomyces cerevisiae. *Biotechnol Bioeng*. 2008.

[66] De Robichon-Szulmajster H. Induction of enzymes of the galactose pathway in mutants of Saccharomyces cerevisiae. *Science*. 1958. 127(3288):28-9.

[67] Angeli, D., Ferrell, J. E. Jr. & Sontag, E. D. Detection of multistability, bifurcations, and hysteresis in a large class of biological positive-feedback systems. *Proc. Natl Acad. Sci. USA* **101**, 1822–1827 (2004).

[68] Hsu C., Jaquet V., Maleki F.,Gencoglu M., Becskei A. Mapping of deterministic and stochastic network activity by feedback splitting. Submitted to *Cell Systems* 2015.

[69] Vashee S., Xu, H., Johnston, S.A. and Kodadek,T. (1993) How do Zn_2 Cys_6 proteins distinguish between similar upstream activation sites. Comparison of the DNA-binding specificity of the GAL4 protein *in vitro* and *in vivo*. *J. Biol. Chem.*, 268, 24699–24706.

[70] Bhat, Paike Jayadeva. *Galactose Regulon Of Yeast*. Berlin: Springer, 2008. Print.

[71] Bhat P J., Hopper J E. Overproduction of the GAL1 or GAL3 protein causes galactose-independent activation of the GAL4 protein: evidence for a new model of induction for the yeast GAL/MEL regulon. *Mol Cell Biol*. 1992.12(6): 2701–2707.

[72] Hawkins KM, Smolke CD. The regulatory roles of the galactose permease and kinase in the induction response of the GAL network in *Saccharomyces cerevisiae*. *J Biol Chem* 2006, 281:13485–13492.

[73] Hsu C., Jaquet V., Maleki F.,Gencoglu M., Becskei A. Mapping of deterministic and stochastic network activity by feedback splitting. Submitted to *Cell Systems* 2015.

[74] Aaron M. Neiman. Sporulation in the Budding Yeast *Saccharomyces cerevisiae*. *Genetics* 2011. 189(3): 737–765.

[75] Gossen, M. and Bujard, H. Anhydrotetracycline, a novel effector for tetracycline controlled gene expression systems in eukaryotic cells. *Nucl. Acids Res.* 1993. 21:4411-4412.

[76] Picotti P, Bodenmiller B, Mueller LN, Domon B, Aebersold R. Full dynamic range proteome analysis of S. cerevisiae by targeted proteomics. *Cell* 2009. 138:795-806.

[77] Murray, Kermit K.; Boyd, Robert K.; Eberlin, Marcos N.; Langley, G. John; Li, Liang; Naito, Yasuhide. Definitions of terms relating to mass spectrometry. (IUPAC Recommendations 2013). *Pure and Applied Chemistry* 2013. 1.

[78] Picotti P, Clément-Ziza M, Lam H, Campbell D S, Schmidt A, Deutsch E W, Röst H, Sun Z, Rinner O, Reiter L, Shen Q, Michaelson J J, Frei A, Alberti S, Kusebauch U, Wollscheid B, Moritz R L, Beyer A, Aebersold R. A complete mass-spectrometric map of the yeast proteome applied to quantitative trait analysis. *Nature* 2013. 494:266–270.